Variation in rock quality between metamorphic domains in the lower levels of the Eastern Segment, Sveconorwegian Province

Linda Lundgren

Dissertations in Geology at Lund University,
Master's thesis, no 324
(45 hp/ECTS credits)

Department of Geology
Lund University
2012

Variation in rock quality between metamorphic domains in the lower levels of the Eastern Segment, Sveconorwegian Province

Master's thesis

Linda Lundgren

Department of Geology
Lund University
2012

Contents

Cover Picture: Hallandia gneiss

Variation in rock quality between metamorphic domains in the lower levels of the Eastern Segment, Sveconorwegian Province

LINDA LUNDGREN

Lundgren, L., 2012: Variation in rock quality between metamorphic domains in the lower levels of the Eastern Segment, Sveconorwegian Province. *Dissertations in Geology at Lund University*, No. 324, 60 pp. 45 hp (45 ECTS credits).

Abstract:

Natural gravel deposits act as aquifers storing ground water but are a finite resource and an important asset to the Swedish community. In order to preserve these assets for the future substitute materials have to be located; crushed rock material (aggregates) is an alternative. Twelve gneiss samples from the Eastern Segment, southwestern Sweden, have been characterized and analyzed for suitability as road or railway aggregates.

Petrographic characteristics including mineral content and meso- and micro-scale textures and structures, explain the rock quality variations in the high grade metamorphic gneiss area in Halland, Eastern Segment. Petrographic characteristics can be used as prospecting tools in the search for material suitable as aggregates. The suitability of the rock materials as aggregates for road or railway was tested by quantitative analyses including crack, mineral grain size and mineral grain size distribution, Foliation index (FIX), perimeter, geochemical and water absorption analyses, and technical properties (Los Angeles, studded tyre, microDeval test analyses).

Low average grain size and high perimeter (total, amphibole+pyroxene, opaque minerals+garnet) show a good correlation with low Los Angeles (LA) values. Samples with high density tend to have a lower Los Angeles/studded tyre ratio. The frequency of fractures has a limited influence on the LA value. A high proportion of very fine or fine grained materials seem to contribute to a better LA value.

The absence of a high grade metamorphic banding (segregation of light and dark minerals), the absence of a pronounced aggregate stretching lineation and the absence of leucosome veins indicate good technical values. The best technical properties are obtained from rocks that have been metamorphosed and deformed at very high temperature conditions (granulite facies). Textures, on a microscopic scale, that show a good correlation to granulite facies metamorphism include reddish brown biotite, low biotite content, brownish green hornblende, pyroxene, antiperthitic feldspars and the absence of titanite and tartan twinning in feldspars.

In the present investigation samples from Dagsås and Ljungby, both located in the Varberg granulite gneiss domain, are the most suitable rock materials as aggregates for road and railway (bounded layers), while samples from Fridhemsberg and Töresjö, located in the Skene migmatite gneiss domain, are the least suitable. Samples from Knobesholm and Vräk are suitable as aggregates for bounded road layers.

Keywords: Los Angeles test, studded tyre test, microDeval test, rock quality, quantitative analyses.

Supervisors: Charlotte Möller, Jenny Andersson, Mattias Göransson and Jan Erik Lindqvist.

Linda Lundgren, Department of Geology, Sölvegatan 12, SE-223 62 Lund, Sweden.
E-mail: linda.lundgren88@hotmail.se

Variationer i bergkvalitet mellan olika metamorfa domäner i de lägre nivåerna av det Östra Segmentet, Svekonovegiska Provinsen

LINDA LUNDGREN

Lundgren, L., 2012: Variationer i bergkvalitet mellan olika metamorfa domäner i de lägre nivåerna av det Östra Segmentet, Svekonorvegiska Provinsen. *Dissertations in Geology at Lund University*, Nr. 324, 60 sid. 45 hp.

Sammanfattning:

Naturliga grusavsättningar är ändliga resurser och verkar som akviferer för grundvatten vilket gör dem viktiga för det svenska samhället. För att kunna bevara dessa värdefulla tillgångar måste ett ersättningsmaterial hittas; krossten (aggregat) är ett bra alternativ. I föreliggande undersökningar har tolv bergartsprov av gnejs från det Östra Segmentet i sydvästra Sverige analyserats för att se hur lämpliga de är att använda som material till väg eller järnväg.

Syftet med de petrografiska beskrivningarna, vilka innefattar mineralinnehåll samt texturer och strukturer i fält och i tunnslip, var att kunna förklara variationer i bergkvalité i de högmetamorfa gnejserna i Halland. Petrografin kan användas som ett prospekteringsverktyg för att hitta passande bergmaterial till väg och järnväg. Genom att jämföra kvantitativa analyser (sprick-, mineral kornstorlek och mineral kornstorleksfördelnings-, Foliations index (FIX), perimeter-, geokemisk- och vattenabsorptionsanalys) med de tekniska egenskaperna (Los Angeles-, kulkvarn- och mikroDevaltester) för gnejserna kunde deras lämplighet bestämmas.

Hög omkrets och lågt kornstorleksmedelvärde korrelerar med låga Los Angelesvärden. Prover med hög densitet tenderar att ha lägre Los Angeles/kulkvarns-förhållande. LA-värdet påverkas till en viss grad av mängden sprickor. En hög andel av väldigt fint eller fint material i proven verkar bidra till ett bättre LA-värde.

Få eller inga ådror, avsaknad av höggradig metamorf bandning (segregation av ljusa och mörka mineral) och avsaknad av aggregatlineation är karaktäristiska strukturer som resulterar i bra tekniska värden. De bästa tekniska egenskaperna erhölls av bergarter som deformerats och metamorfoserats under mycket höga temperaturer (granulitfacies). Microtexturer som visar en bra correlation till högtemperatur metamorfos är: rödbrun biotit, låg biotithalt, brungrönt hornblende, pyroxen, antipertitisk fältspat, samt avsaknad av titanit och avsaknad av mikroklin tvillingar i fältspat.

Gnejs från Dagsås och Ljungby, båda från Varbergs granulit- och gnejsdomän, är de två bergarter av de undersökta bergmaterialen som bäst uppfyller kraven för bergmaterial till bundna väg– och järnvägslager, medan gnejs från Fridhemsberg och Töresjö, båda från Skenes migmatitgnejsdomän är de minst lämpliga. Gnejs från Knobesholm och Vräk är lämpliga som aggregat till bundna väglager.

Nyckelord: Los Angelesvärde, kulkvarnsvärde, microDevalvärde, bergkvalitet, kvantitativa analyser

Ämnesinriktning: Berggrundsgeologi

Linda Lundgren, Geologiska institutionen, Lunds universitet, Sölvegatan 12, SE-223 62 Lund, Sverige.
E-post: linda.lundgren88@hotmail.se

1. Introduction

Natural gravel deposits are an important resource for the community and should be preserved for at least two reasons. First, the deposits are finite and have to be preserved for the future for products where there are no replacements known. Second, the deposits often store groundwater which is very important to the community. In order to save these aquifers and valuable gravel assets it is important to preserve the present deposits and find replacement materials corresponding to the natural ones. Crushed rock (aggregates) is a good alternative.

Bedrock and rock quality mapping has been carried out by the Geological Survey of Sweden in the studied area (Falkenberg). Observations and data from the mapping have been used to divide the bedrock into different domains based on similarity in mineralogy and textures. Representative samples were collected from each bedrock domain. Gneisses in the Laholm-Halmstad and Varberg-Kungsbacka areas show variations in rock quality that have been difficult to explain (Göransson et al., 2008; Persson & Göransson, 2010a).

Quantitative analyses carried out in this project include studded tyre test (A_N), microDeval test (M_{DE}), Los Angeles test (LA), density (D), micro, geochemical and water absorption analyses. Geochemistry was made for all gneisses except for samples from Fridhemsberg and Töresjö. Qualitative descriptions for all twelve rock samples are based on field observations and polarized microscopy. The results from the quantitative and qualitative analyses determine the suitability of the investigated gneisses as aggregates for road or railway.

The objective of this study has been to attain detailed petrographic and geological knowledge to explain variations in rock quality in the high grade metamorphic gneisses in Halland. This knowledge can be used as prospecting tools. Another aim is to correlate properties of the investigated gneisses (microtextures, mineral content, frequency of fractures, mineral grain size and distribution, Foliation index (FIX), perimeter analysis, geochemical analyses and water absorption analysis) with their technical properties, and assess how appropriate these rock materials work as aggregates for road and/or railway construction.

2. Geological setting

2.1 Regional geology

The sampled area is located in the Halland county, southwestern Sweden which is a part of the Sveconorwegian Orogen (Fig. 1).

In late Mesoproterozoic to early Neoproterozoic time the Fennoscandian continent was reworked in its southwestern parts by accretion and continent-continent collision which resulted in a c. 500 km wide orogenic belt, the Sveconorwegian Orogen (Bingen et al., 2008b). The Sveconorwegian orogenic belt is overlain in the northwest by the Caledonian nappes and restricted to the east by the Sveconorwegian Frontal Deformation Zone (Fig. 1; Bingen et al., 2008a). Sveconorwegian high-grade metamorphism took place during different events in different parts of the orogen between 1.14 and 0.90 Ga (Bingen et al., 2008b). The orogen consists of five principal segments which are separated by Sveconorwegian shear zones (Figs. 1 and 2). The Eastern Segment is the easternmost segment and restricted to the area between the Sveconorwegian Frontal Deformation Zone in the east and the Mylonite Zone in the west (Berthelsen, 1980; Wahlgren et al., 1994).

Based on the imprint of Sveconorwegian deformation, the Eastern Segment can be divided into three tectonic levels (Fig. 2). The upper tectonic level (roughly corresponding to the Protogine Zone) is characterized by non-penetrative Sveconorwegian deformation. Rocks in the middle level show penetrative Sveconorwegian deformation at amphibolite facies conditions. The lower tectonic level is characterized by penetrative high-grade deformation and at 0.97 Ga large parts of the lower level were buried to at least 35 km depth which resulted in metamorphism at high-pressure granulite to upper amphibolites facies conditions (Johansson et al., 1991; Wang & Lindh, 1996; Möller, 1998). Eclogite-bearing gneiss units are also present and are evidence of even deeper burial, > 50

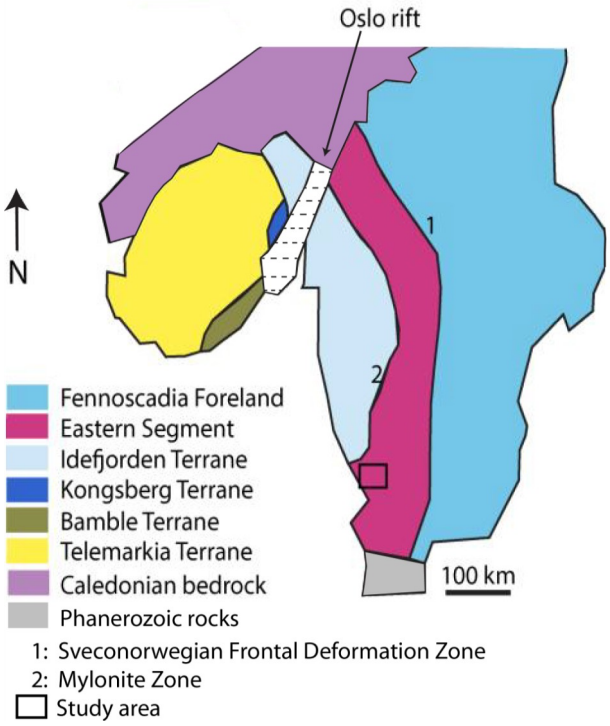

Fig. 1. Simplified domain map of southwestern Scandinavia showing the location of the Sveconorwegian Orogen, including lithotectonic domains and significant shear zones with respect to the Fennoscandian foreland, Oslo rift and Caledonian front. Modified from Bingen et al. (2008a).

km (Möller 1998, 1999). Ductile structures in the Eastern Segment are characterized by E-W trending folds overprinted and rotated by younger N-S trending structural features (Möller et al., 2007).

The Eastern Segment is mainly made up of 1.81-1.64 Ga granitic to syenitoid gneisses that are similar in age and composition to rocks east of the Sveconorwegian orogen (Söderlund et al., 2002; Andersson et al., 2006; Möller et al., 2007; Wik et al., 2006, 2009). Younger protholith rocks are 1560 Ma old mafic dykes, 1460-1380 Ma felsic to mafic and 1250-1200 Ma granite to syenitoid intrusions. The Eastern Segment has also been affected by high-grade metamorphism of a pre-Sveconorwegian event, at 1.46-1.38 Ga Hallandian orogenesis (Hubbard, 1978; Möller et al., 2007). The Hallandian event included regional scale migmatitization and formation of a gneissic layering at 1.46-1.42 Ga, (Möller et al., 2007; Brander et al., 2012) and intrusion of granite and charnockite, including local charnockitization of the host gneisses at 1.41-1.38 Ga (Hubbard & Whitley, 1979; Harlov et al., 2006; Rimsa et al., 2007).

2.2 Geology of the Falkenberg area

The investigated area, marked with a light blue line in figure 3 (the Falkenberg project area of the Geological Survey of Sweden), is located in the lower tectonic level of the Eastern Segment (Figs. 1 and 2). It comprises a heterogeneous gneiss complex divided in to sub-domains based on the results of ongoing SGU mapping and previously published literature. Each sub-domain show special mineralogical and textural properties which are characteristic for the sub-domain, however not by every outcrop. The sub-domains are the Varberg granulite gneiss domain, the Hallandia gneiss domain, the Skene migmatite gneiss domain and the Svarten gneiss domain.

2.2.1 Varberg granulite gneiss domain

In the Varberg granulite gneiss domain (green area in Fig. 3) high-temperature metamorphism and charnockitization is at least locally associated with 1.4 Ga old magmatism and the gneiss complex host both magmatic and metamorphic charnockites (Hubbard, 1978). Gneisses in this area are characterized by their dark color (grey- greenish grey) and variable presence of leucosome veins. When present, leucosome are discrete and strongly deformed. Relict magmatic textures make it possible to tell the protolith of most of the gneisses. The gneisses commonly lack distinct metamorphic segregation of light and dark mineral phases on scales larger than c. 5 mm. Garnet was identified only rarely in outcrops and in hand specimens.

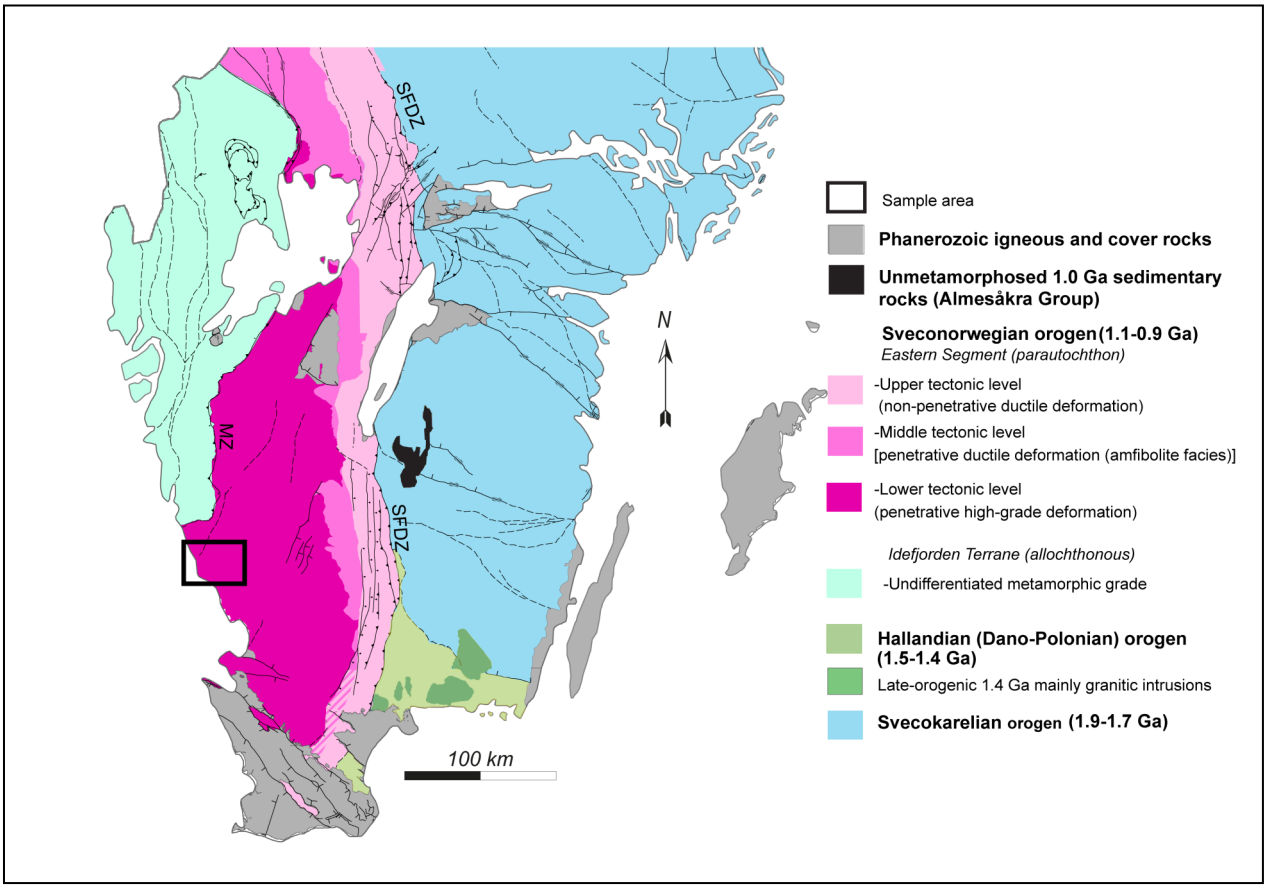

Fig. 2. Principal geological units in southern Sweden based on the Geological Survey of Sweden bedrock map database at scale 1:1000.000, showing principal lithological and tectonic boundaries. The sample area, marked with a black square, is located in the Halland county.

2.2.2 Hallandia gneiss domain

The gneisses in the southern part of the study area (blue area in Fig. 3) are polymetamorphic and contain one or two generations of leucosome veins dated at 1.43 and 0.97 Ga and two generations of granite pegmatite dykes dated at 1.40 and 0.95 Ga respectively (Möller et al., 2007). Pink leucosome veins are common and folded. Field relations between the different vein generations demonstrate polyphase high-grade metamorphism and deformation. The 1.43 Ga migmatitic gneissic layering is cut by 1.40 Ga pegmatitic materials which in turn is tightly folded and stretched (Möller et al., 2007). The youngest 0.95 Ga dykes are undeformed and cross-cut ductile deformation structures.

A pronounced lineation and foliation is characteristic for these gneisses. The extensively veined and folded gneisses in the Hallandia gneiss domain are esthetically appealing and sought after by the industry. The gneisses are used as dimension stones and commonly referred to as Hallandia gneiss, Bårarp gneiss or Halmstad gneiss.

2.2.3 Skene migmatite gneiss domain

Migmatites are composed of various components: melanosome, leucosome and mesosome (Winter, 2001). The melanosome is the darkest material and commonly boarder the light material i.e. the leucosome. The mesosome has an intermediate composition.

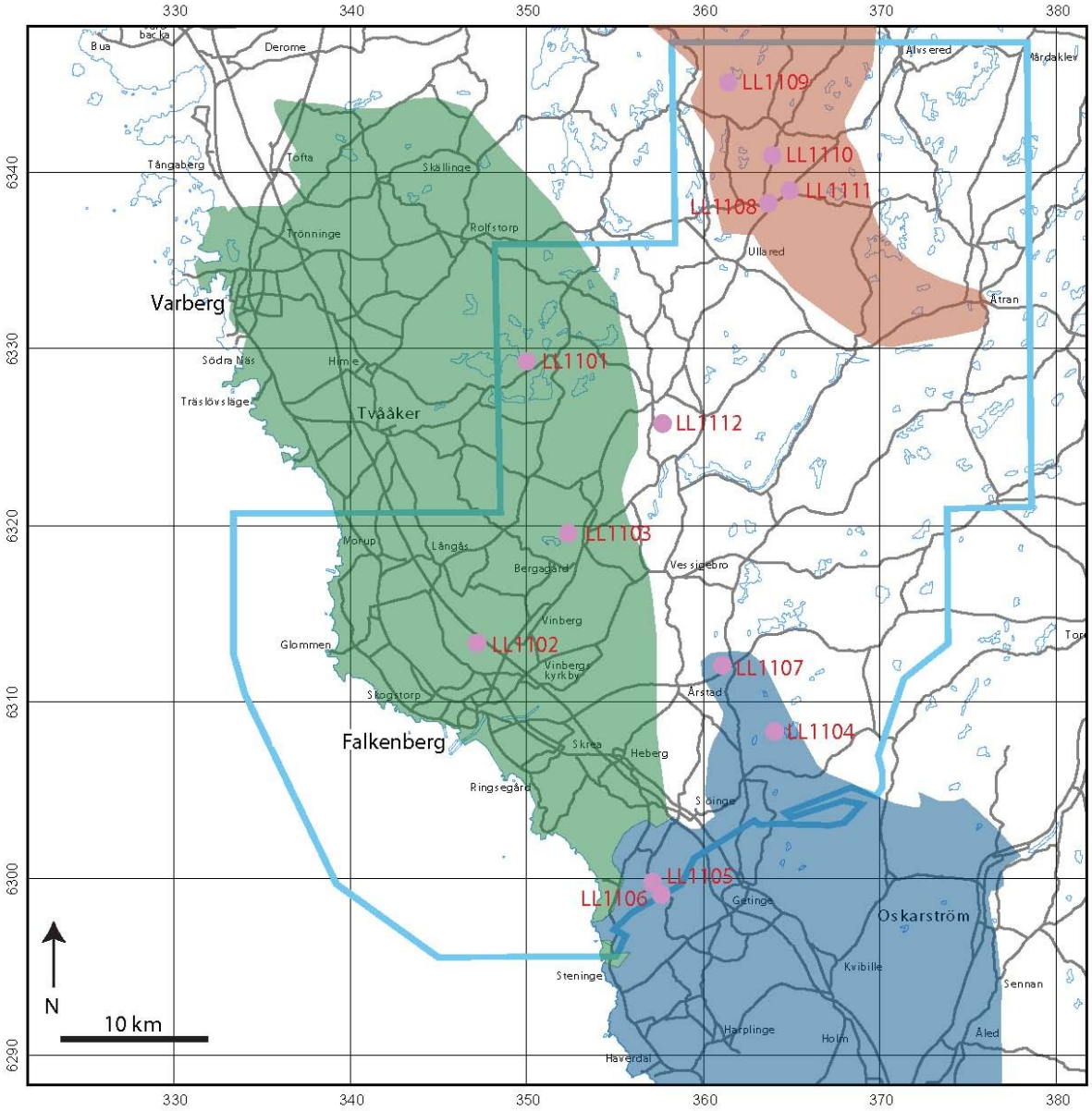

Fig. 3. The investigated area ("Falkenberg area") is marked with a light blue line. The boundaries between the Varberg (green color), Skene (red color), Hallandia (blue color) and Svarten domains (described in the text) are approximate and parallel to the regional foliation and magnetic anomaly trend lines. The sketch is based on unpublished preliminary data from the Geological Survey of Sweden bedrock mapping project in Falkenberg community and C. Möller, Lund University, December 2012.

A regional extensive sub-domain, located between Fagered in the south and Härryda-Bollebygd in the north, is characterized by stromatic migmatite gneiss (Skene gneiss) hosting disrupted and amphibolitized eclogite lenses. The southern part of this domain was investigated in the present study, here referred to as the Skene migmatite gneiss domain (red area in Fig. 3). Typical rocks in this domain are stromatic migmatitic gneisses with penetrative and extensive metamorphic segregation of felsic and mafic material forming a high-grade banding. Primary magmatic textures such as relict augen or relict coarse-medium texture are rarely present. Light reddish leucosome veins make up about 5-10 vol %. The minerals making up the veins are commonly unstrained, uneven grained and has a sugary texture. Occasionally, the leucosomes, show pinch and swell structures. The veins and layering locally show tight to isoclinal folding.

2.2.4 Svarten gneiss domain

The Svarten Zone is a roughly N-S-trending structure, located in the Eastern Segment and bounding the Varberg domain to the west (Fig. 3). The tectonic role of this structure is still not clearly understood. Only one sample was collected in this domain. Gneisses in the Svarten domain are heterogeneous, commonly strongly deformed with a pronounced stretching defined by deformed pink feldspar aggregates. A relict magmatic fabric is present locally; the gneisses are commonly veined.

3. Description of sample sites

Twelve samples were collected from the investigated area. Sample localities are marked with light purple dots and the sampled sub-domains (1-4 above) have different colors in figure 3 (except the Svarten gneiss domain since only one sample is restricted to this domain).

Three samples (Dagsås = LL1101, Stavsjö = LL1102 and Ljungby = LL1103) are located in the Varberg granulite gneiss domain, located in the western area of the investigated area (Fig. 3). In the south, samples Knobesholm (LL1104), Hallandssten (LL1105), Mokrik (LL1106) and Abild (LL1107) are restricted to the Hallandia gneiss domain. Four samples (Fridhemsberg = LL1108, Töresjö = LL1109, Toppeberg = LL1110 and Vräk = LL1111) are located in the Skene migmatite gneiss domain in the northeast. From the Svarten gneiss domain, in the centre of the investigated area, one sample (Köinge, LL1112) was collected.

Field observations from the sample localities are given below according to the domain sub-division and a brief summary are found in Appendix 2.

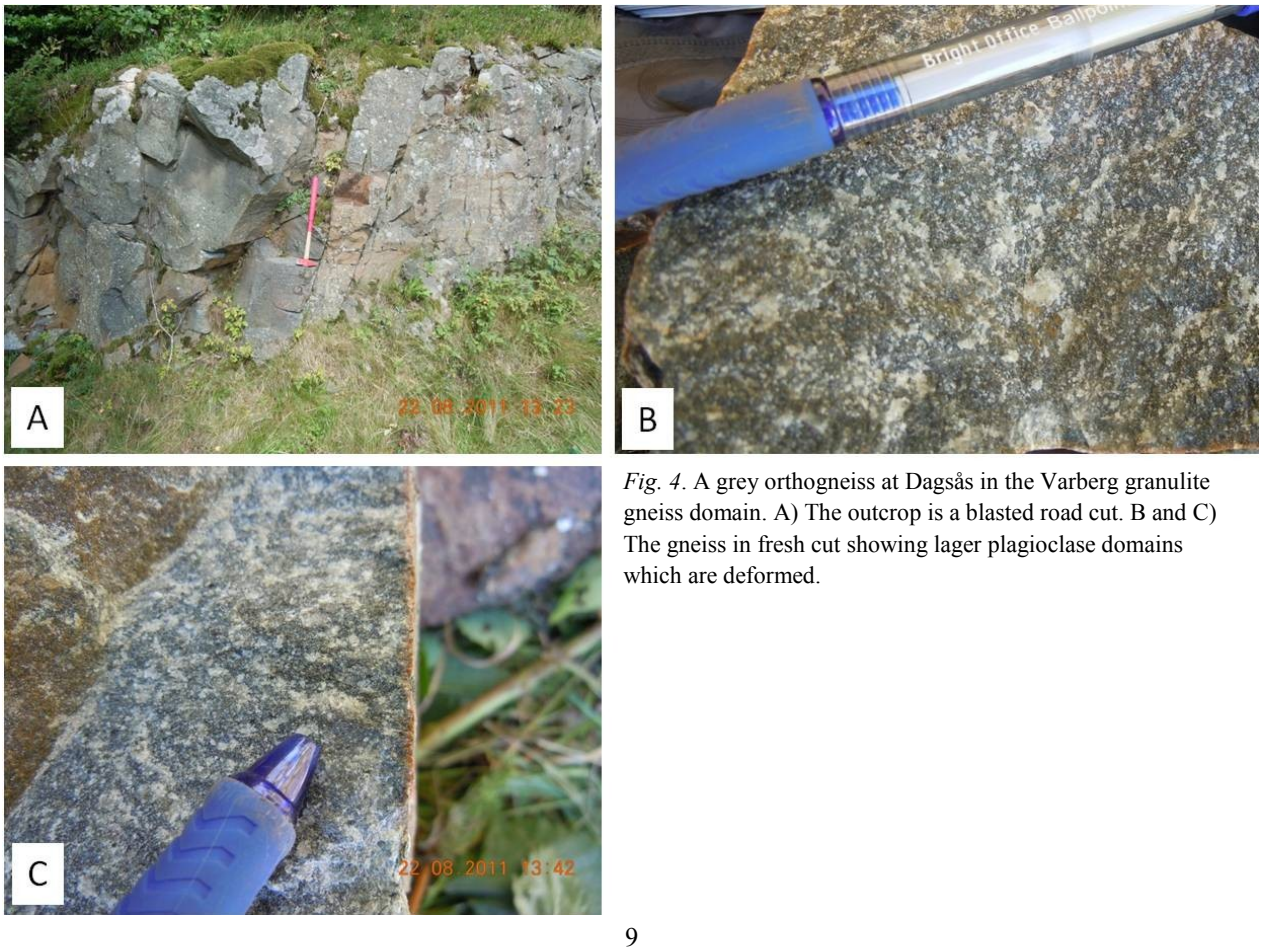

Fig. 4. A grey orthogneiss at Dagsås in the Varberg granulite gneiss domain. A) The outcrop is a blasted road cut. B and C) The gneiss in fresh cut showing lager plagioclase domains which are deformed.

3.1 Varberg granulite gneiss domain

Many of the gneisses in this area have a granulite facies mineral assemblage, with antiperthite and pyroxene as major components. Many gneisses lack a distinct gneissic layering (metamorphic segregation of dark and light minerals phases), veins are sparse and the absence of a lineation occurs locally. Sometimes the gneisses are dark in color, due to a high content of mafic minerals.

3.1.1. Dagsås (LL1101)

The outcrop is a blasted road cut (Fig. 4A) located in the area of Lake Humsjön. The rock is an uneven grained grey, relatively dark orthogneiss (Figs. 4B and C), rusty brown on weathered surfaces. It is penetratively foliated but has no metamorphic banding. No augen, veins or lineation can be seen on a macroscopic scale; small garnet crystals was identified with a hand lens. Large deformed plagioclase domains are present in the fine grained grey groundmass (Fig. 4B and C). Two set of fractures are present. The protholith of this orthogneiss has been dated at 1.7 Ga; it is affected by 1.45 Ga metamorphism (Söderlund et al., 2002).

3.1.2 Stavsjö (LL1102)

Släryds Grus och Entrepenad AB runs the Stafsinge 6:4 quarry. Allmost all the quarried material during 2005-2009 were used for roads and the rest for concrete. The production data was collected from the Geological Survey of Sweden and are compiled in Appendix 1.

The walls in the quarry are heavily fractured; blocks have fallen to the ground or remain loose on the walls (Fig. 5A). Relict uneven grained reddish grey gneiss dominates the quarry (Figs. 5B and C). Amphibolite occurs locally as larger lenses. Weathered surfaces are yellowish brown to rusty colored. The grey groundmass is medium grained. Aggregates are dominated by pink K-feldspar which shows that the gneiss once was unevenly grained (Figs. 5 B and C). Veins are extensive and uniform in thickness (0.5-3 cm thick; Fig. 5B). They are medium to coarse grained and have a granitic composition. Red fractures (123°/66°SW) occasionally cut the gneissosity which is defined by dark minerals, veins and elongated feldspar aggregates.

Fig. 5. A reddish grey gneiss at Stavsjö located in the Varberg granulite gneiss domain. A) Rock walls in the quarry are fractured. B) The gneiss contains pink K-feldspar rich veins and aggregates. C) Larger deformed pink K-feldspar aggregates give the gneiss an uneven grained appearance.

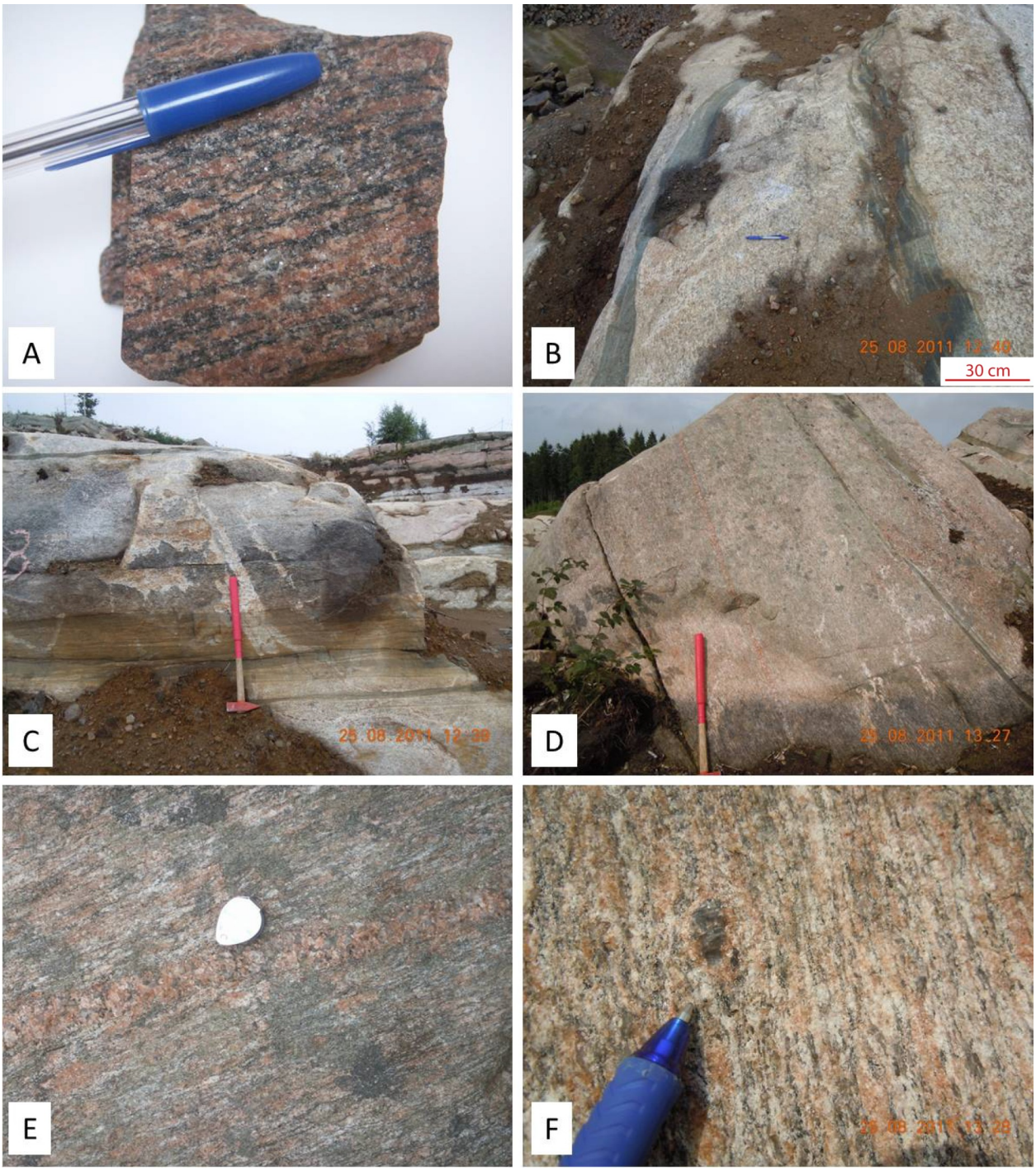

Fig. 6. A reddish grey gneiss in the Ljungby quarry located in the Varberg granulite gneiss domain. A) This reddish grey gneiss dominates in the quarry. B) Alternation of the gneiss and amphibolite layers define a lithological layering. C) The gneiss show lithological layering where the fine grained dark layers are extensive and 2-20 cm thick. D) Felsic thin dykes, slightly discordant to the lithological layering. E) The felsic dykes are 3-20 cm thick and contain unstrained felsic minerals. F) Some feldspar aggregates have a remnant of megacrystic orthoclase in the core.

3.1.3 Ljungby (LL1103)

Skanska runs the Ljungby-Prästgård 2:1 quarry. All quarried material during 2011 and 2012 were used for roads (Skanska, Jan Heltegen, personal communication, 17th of October 2012). The production data are summarized in Appendix 1.

Blasted rock walls show that there is a variety of rocks within the quarry.

The lower part of the quarry is dominated by a red gneiss. The gneiss is reddish both in fresh cut and on exposed weathered surfaces. Alternating gneiss and amphibolite layers form a lithological layering (352º/32ºE). The amphibolites are fine grained, horizontally extensive and ≤ 20 cm thick. The fine to medium grained red gneiss is leucocratic and the lack of dark minerals makes it difficult to pick out a foliation. Felsic veins, relict coarse grained, are parallel to the lithological layering, and minerals inside the veins e.g. quartz are strongly deformed and stretched.

The quarry is dominated by an uneven grained reddish grey gneiss which was sampled for further investigation (Fig. 6A) The gneiss is layered with alternating dark and felsic layers (Figs. 6B and C). Dark fine grained amphibolite layers (353º/33ºE) are even grained, dark grey, but has a yellowish to rusty brown color on weathered surfaces (appears to weather more easily than the gneiss). The dark layers are horizontally extensive (several meters), unevenly thick (2-20 cm) and contain felsic veins (Fig. 6B). The veins are thin (0.5 cm thick) and concordant with the layering. The grey groundmass is fine grained. Veins, augen and strong foliation (324°/34°NE) in the gneiss are parallel to the lithological layering. Coarse grained felsic veins (333º/32ºNE) are slightly discordant to the lithological layering (Fig. 6D). They are extensive (several meters), 3-20 cm thick, and contain unstrained felsic minerals (Fig. 6E). The gneiss is discretely veined and lack other metamorphic segregations. Augen consist of elongated pink K-feldspar; the least deformed aggregates are ≤ 2 cm long and ≤ 1 cm thick, whereas the most deformed form veins are 4-10 cm long and 0.5-1 cm thick. Dark brown orthoclase crystals occasionally occur as cores in some feldspar aggregates (Fig. 6F). The appearance of this gneiss, with respect to the light color, presence of augen and veins, strong foliation and lithological layering is characteristic of some but not all rocks in the Varberg granulite gneiss domain.

3.2 Hallandia gneiss domain

Gneisses restricted to this area are polymetamorphic and contain at least three generations of leucosome veins and dykes (dated at 1.43, 1.40 and 0.95 Ga respectively; Möller et al., 2007). Pink veins are common, folded and strongly deformed. An aggregate lineation is commonly pronounced as are a gneissic layering and foliation. The rocks commonly show reddish grey color.

3.2.1 Knobesholm (LL1104)

Slättelynga Grus AB runs the Torkelstorp 5:1 quarry. Production data (collected from the Geological Survey of Sweden) shows that the main part of the quarried material between 2005 and 2009 were used for roads. The production data are compiled in Appendix 1.

The rock material in the quarry is homogenous, with the exception of a metabasic layer (258/20N, 1.5-2 m thick, horizontally extensive and parallel to the lineation in the gneiss), and is dominated by uneven grained reddish grey gneiss. The gneiss is reddish grey in fresh cut and rusty brown on weathered surfaces (Figs. 7A and B). The gneiss contain several generations of veins. Veins and elongated augen are common and dominated by K-feldspar. Veins are commonly isoclinally folded (tightly folded; Fig. 7C). Some fine grained K-feldspar aggregates contain remnants of orthoclase in the core. The grey groundmass is fine to medium grained. The foliation is weak and defined by dark minerals. Lineation is pronounced and defined by deformed pink K-feldspar aggregates and biotite (Figs. 7D and E).

3.2.2 Hallandssten (LL1105)

The company Hallandssten AB owns and runs the Eftra-Svenstorp 1:19 quarry. Most of the quarried material during 2005-2009 was thrown away but the remaining material was used as ornamental stones. Production data was collected from the Geological Survey of Sweden and a compilation is found in Appendix 1.

Uneven grained reddish grey gneiss with augen and veins (both dominated by pink K-feldspar) dominate the quarry (Figs. 8A and B). Weathered surfaces are yellowish brown to rusty brown. The grey groundmass is fine to medium grained. Elongated pink augen/feldspar aggregates (1-2 cm large) occasionally show orthoclase core (Fig. 8C) and define a pronounced lineation. Reddish leucosome veins (≤ 10 cm long and 0.5-4 cm thick) are common and often moderate to tightly folded, penetrating and locally surrounded by dark selvage of biotite (Fig. 8A). There are two sets of folded veins which crosscuts eachother at a high grade angle (Figs. 8B and D). The axial plane foliation (343/40E) of the veins is defined by Fe-Mg rich minerals (hornblende, biotite and opaques) and is less pronounced than the lineation.

3.2.3 Mokrik (LL1106)

The company Mobjer Sten AB owns and runs the Äskered 3:1, 7:1 quarry. Production data was collected from the Geological Survey of Sweden and shows that all material quarried in 1996 was used as dimension stone. During 1997-2009 material used as ornamental stone was quarried; between 1997-2001 quarried material was also used for roads. The production data are summarized in Appendix 1.

An uneven grained, foliated (340/25E) and fol-

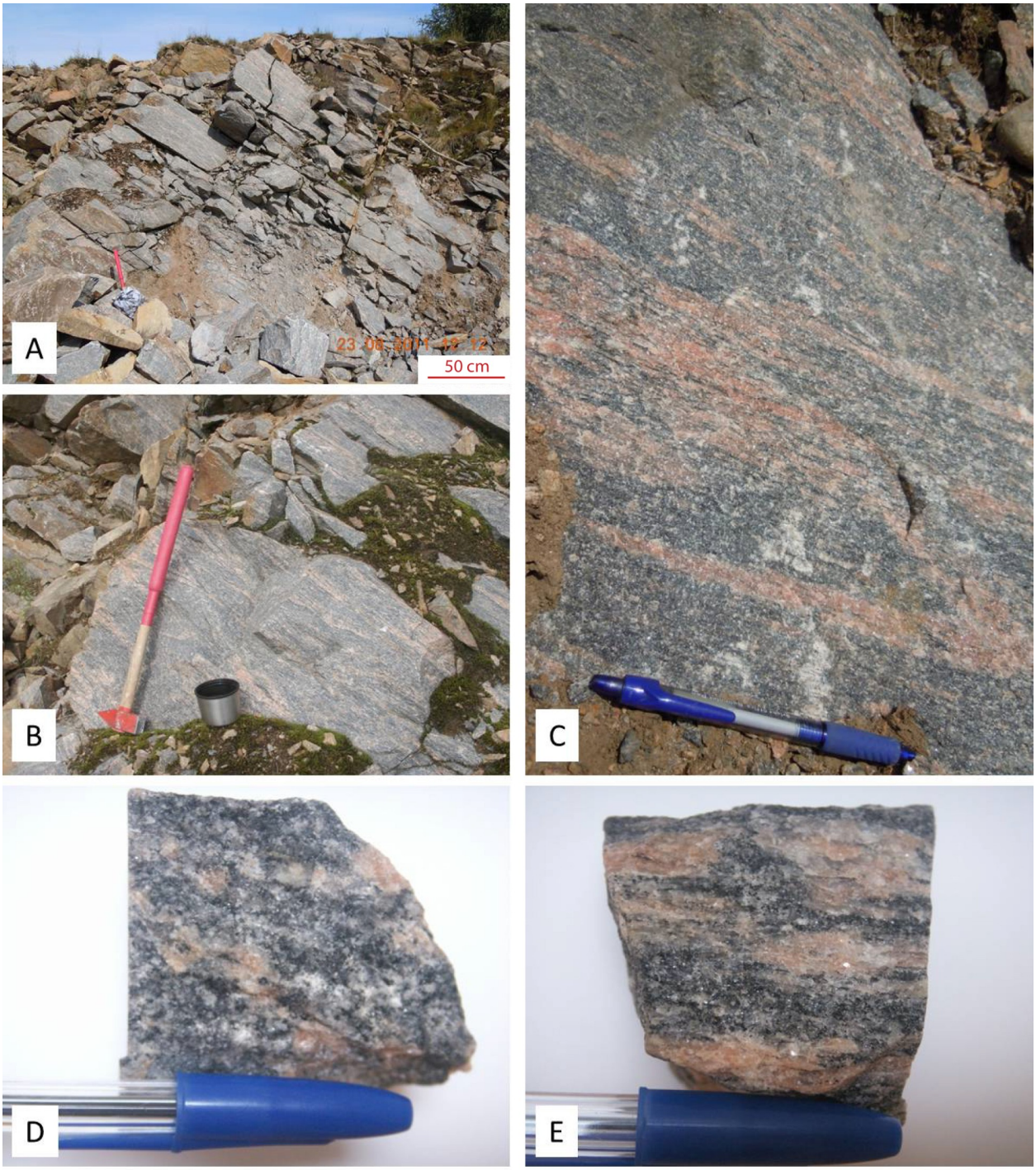

Fig. 7. Reddish grey gneiss in a quarry at Knobesholm in the Hallandia gneiss domain. A and B) Reddish grey gneiss. C) Pink aggregates and veins, K-feldspar dominated, are common. Leucosome veins are often isoclinally folded. D and E) A pronounced lineation is defined by elongated K-feldspar dominated aggregates and biotite.

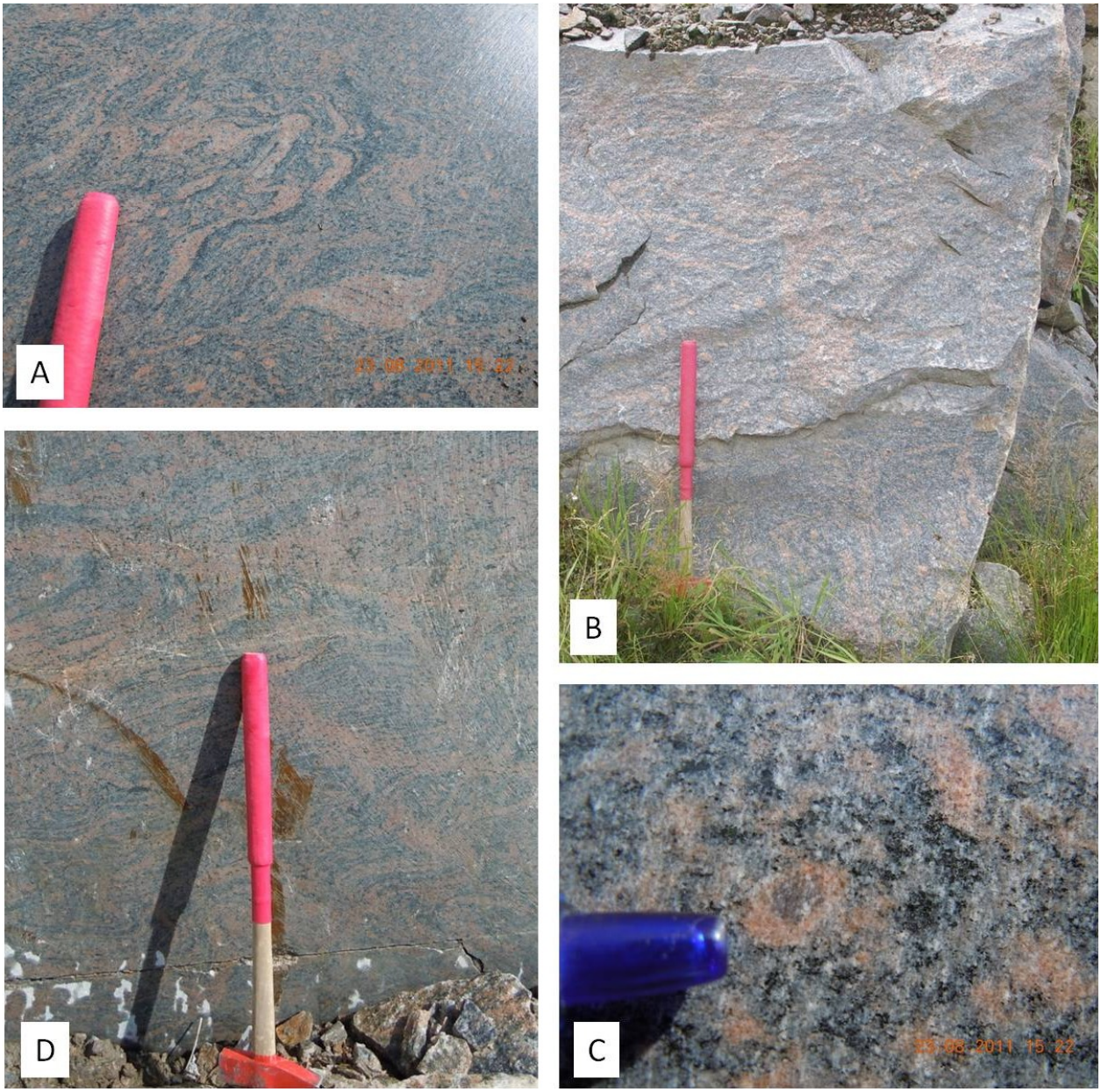

Fig. 8. Reddish grey gneiss at Hallandssten in the Hallandia gneiss domain. A) Pink veins are common, often folded and locally bordered by a dark selvage of biotite. B) The gneiss has two sets of folded pink veins. The scale, a red hammer, is 65 cm. C) Orthoclase occasionally occurs as cores in larger pink feldspar aggregates. D) Two sets of leucosome veins occur in the Hallan-

ded reddish grey gneiss dominate the quarry (Figs. 9A-C). The gneiss is yellowish brown to rusty colored on weathered surfaces. The grey groundmass is medium grained. A pronounced lineation is defined by stretched pink K-feldspar aggregates in folded veins; axial plane foliation is defined by oriented Fe-Mg mineral phases (hornblende, opaques and biotite; Fig. 9D) which make the veins appear slightly blurry. Reddish leucosome (dominated by K-feldspar) is common and occur as thin veins (≤ 5 cm thick) and layers (≤12 cm thick and several meter long). Both features are horizontally extensive, isoclinally folded (moderate to tightly folded; Fig. 9B) and are locally surrounded by a selvage of dark minerals (Fig. 9C). There are two sets of veins where one type cross cuts the other with an high angle, similar to the gneiss at Hallandssten. Yellowish brown fractures (251/68N, 248/68N) cut the gneiss. The gneiss contains disrupted metabasic bodies with various sizes (≤ 10 cm-1 m long and c. 50 cm thick). Various shapes of these fragments are present: round, folded bands and elongated boudinaged ones (Fig. 9C). A bleached zone usually surrounds the fragments and constitute of quartz, plagioclase and minor or no pink K-feldspar (Fig. 9C).

3.2.4 Abild (LL1107)

A temporary blasted rock wall was exposed at a construction site, however not very well exposed due to

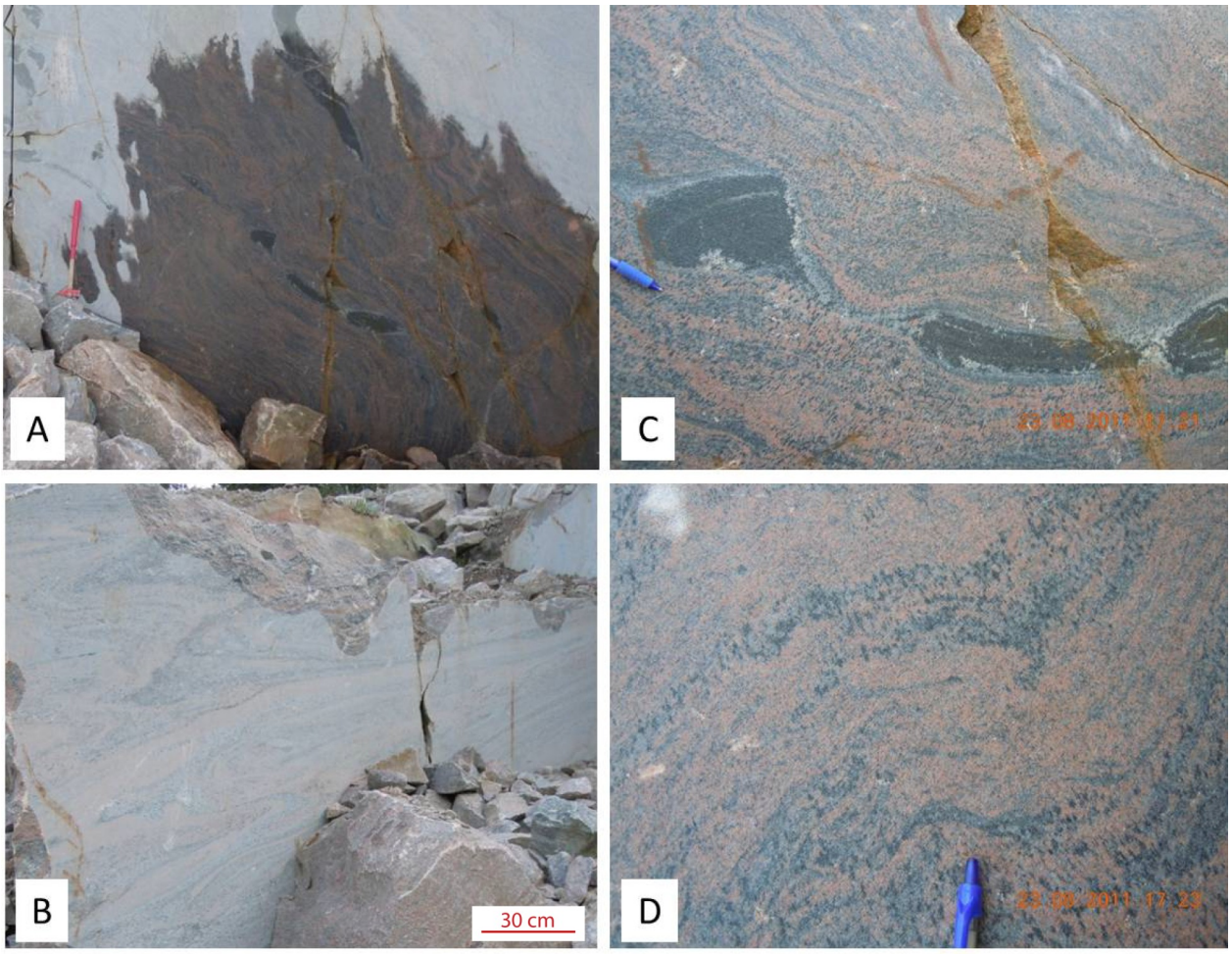

Fig. 9. Reddish grey gneiss in the Mokrik quarry, located in the Hallandia gneiss domain. A) A folded and reddish grey gneiss dominates the quarry. B) Horizontally extensive pink leucocratic veins (≤ 5 cm thick and several meters long) and layers (≤12 cm thick and several meters long) are common and often tightly folded. C) A dark mineral selvage often surrounds the pink veins. Disrupted metabasic bodies within the gneiss are surrounded by a bleached zone. D) Folded pink veins show a slightly blurry appearance, and have developed an axial planar foliation defined by dark mineral aggregates (hornblende, opaques and biotite).

soil cover and loose boulders. Uneven grained reddish grey gneiss dominates the outcrop (Fig. 10A). The grey groundmass is medium grained. Pink veins and augen are common and dominated by K-feldspar. Tightly folded veins occur locally (Fig. 10A). Augen are deformed with the least deformed aggregates are elongated by 2:1 (0.5-2 cm thick and 1-4cm long) and the most deformed form vein-like aggregates 2-5 cm thick (Fig. 10B). Elongated K-feldspar aggregates in the veins define a stretching lineation (Fig. 10C). Some hand specimens contain minor amounts of sulfides.

A lens of red, coarse grained, even grained gneiss occurs in the reddish grey gneiss. An east trending lineation is defined by quartz, biotite and K-feldspar aggregates. Dark larger crystals occur in the lens and are deformed to various degree. Some dark crystals, possibly allanite, have brown halos.

3.3 Skene migmatite gneiss domain

Migmatitic gneisses restricted to the Skene migmatite gneiss domain show stromatic banding (extensive and penetrative segregation of leucosome and mesosome). Commonly, no primary magmatic textures, e.g. relict augen, are present. One generation of unstrained leucosome, with sugary textured veins are present. Veins are often folded.

3.3.1 Fridhemsberg (LL1108)

A blasted and well exposed outcrop shows an undulating surface (wavelength ca. 10 m; Fig. 11A) of a folded stromatic migmatite gneiss which is pink-whitish grey in fresh cut and white to yellowish brown on weathered surfaces. The rock has a pronounced gneissic layering which is defined by metamorphic segregation (stromatic layering) of dark mesosome and light leucosome, which is dipping gently toward E (321º/15ºE).

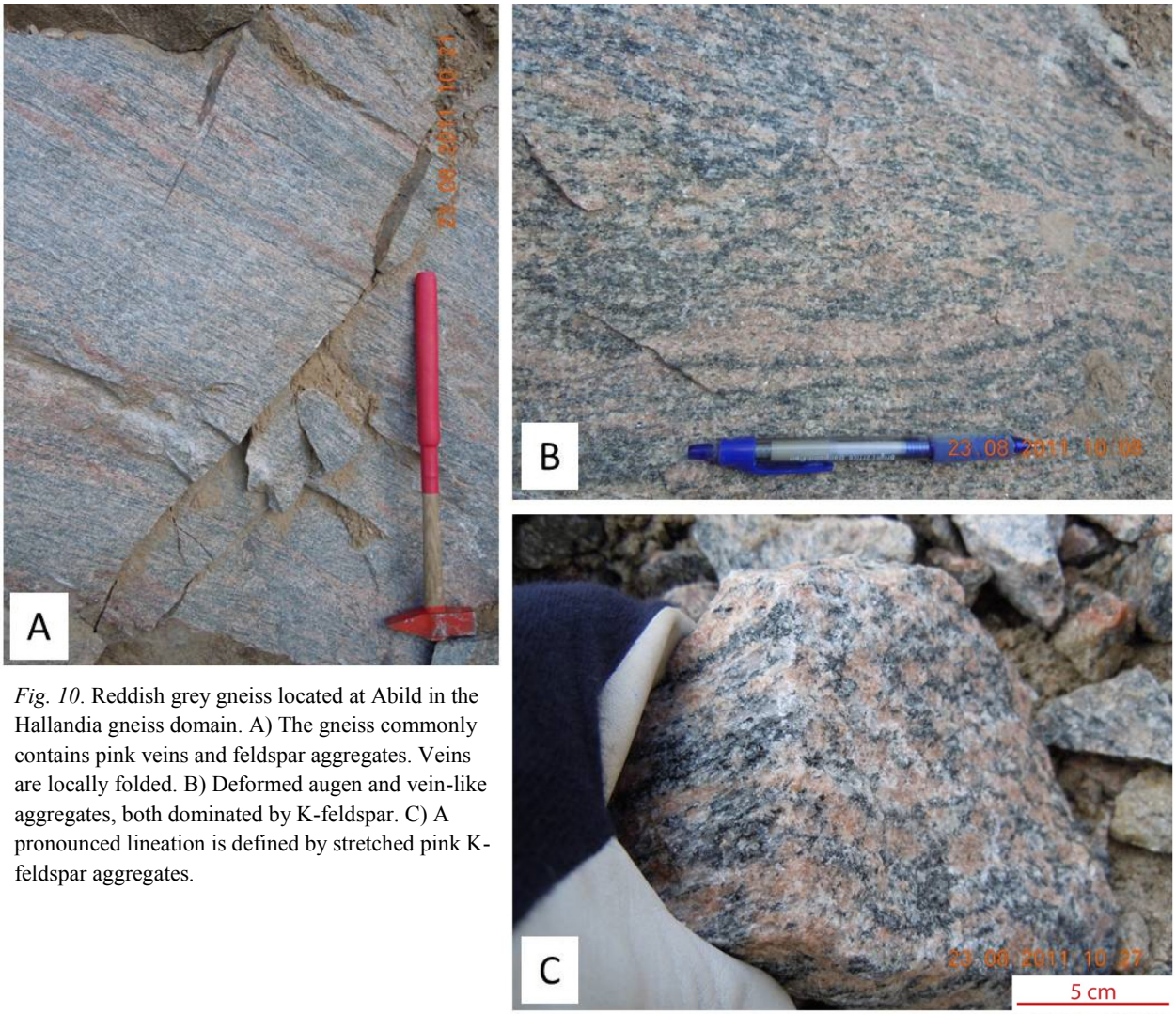

Fig. 10. Reddish grey gneiss located at Abild in the Hallandia gneiss domain. A) The gneiss commonly contains pink veins and feldspar aggregates. Veins are locally folded. B) Deformed augen and vein-like aggregates, both dominated by K-feldspar. C) A pronounced lineation is defined by stretched pink K-feldspar aggregates.

The fine grained mesosome lack pink K-feldspar but contains quartz, plagioclase and hornblende. A locally developed lineation is defined by pegmatitic aggregates and gently plunging to the E (90º/16ºE). There are three types of pink leucosome; thin (< 1 cm thick; Fig. 11B) evenly grained pink layers, 1-3 cm thick pink layers and > 3 cm thick coarse pegmatitic layers with hornblende aggregates (2-3 cm diameter; Figs. 11C and D). The first types of leucosome are surrounded by biotite-hornblende selvage (melanosome). A penetrative stromatic layering is defined by all three types of veins (Figs. 11C and D). The coarse grained leucosome consists of unstrained minerals and has a sugary texture (Fig. 11E). Dark fine grained lenses are elongated and parallel to the gneissic layering (Figs. 11B and C). Garnet can be spotted with the naked eye.

3.3.2 Töresjö (LL1109)

Stromatic migmatitic gneiss is exposed in a small road cut near Lake Töresjö (Fig. 12A). The rock is grey with uneven grained white-pinkish leucosome. The gneiss is yellowish brown to rusty colored on weathered surfaces. Gneissic layering is defined by metamorphic segregation of dark mesosome and light leucosome (Figs. 12 B and C). The grey groundmass (mesosome) is fine to medium grained. Coarse grained white-pinkish veins (dominated by K-feldspar) are common and horizontally continuous over distances of meters (some are ≤ 3 cm wide while others ≥ 3 cm wide) and define a stromatic layering (Figs. 12 B and C). The leucosome show variation in thickness; locally coarse pegmatitic bands are boudinaged showing pinch and swell structures. The coarse grained leucosome consists of unstrained minerals and has a sugary texture (Figs. 12 D and E). Veins are surrounded by dark mineral selvage (melanosome; Fig. 12 B).

3.3.3 Toppeberg (LL1110)

A discretely veined granitic gneiss dominates the outcrop (Fig. 13A). In fresh cut the uneven grained gneiss is pinkish grey (Figs.13B and C) and yellowish brown to rusty colored on weathered surfaces. The grey groundmass is fine to medium grained. Elongated augen, dominated by pink K-feldspar aggregates, (0.5-3 cm long and 1-2 cm thick) define a weak lineation (60º/32ºNE; Figs. 13B and C). Unstrained pinkish veins (≤ 10 cm long and 1-2 cm thick) occur locally and

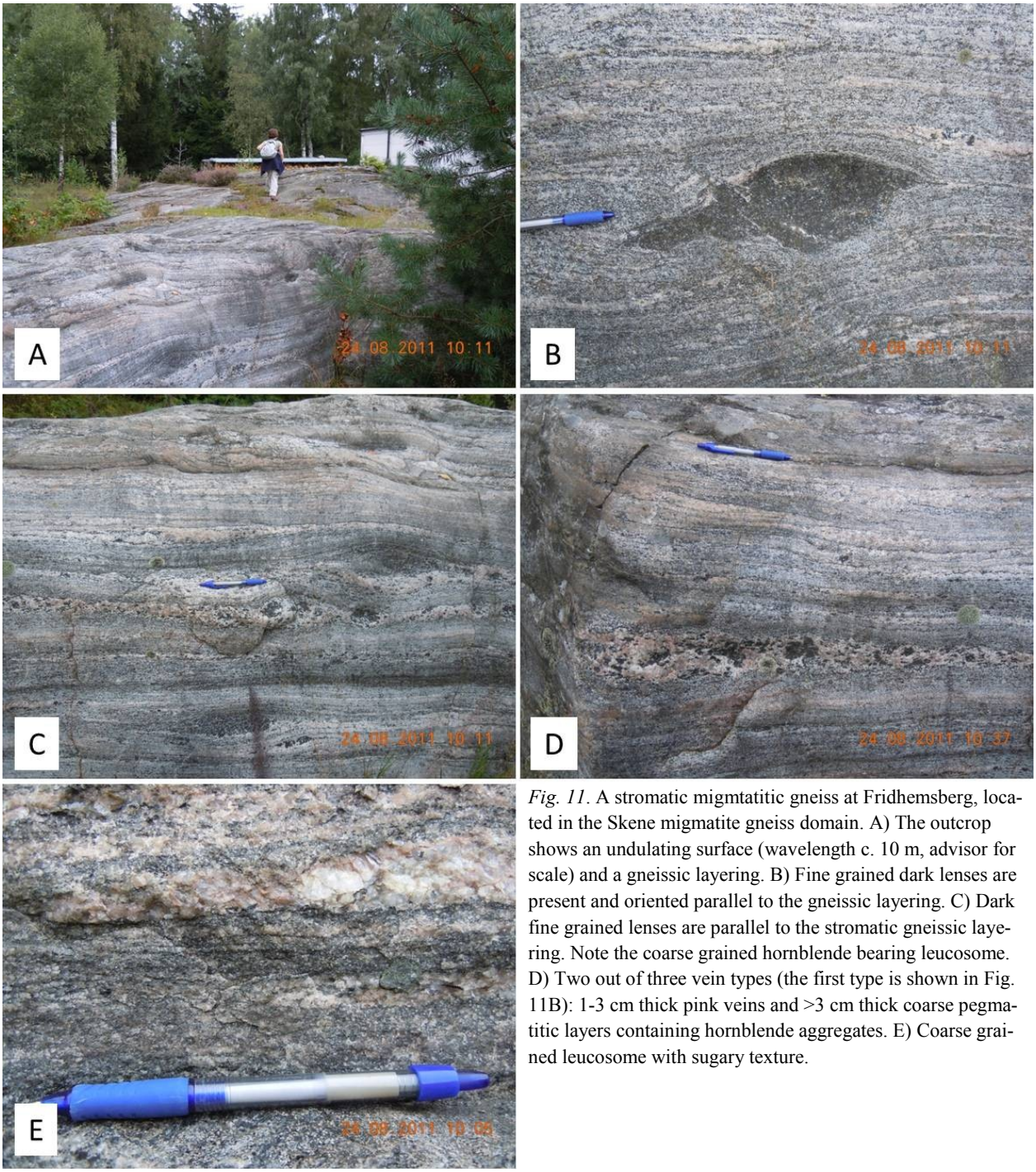

Fig. 11. A stromatic migmtatitic gneiss at Fridhemsberg, located in the Skene migmatite gneiss domain. A) The outcrop shows an undulating surface (wavelength c. 10 m, advisor for scale) and a gneissic layering. B) Fine grained dark lenses are present and oriented parallel to the gneissic layering. C) Dark fine grained lenses are parallel to the stromatic gneissic layering. Note the coarse grained hornblende bearing leucosome. D) Two out of three vein types (the first type is shown in Fig. 11B): 1-3 cm thick pink veins and >3 cm thick coarse pegmatitic layers containing hornblende aggregates. E) Coarse grained leucosome with sugary texture.

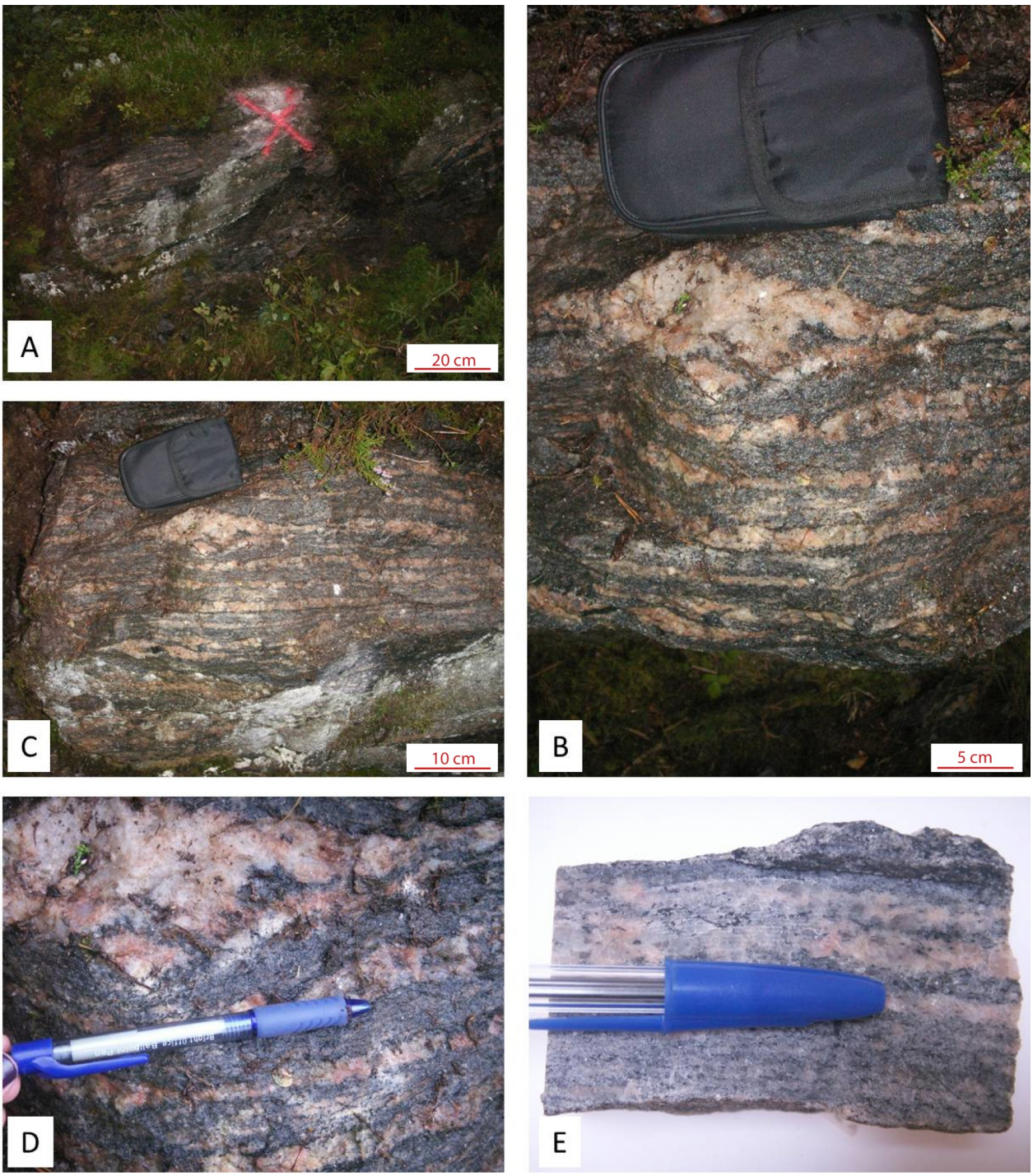

Fig. 12. Stromatic migmatitic gneiss located at Töresjö in the Skene migmatite gneiss domain. A) An uneven grained grey migmatitic gneiss. B) Veins are surrounded by a dark mineral selvage and define a stromatic layering. A gneissic layering is also present. C) The migmatitic gneiss show metamorphic segregation of light leucosome and dark mesosome defining a gneissic layering. D and E) Unstrained leucosome with minerals showing sugary texture.

contain minerals with sugary texture (Figs. 13D and E). A weak foliation (353º/32ºE), present in the groundmass, is defined by dark minerals and occur parallel to the veins.

Features that make the appearance of this gneiss atypical, for rocks occurring within the Skene migmatite gneiss domain, are: the presence of lineation, the presence of remnants of a magmatic texture (such as augen and a relict uneven grained texture), the absence of penetrative metamorphic segregation of felsic leucosome and dark mesosome and the absence of a pronounced stromatic layering.

3.3.4 Vräk (LL1111)

The western side of the blasted road cut is dominated by an uneven grained grey gneiss (Fig. 14A-C). Weathered surfaces show rusty brown to grey color. The grey groundmass is fine to medium grained. Stretched aggregates, dominated by bright pink K-feldspar, define a distinct lineation (Figs. 14B and C). Red fractures occur perpendicular to the weak foliation which is defined by dark minerals.

This gneiss does not show typical appearance for a rock located in the Skene migmatite gneiss domain due to the presence of a distinct stretching lineation, the absence of veins, the absence of penetrative meta-

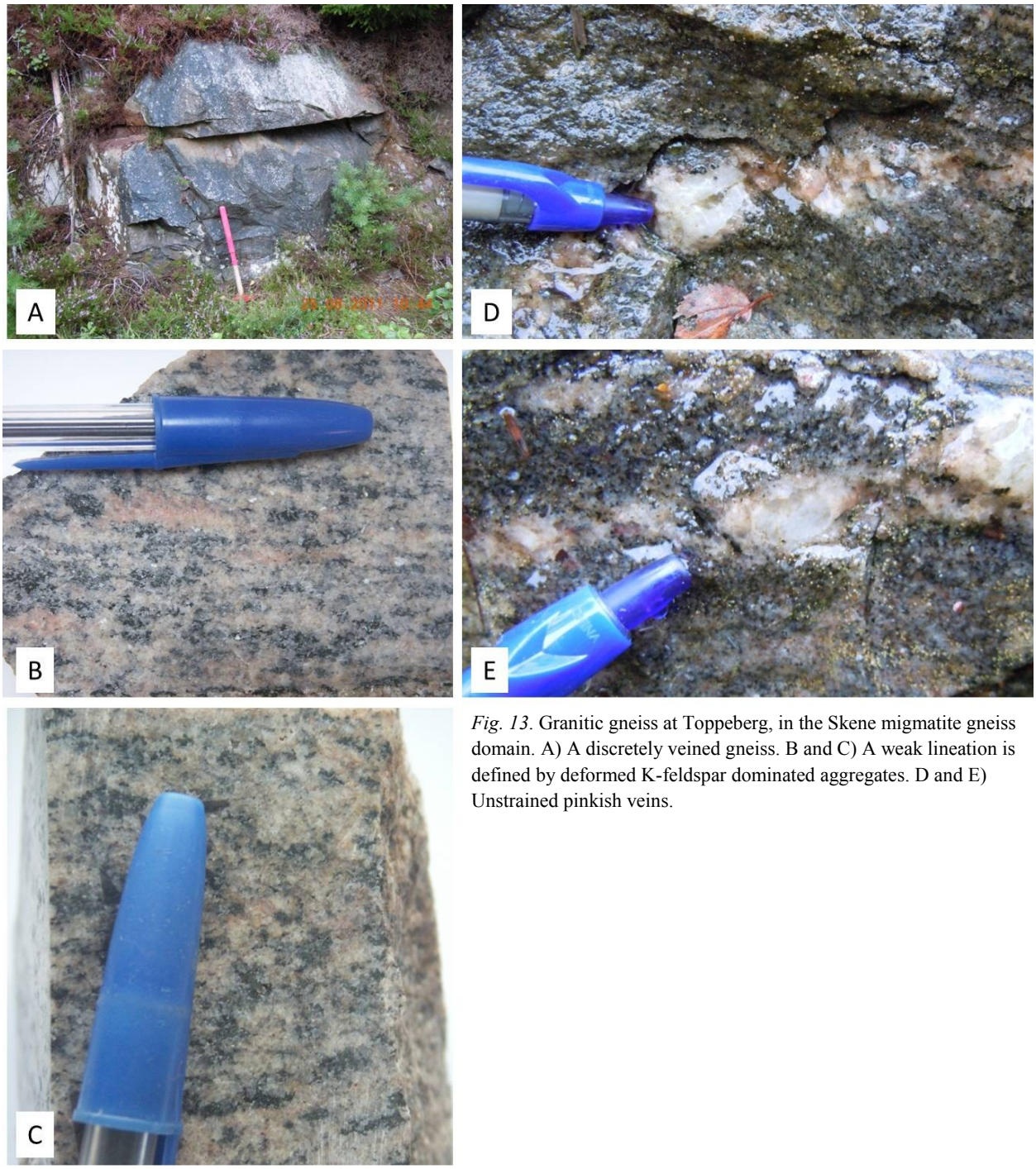

Fig. 13. Granitic gneiss at Toppeberg, in the Skene migmatite gneiss domain. A) A discretely veined gneiss. B and C) A weak lineation is defined by deformed K-feldspar dominated aggregates. D and E) Unstrained pinkish veins.

morphic segregation of felsic leucosome and dark mesosome and the absence of a stromatic layering.

3.4 Svarten gneiss domain

Gneisses in this domain generally have a pronounced stretching lineation which is defined by deformed feldspar and quartz aggregates. The rocks are often devoid of migmatitic strucutres and relict magmatic texture is sometimes present.

3.4.1 Köinge (LL1112)

Uneven grained pinkish grey gneiss composes the blasted outcrop, located in the vicinity of a road in a farming area (Fig. 15A and B). The gneiss is pink-whitish grey to rusty brown on weathered surfaces. The grey groundmass is fine grained and veins are absent. Elongated pink aggregates (1-2 cm long), dominated by K-feldspar, define a weak stretching lineation (Figs. 15C and D). The gneissosity (38/16E) is defined by dark minerals cross cut by red fractures (45-53 E; Figs. 15E and F).

Fig. 14. Grey gneiss at Vräk, in the Skene migmatite gneiss domain, with advisors Jenny Andersson and Mattias Göransson from SGU in action. A) Grey gneiss dominates the western part of the outcrop. B and C) A distinct lineation is defined by stretched aggregates, dominated by bright pink K -feldspar.

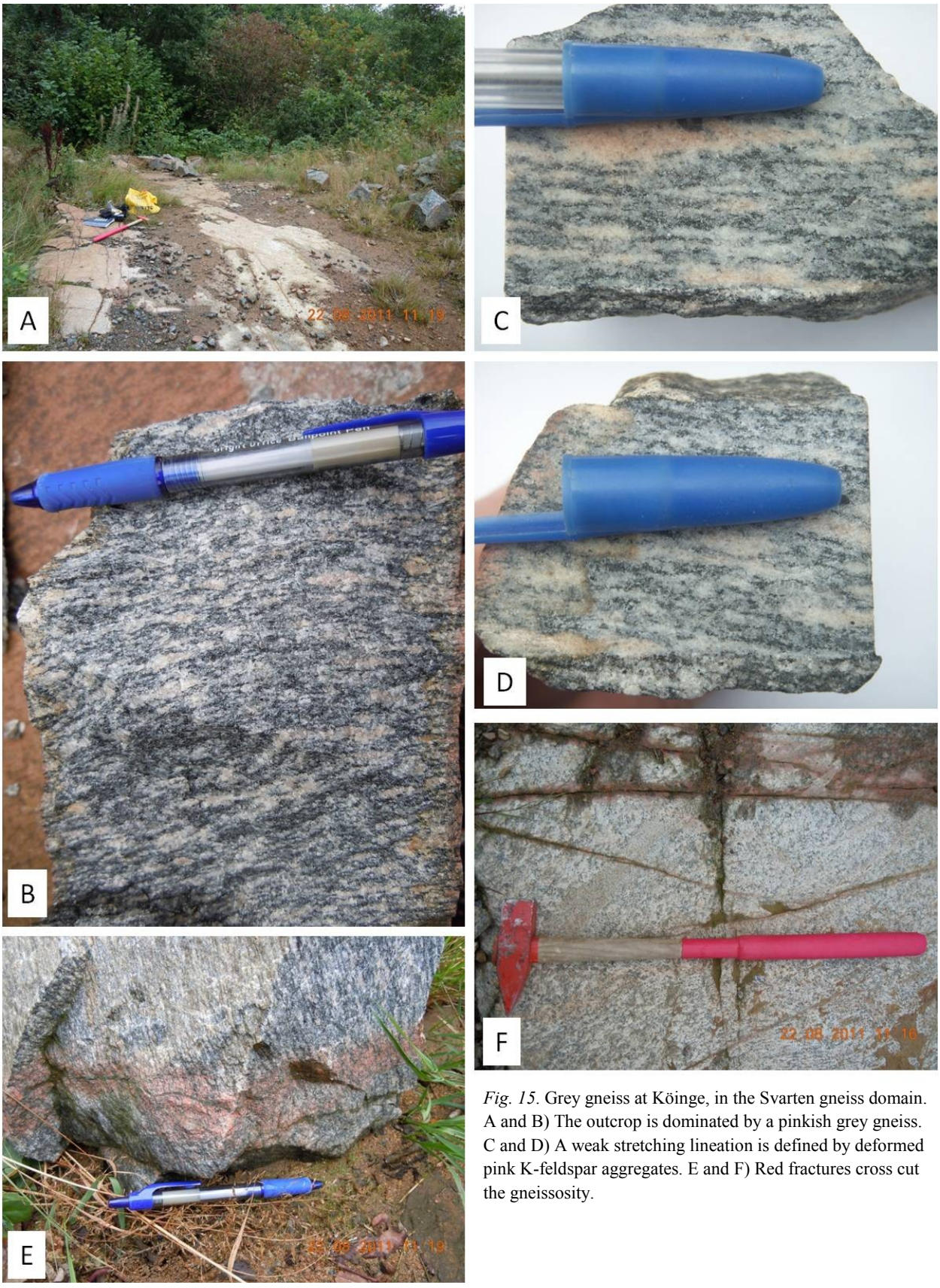

Fig. 15. Grey gneiss at Köinge, in the Svarten gneiss domain. A and B) The outcrop is dominated by a pinkish grey gneiss. C and D) A weak stretching lineation is defined by deformed pink K-feldspar aggregates. E and F) Red fractures cross cut the gneissosity.

4. Thin section descriptions

Two polished thin sections were made for each sample. Cuts were made parallel and perpendicular to the lineation (if present) and perpendicular to the foliation (Table 1).

Thin section descriptions from all sample localities are summarized in Appendix 3.

4.1 Varberg granulite gneiss domain

Characteristic for the gneisses in the Varberg granulite gneiss domain is the presence of antiperthitic plagioclase and the low content of biotite. Biotite is red-brown and hornblende brown-green. Titanite and microcline is absent. Orthoclase is present and in places occurs as augen.

4.1.1 Dagsås (LL1101 F1 and F2)

The orthogneiss at Dagsås is made up of feldspars, quartz, hornblende, pyroxene, garnet and biotite. Accessory minerals are opaque minerals, apatite and zircon.

The two thin sections from Dagsås show the same microtextures and are uneven grained. The grain size varies from 0.05 mm to 2.75 mm. The foliation (Figs. 16A and B) is defined by thin bands and lenses of dark minerals (hornblende, clinopyroxene, orthopyroxene opaque minerals, almandine rich garnet, and biotite) alternating with feldspar rich domains containing quartz ribbons (0.25-1mm wide and up to 4.45 mm long; Fig. 16A) and quartz lenses (Fig. 16A). The quartz ribbons are made up of relatively unstrained grains (lower left in Fig. 16A). Feldspars are antiperthitic, granoblastic to irregular and often have complex grain boundaries. Albite twins occur occasionally and tartan twinning is absent. Myrmekitization is modest. A large single plagioclase megacryst (0.5-1mm wide and 1.75 mm long) follows the foliation and is occasionally antiperthitic. Biotite is red-brown and hornblende brown-green. Biotite content is very low and titanite is absent. Orthopyroxene shows a rus-

Table 1. Locality name, sample ID, coordinates (SWEREF) and the orientation of the thin sections in relation to the foliation or lineation in the rock.

			Coordinates	
Locality name	Sample ID	Orientation	Northing	Easting
Dagsås	LL1101 F1	Perpendicular to the foliation	6329200	350077
	LL1101 F2	Perpendicular to the foliation		
Stavsjö	LL1102 F1	Perpendicular to the foliation	6313111	347230
	LL1102 F2	Perpendicular to the foliation		
Ljungby	LL1103 F1	Perpendicular to the foliation	6319627	352432
	LL1103 F2	Perpendicular to the foliation		
Knobesholm	LL1104 TL	Perpendicular to the lineation	6308420	363936
	LL1104 PL	Parallel to the lineation		
Hallandssten	LL1105 F1	Perpendicular to the foliation	6299914	357081
	LL1105 F2	Perpendicular to the foliation		
Mokrik	LL1106 F1	Perpendicular to the foliation	6299007	357503
	LL1106 F2	Perpendicular to the foliation		
Abild	LL1107 TL	Perpendicular to the lineation	6311798	361020
	LL1107 PL	Parallel to the lineation		
Fridhemsberg	LL1108 F1	Perpendicular to the foliation	6338122	363789
	LL1108 F2	Perpendicular to the foliation		
Töresjö	LL1109 F1	Perpendicular to the foliation	6344875	361194
	LL1109 F2	Perpendicular to the foliation		
Toppeberg	LL1110 F1	Perpendicular to the foliation	6340939	364276
	LL1110 F2	Perpendicular to the foliation		
Vräk	LL1111 TL	Perpendicular to the lineation	6338922	364958
	LL1111 PL	Parallel to the lineation		
Köinge	LL1112 TL	Perpendicular to the lineation	6325958	357819
	LL1112 PL	Parallel to the lineation		

ty color and looks porous and weathered (Fig. 16B). The opaque minerals are iron oxides (titanomagnetite and lamella of hematite and magnetite in the same grains) and iron sulfide (pyrite).

4.1.2 Stavsjö (LL1102 F1 and F2)

Feldspars, quartz, hornblende and biotite are the major constituents of the gneiss at Stavsjö. Accessory minerals are opaque minerals, apatite and zircon.

The two thin sections show similar microtextures and are uneven grained. The grain size varies from 0.1 mm to 7.75 mm. The foliation (Figs. 17A and B) is defined by bands and lenses of dark minerals (hornblende, biotite and opaque minerals) alternating with feldspar rich domains containing few distinct quartz ribbons (mm-wide and up to 10 mm long; Fig.17A) and felsic deformation bands (mm-wide and up to 4.43 mm long). Quartz ribbons are composed of relatively unstrained grains (Fig. 17A). In thin section LL1102 F1 the foliation is folded. Feldspars are granoblastic to irregular, show straight grain boundaries and antiperthite is sparse. Microcline is common and albite twins occur occasionally. Some feldspar grains are moderately to severely sericitized. Dark minerals are often randomly oriented (Fig. 17B). Biotite is dark-brown and hornblende blue-green. Biotite occurs as sub- to euhedral individual grains and occasionally as aggregates. Few elongated opaque minerals have a corona of titanite.

The amount and presence of microcline, titanite and biotite but also the color of biotite and hornblende (dark-brown and blue-green respectively) is not typical for rocks located in the Varberg granulite gneiss domain.

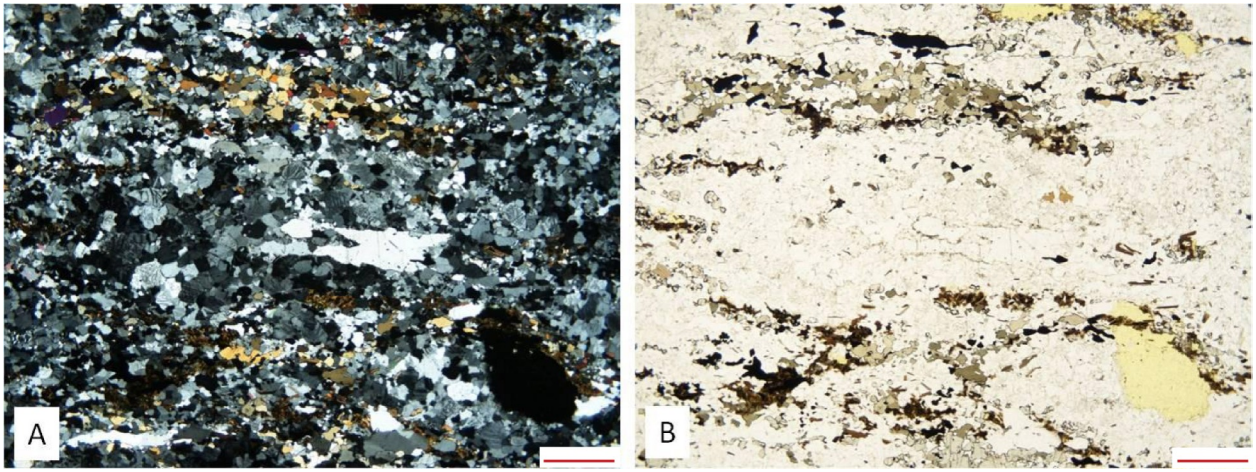

Fig. 16. Photomicrographs of thin section LL1101 F1 of a grey orthogneiss at Dagsås located in the Varberg granulite gneiss domain. The red scale bar = 1 mm. A) Crossed polarized light; The foliation is defined by dark bands and lenses alternating with felsic domains. Quartz ribbons, lower left, (composed of relatively unstrained grains) and quartz lenses are present in the felsic domains. B) Plane polarized light; Bands and lenses of dark minerals alternating with felsic domains define a foliation. Orthopyroxene shows a rusty color and looks porous and weathered.

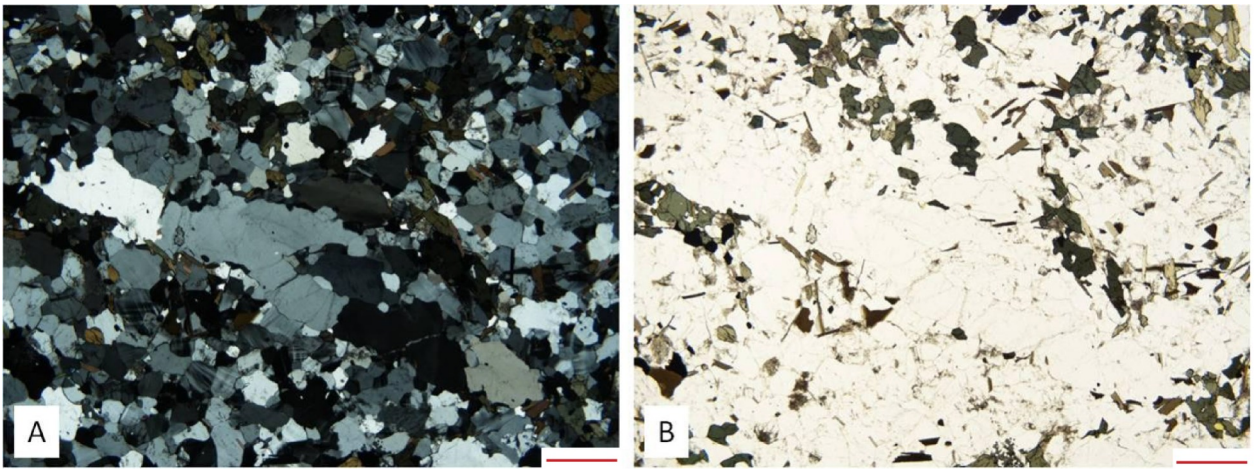

Fig. 17. Photomicrographs of thin section LL1102 F2 of a reddish grey gneiss at Stavsjö located in the Varberg granulite gneiss domain. The red scale bar = 1 mm. A) Crossed polarized light; The foliation is defined by bands and lenses of dark minerals alternating with feldspar rich domains containing distinct quartz ribbons (made up of relatively unstrained grains). B) Plane polarized light; Dark minerals are randomly oriented and they occur as bands and lenses which alternate with feldspar rich domains and define a foliation.

4.1.3 Ljungby (LL1103 F1 and F2)

Quartz, feldspars, hornblende, garnet, clinopyroxene and biotite are the major constituents of the gneiss at Ljungby. Accessory minerals are opaque minerals, apatite and zircon.

Both thin sections of this sample show similar microtextures and are uneven grained. The grain size varies between 0.075 mm and 3.2 mm. The strong foliation (Figs. 18A-C) is defined by thin bands of dark minerals (hornblende, opaque minerals, garnet, clinopyroxene and biotite) alternating with feldspar rich domains containing distinct quartz ribbons (often mm-wide and up to 4.1 mm long; Figs. 18A and C) and elongated quartz grains (Fig. 18A). Some quartz ribbons consist of relatively unstrained grains. Feldspars are antiperthitic, moderately sericitized and show simple grain boundaries. Albite twins occur occasionally and tartan twinning is absent. Alkali feldspar occurs occasionally as granoblastic polycrystalline domains (centre of Fig. 18C) and show rusty colored alteration. A few orthoclase augen are present with exsolution lamella (Fig. 18D). Clinopyroxene shows severe rusty colored alteration. Biotite is red-brown and hornblende brown-green. Biotite grains, some are chloritized, occur only sparsely and are parallel to the foliation. Titanite is absent.

4.2 Hallandia gneiss domain

Gneisses in the Hallandia gneiss domain have antiperthitic plagioclase. Biotite is red-brown and hornblende is brown-green. Clinopyroxene and microcline are rare and titanite is absent. Orthoclase was found occasionally.

4.2.1 Knobesholm (LL1104 TL and PL)

The gneiss at Knobesholm consists of quartz, feldspars, hornblende and biotite. Accessory minerals are opaque minerals, apatite, zircon and allanite.

The rock is uneven grained and the different

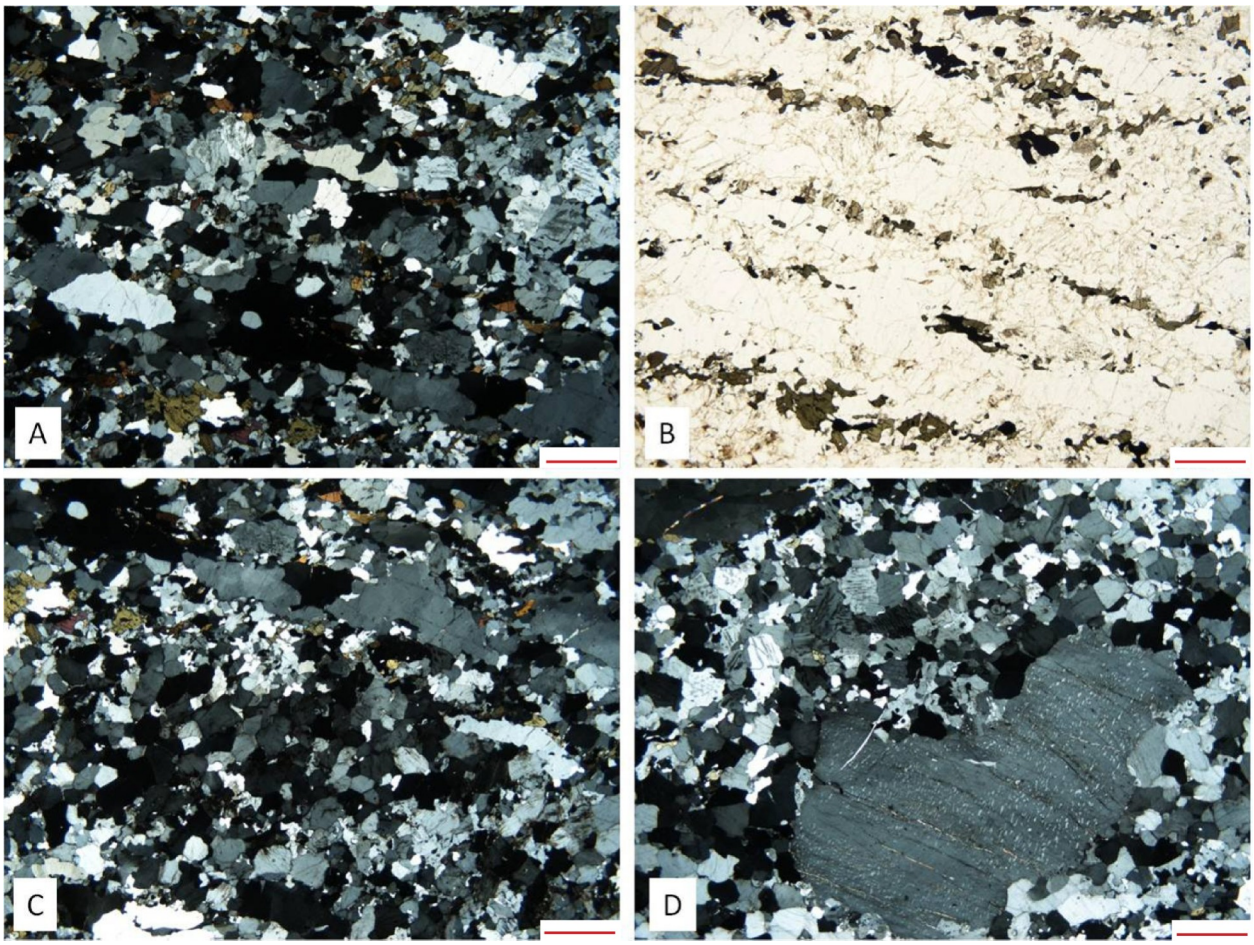

Fig. 18. Photomicrographs of thin section LL1103 F1 and F2 of a reddish grey gneiss at Ljungby located in the Varberg granulite gneiss domain. The red scale bar = 1 mm. A) Crossed polarized picture of thin section LL1103 F2; Bands of dark minerals alternating with feldspar rich domains containing quartz ribbons and elongated quartz grains define a strong foliation. B) Plane polarized picture of thin section LL1103 F2; Feldspar rich domains alternate with bands of dark minerals define a foliation. C) Crossed polarized picture of thin section LL1103 F2; Quartz ribbon made up of relatively unstrained grains, upper part of the image, and granoblastic alkali feldspar domain in the centre of the image. D) Crossed polarized picture of thin section LL1103 F1; Large orthoclase augen with exsolution lamella.

sections (parallel and perpendicular to the lineation) show variation in microtextures. The grain size varies between 0.2 mm and 4.7 mm. The foliation (Figs. 19A-D) is defined by elongated aggregates and bands of dark minerals (hornblende, biotite and opaque minerals) alternating with feldspar rich domains containing distinct straight quartz ribbons (thin section LL1104 PL; 0.23-1.38 mm wide and up to 20 mm long; Fig.19A), more diffuse quartz ribbons (thin section LL1104 TL; 0.3-0.58 mm wide and up to 3.45 mm long) and elongated felsic grains (thin section LL1104 TL; 0.37-1 mm wide and up to 4.7 mm long; Fig. 19C). Quartz ribbons define a pronounced lineation and consist of large, relatively unstrained grains (Fig. 19A). Elongated quartz grains are parallel to the foliation (Fig. 19C) and is folded in the thin section cut perpendicular to the lineation (LL1104 TL; Fig. 19D). Feldspars are occasionally antiperthitic, often irregular, moderately to severely sericitized and show smooth grain boundaries. Alkali feldspar occurs as granoblastic monomineralic domains. A few small grains show tartan twinning. Individual grains of dark minerals are randomly oriented with one exception: biotite (both individual grains and aggregates, LL1104 PL) is parallel to the foliation and lineation. Biotite is red-brown and hornblende brown-green. Titanite and pyroxene is absent.

4.2.2 Hallandssten (LL1105 F1 and F2)

The major constituents of the gneiss at Hallandssten are feldspars, quartz, hornblende and biotite. Accessory minerals are opaque minerals, apatite, zircon and allanite.

The rock is uneven grained and the two thin sections show a slight variation in microtextures. The grain size varies between 0.05 mm to 6.05 mm. The foliation (Figs. 20A-D) is defined by lenses and thin

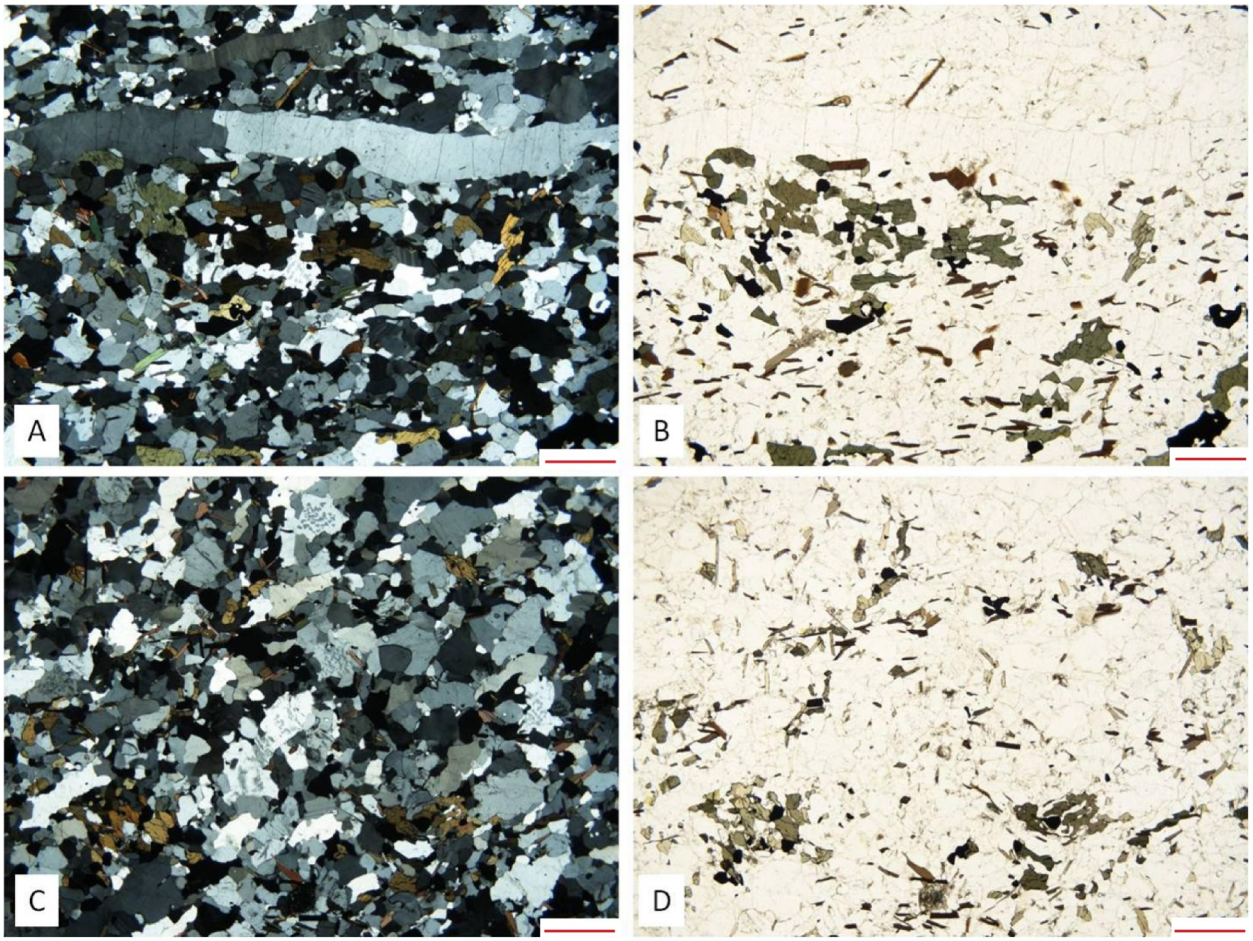

Fig. 19. Photomicrographs of thin section LL1104 PL and TL of a reddish grey gneiss at Knobesholm located in the Hallandia gneiss domain. The red scale bar = 1 mm. A) Crossed polarized picture of thin section parallel to the lineation; Feldspar rich domains alternating with bands and elongated aggregates of dark minerals define the foliation. Straight and large quartz ribbons define a lineation. B) Plane polarized picture of thin section LL1104 PL; Quartz ribbons define a pronounced lineation while alternation of feldspar rich domains with aggregates and bands of dark minerals define a foliation. C) Crossed polarized picture of thin section perpendicular to the lineation; Elongated quartz grains occur in the feldspar rich domains. D) Plane polarized picture of thin section LL1104 TL; The foliation, defined by bands and lenses of dark minerals alternating with feldspar rich domains, is folded.

bands of dark minerals (hornblende, biotite and opaque minerals) alternating with feldspar rich domains containing distinct straight quartz ribbons (in thin section LL1105 F1; 0.5-1 mm wide and up to 7.3 mm long; Fig. 20C) and elongated quartz grains (often 0.25-1 mm wide and up to 6.05 mm long; Fig. 20D). The lineation is defined by quartz ribbons which are made up of relatively unstrained grains (Fig. 20C). Feldspars are irregular, occasionally antiperthitic and have smooth grain boundaries. Albite twins are well developed and feldspars are occasionally moderately to severely sericitized. Alkali feldspar occurs as granoblastic domains (Fig. 20C) and show rusty colored alteration. Tartan twinning, pyroxene and titanite are absent. Both thin sections show that individual grains and aggregates of dark minerals generally are oriented parallel the foliation (Fig. 20B). Biotite is red-brown and hornblende is brown-green. A few biotite grains are partly chloritized.

4.2.3 Mokrik (LL1106 F1 and F2)

Feldspars, quartz, hornblende, biotite, clinopyroxene and garnet are the major constituents of the Hallandia gneiss at Mokrik. Accessory minerals are opaque minerals, apatite, zircon and allanite.

The rock is uneven grained and the two thin sections show similar microtextures. The grain size varies between 0.05 mm and 7.2 mm. The foliation is defined by bands of dark minerals (hornblende, biotite, opaque minerals, clinopyroxene and garnet) alternating with feldspar rich domains containing few distinct quartz ribbons (0.5-1 mm wide and up to 5.75 mm long), quartz lenses (0.5-1 mm wide and up to 5.75 mm long) and elongated quartz grains (up to 7.2 mm long; Figs. 21A and B). Quartz ribbons consist of relatively unstrained grains and the ones that are distinct and straight define a lineation. Feldspars are irregular, occasionally antiperthitic and show smooth grain

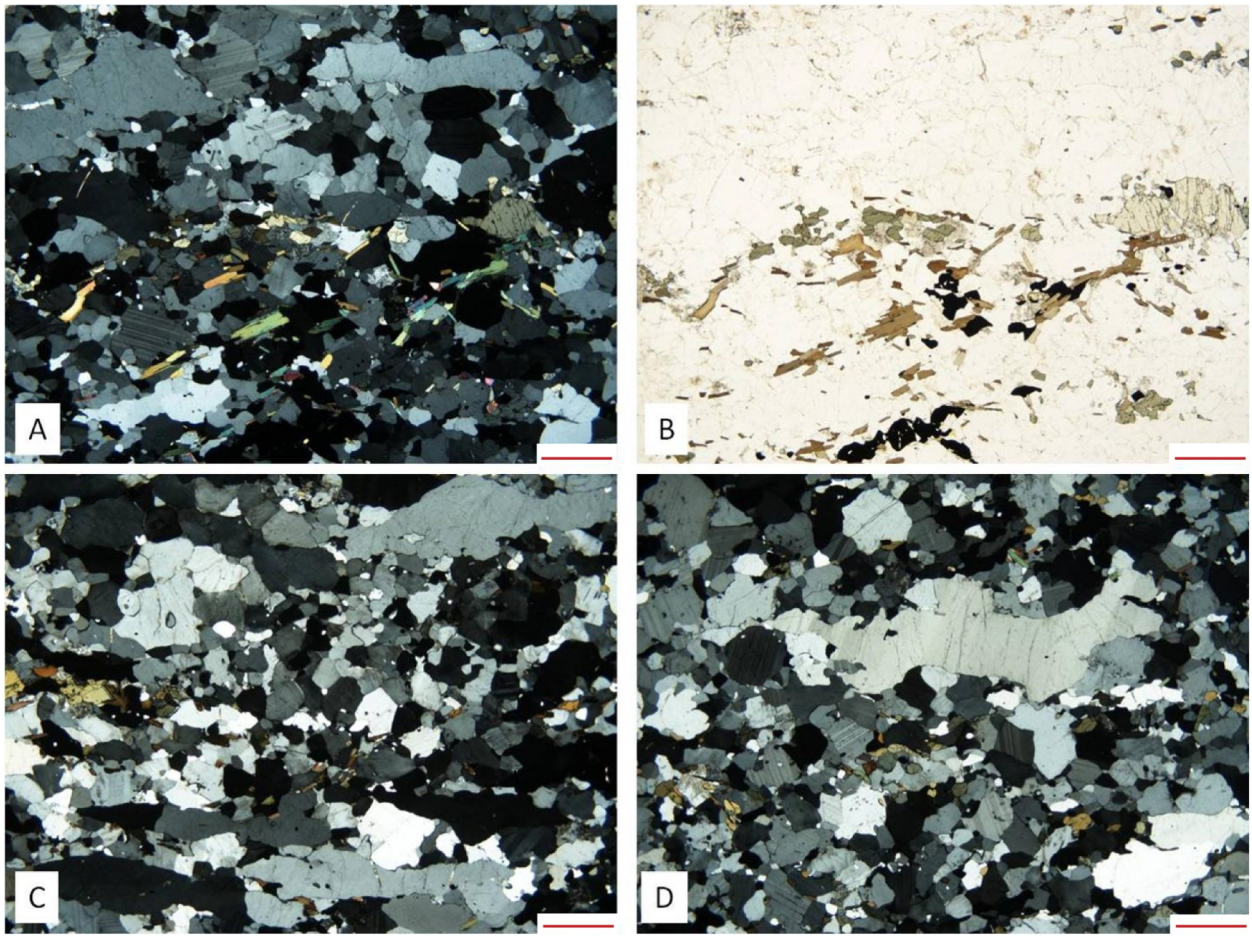

Fig. 20. Photomicrographs of thin section LL1105 F1 and F2 of a reddish grey gneiss at Hallandssten located in the Hallandia gneiss domain. The red scale bar = 1 mm. A) Crossed polarized picture of thin section LL1105 F1; Alternation of feldspar rich domains with lenses and bands of dark minerals define a gneissic foliation. B) Plane polarized picture of thin section LL1105 F1; Lenses and thin bands of dark minerals alternating with feldspar rich domains define a foliation. Dark mineral (individual grains and aggregates) are parallel to the foliation. C) Crossed polarized picture of thin section LL1105 F1; Straight quartz ribbons, lower part of the picture, define a lineation and granoblastic alkali feldspar are present. D) Crossed polarized picture of thin section LL1105 F2; Elongated quartz grains are parallel to the foliation.

boundaries. Albite twins are well developed and some feldspars are occasionally moderately to severely sericitized. Alkali feldspar occurs as granoblastic domains (Fig. 21A) and show rusty colored alteration. Individual biotite grains (and small aggregates), hornblende and opaque minerals generally follow the foliation (Fig. 21B) which is folded in thin section LL1106 F2. Biotite is red-brown and hornblende is brown-green. A few biotite grains are partly chloritized. Opaque minerals are iron oxides (titanomagnetite, lamella of hematite and magnetite in the same grains) and iron sulfide (pyrite). Tartan twinning and titanite are absent while clinopyroxene occurs occasionally and show rusty colored alteration.

4.2.4 Abild (LL1107 TL and PL)

The gneiss at Abild is mainly made up of quartz, feldspars, biotite and hornblende. Accessory minerals are opaque minerals, allanite, apatite and zircon.

The rock is uneven grained and the thin sections show slight variation in microtextures. The grain size varies between 0.05 mm and 16.45 mm. The lineation is defined by oriented individual biotite grains and aggregates (Figs. 22A-D). Dark minerals (biotite, hornblende and opaque minerals) form domains which alternate with the feldspar rich domains containing distinct quartz ribbons (occur in the thin section cut parallel to the lineation; 0.375- 1.5 wide and up to 21.05 mm long; Fig. 22A), a few felsic deformation bands of quartz and feldspars (0.33-1.38 mm wide and 3.88-4.5 mm long) and elongated felsic grains (0.35-1.05 mm wide and 1.43-3.23 mm long; see Fig. 22C). Quartz ribbons are made up of relatively unstrained grains (Fig.22A) and define a pronounced lineation. Feldspars are occasionally antiperthitic, irregular, show smooth grain boundaries and are moderate to severely sericitized. Alkali feldspar occurs occasionally as granoblastic domains (Fig. 22A). Tartan twinning is common and some microcline grains have an orthoclase core. Dark minerals (except biotite) are generally randomly oriented in the section cut perpendicular to the lineation (Figs. 22 C and D) and parallel to the lineation in the thin section cut parallel to the lineation (Figs. 22A and B). Biotite is red-brown and hornblende is mostly blue-green. Pyroxene and titanite are absent.

The blue-green color of hornblende and the abundance of tartan twinning are atypical for rocks in the Hallandia gneiss domain.

4.3 Skene migmatite gneiss domain

Gneisses in this area are composed of microcline, plagioclase, quartz, biotite, hornblende and titanite. Biotite is dark-brown and hornblende is blue-green. Biotite commonly occurs as aggregates, bands and individual grains. Microcline twinning is common and well developed. Orthoclase occurs only sparsely as cores in some microcline augen. Garnet and antiperthite is rare. The high grade banding and components (meso-, leuco- and melanosome) of the migmatites are difficult to observe at a microscopic scale and is much better examined and described in the field.

4.3.1 Fridhemsberg (LL1108 F1 and F2)

Feldspars, quartz, hornblende and biotite are the major components of the migmatitic gneiss at Fridhemsberg. Accessory minerals are opaque minerals, apatite, zircon and allanite.

The rock is uneven grained and the two thin sections show the same microtextures. The grain size varies between 0.2 mm to 3.25 mm. The foliation (Figs. 23A-D) is defined by bands of dark minerals (biotite, hornblende and opaque minerals) alternating with felsic domains containing elongated feldspar and quartz grains (0.6-1 mm wide and up to 3.25 mm long;

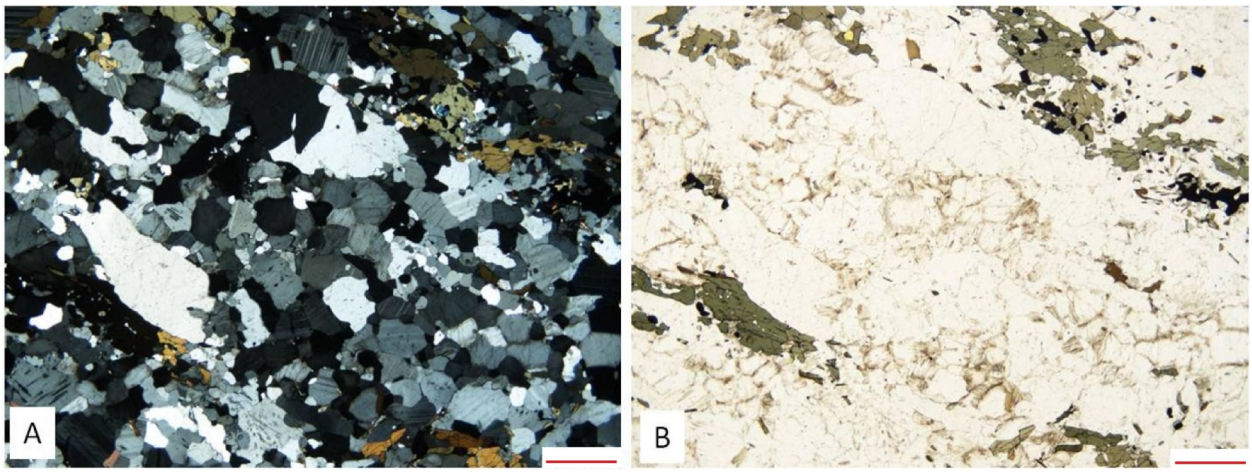

Fig. 21. Photomicrographs of thin section LL1106 F1 of a reddish grey gneiss at Mokrik located in the Hallandia gneiss domain. The red scale bar = 1 mm. A) Crossed polarized light; Feldspar rich domains alternate with dark mineral bands and define a foliation. Quartz ribbons, elongated quartz grains and granoblastic alkali feldspar occur in the feldspar rich domains. B) Plane polarized light; Biotite, hornblende and opaque minerals are oriented parallel to the foliation which is defined by feldspar rich domains alternating with bands of dark minerals.

Figs. 23A and C). Minerals in the felsic domains are irregular, moderate to severely sericitized with sutured but smooth grain boundaries. Microcline is common and tartan twinning is well developed. A few microcline augen are present and one or two contain a core of orthoclase. A few plagioclase grains are antiperthtitic and myrmekite occurs sparsely. Hornblende grains and biotite as sub- to euhedral individual grains, aggregates and bands are parallel to the foliation (Figs. 23B and D). Biotite is dark-brown and hornblende is blue-green. A few biotite grains are partly chloritized. Garnet and titanite are absent.

4.3.2 Töresjö (LL1109 F1 and F2)

The major constituents of the migmatitic gneiss at Töresjö are feldspars, quartz, biotite and garnet. Accessory minerals are opaque minerals, titanite, allanite, apatite and zircon.

The rock is uneven grained and the two thin sections show the same microtextures. The grain size varies between 0.125 mm and 5.9 mm. The foliation (Figs. 24A-D) is defined by bands of dark minerals (biotite, opaque minerals, titanite and garnet) alternating with felsic domains containing smaller (0.13-0.6 mm wide and 1.05-2.45 mm long; Figs. 24A and C) and larger elongated felsic grains (0.3-1.63 mm wide and up to 5.5 mm long; Fig. 24C). Felsic minerals are irregular, occasionally moderate to severely sericitized with sutured but smooth grain boundaries. Microcline is common and tartan twinning is well developed. A few microcline augen have an orthoclase core: some augen are several mm large, the largest ones are up to 5 mm (Fig. 24C). Plagioclase has well developed albite twins and is not antiperthitic. Myrmekitization occur locally. Individual grains of dark minerals and aggregates, bands and individual grains of biotite are paral-

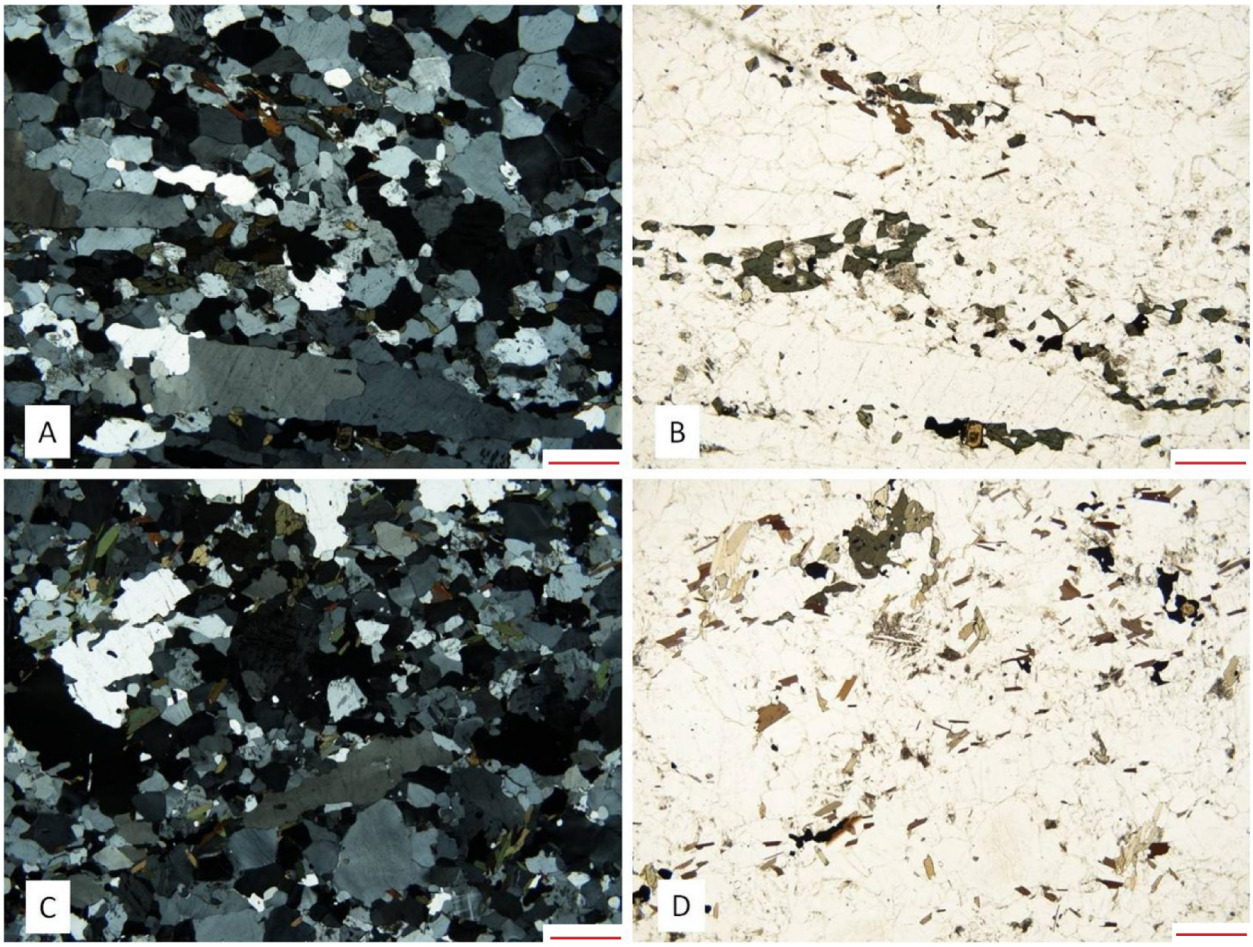

Fig. 22. Photomicrographs of thin section LL1107 PL and TL of a reddish grey gneiss at Abild located in the Hallandia gneiss domain. The red scale bar = 1 mm. A) Crossed polarized picture of thin section parallel to the lineation; Oriented individual grains and aggregates of biotite define a lineation. Hornblende and opaque minerals are parallel to the lineation. Distinct quartz ribbons, lower part of the image, and granoblastic alkali feldspar, upper right corner, occur in the feldspar rich domains. B) Plane polarized picture of thin section LL1107 PL; Dark minerals are parallel to the lineation which is defined by aggregates and oriented individual biotite grains. C) Crossed polarized picture of thin section perpendicular to the lineation; Dark minerals (except biotite) are randomly oriented and elongated felsic grains occur in the feldspar rich domains. D) Plane polarized picture of thin section LL1107 TL; Individual grains of hornblende and opaque minerals appear randomly oriented and not oriented parallel to the lineation, whereas biotite grains and aggregates are oriented.

lel to the foliation (Figs. 24B and D). Biotite is sub- to euhedral, dark-brown and few grains are partly chloritized. Titanite occurs as individual grains and as coronas around few opaque minerals. Garnet is rare and hornblende is absent.

The absence of hornblende in this gneiss is not typical for rocks occurring in the Skene migmatite gneiss domain.

4.3.3 Toppeberg (LL1110 F1 and F2)

The gneiss at Toppeberg is mainly made up of feldspars, quartz, hornblende and biotite. Accessory minerals are opaque minerals, titanite, apatite, zircon and allanite.

The rock is uneven grained and the two thin sections show similar microtextures. The grain size varies from 0.125 mm to 3.65 mm. The weak foliation (Figs. 25A and B) is defined by diffuse bands and lenses of dark minerals (hornblende, biotite and opaque minerals) alternating with feldspar rich domains. The foliation is folded in thin section LL1110 F1. Mineral grains in the felsic domains are slightly elongated and parallel to the foliation (Fig. 25A). Feldspars are irregular, moderately to severely sericitized and have relatively smooth grain boundaries. Plagioclase is common but albite twins are not well developed and antiperthite is rare. Microcline show well developed tartan twinning. Myrmekite is sparse. Biotite is often partly chloritized and occurs occasionally as aggregates. Biotite is dark-brown and hornblende is blue-green; individual grains are oriented parallel to the foliation (Figs. 25A and B). The opaque minerals are iron oxides (lamella of titanomagnetite and hematite in the same grains and lamella of hematite and magnetite in the same grains). Titanite occurs as a few individual grains and as coronas around opaque minerals. Garnet is absent.

4.3.4 Vräk (LL1111 TL and PL)

Feldspars, quartz, biotite and hornblende are the major constituents of the gneiss at Vräk. Accessory minerals are opaque minerals, apatite, zircon and allanite.

The rock is uneven grained and the two thin sections show variation in microtextures. The grain

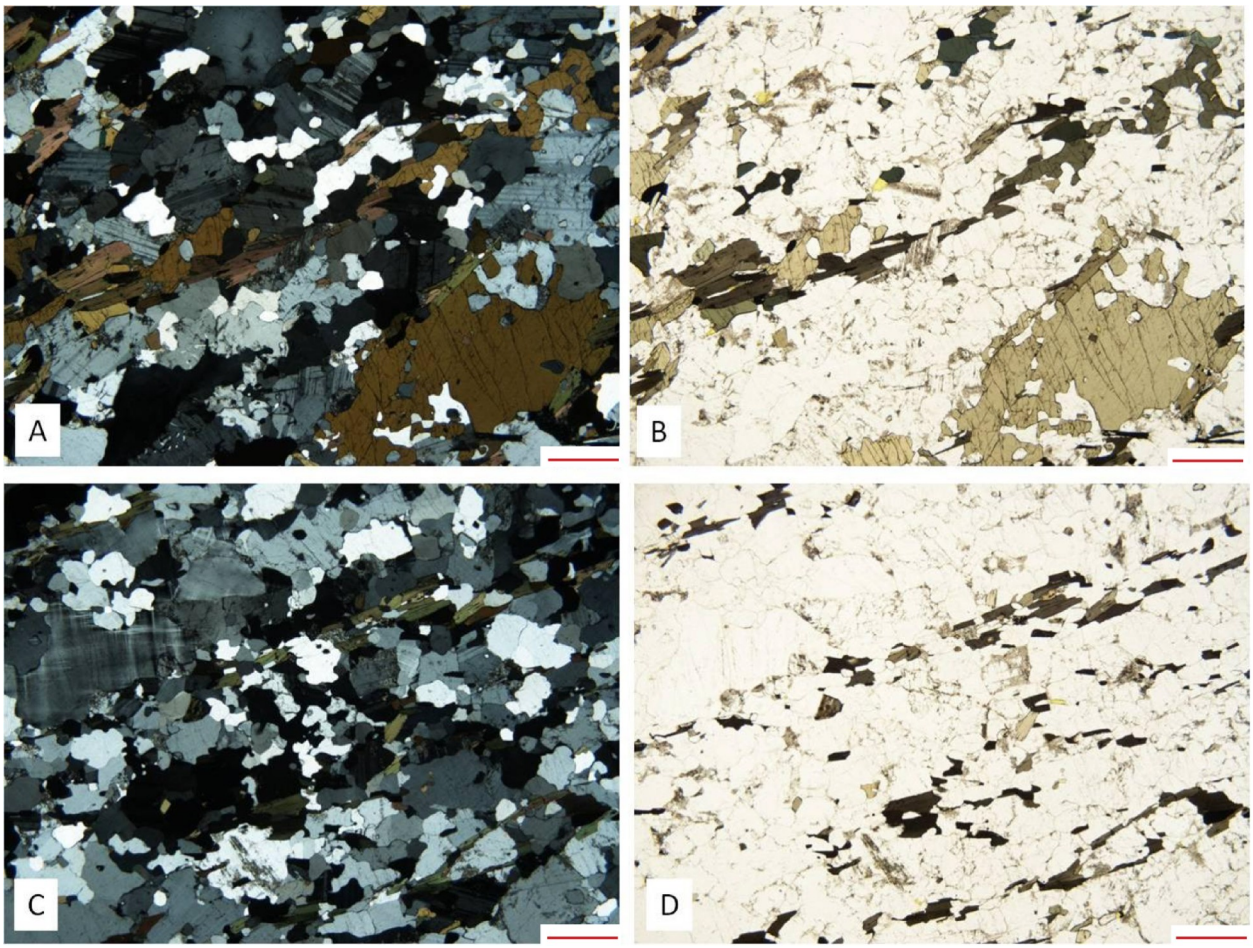

Fig. 23. Photomicrographs of thin section LL1108 F1of a pink-whitish grey migmatitic gneiss at Fridhemsberg located in the Skene migmatite gneiss domain. The red scale bar = 1 mm. A and C) Crossed polarized light; Felsic domains (containing elongates felsic grains) alternate with dark mineral bands and define a foliation. B and D) Plane polarized light; Aggregates, bands and individual grains of biotite and grains of hornblende are parallel to the foliation which is defined by alternation of felsic domains and bands of dark minerals.

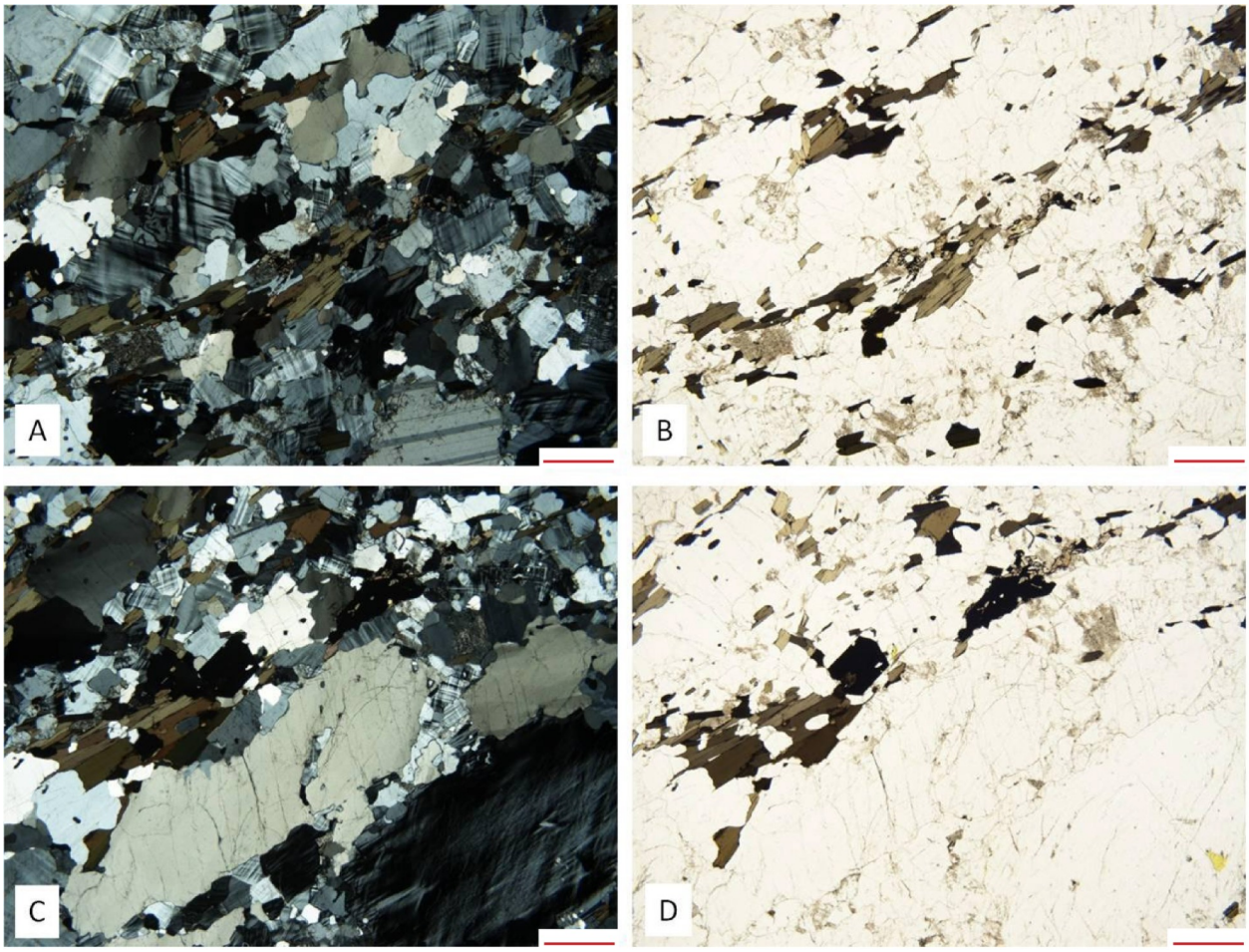

Fig. 24. Photomicrographs of thin section LL1109 F1 of a migmatitic light grey gneiss at Töresjö located in the Skene migmatite gneiss domain. The red scale bar = 1 mm. A) Crossed polarized light; Fine grained felsic grains are parallel to the foliation which is defined by felsic domains alternating with bands of dark minerals. B and D) Plane polarized light; Dark minerals are parallel to the foliation defined by bands of dark minerals alternating with felsic domains. C) Crossed polarized light; Small and larger felsic grains and augen are parallel to the foliation.

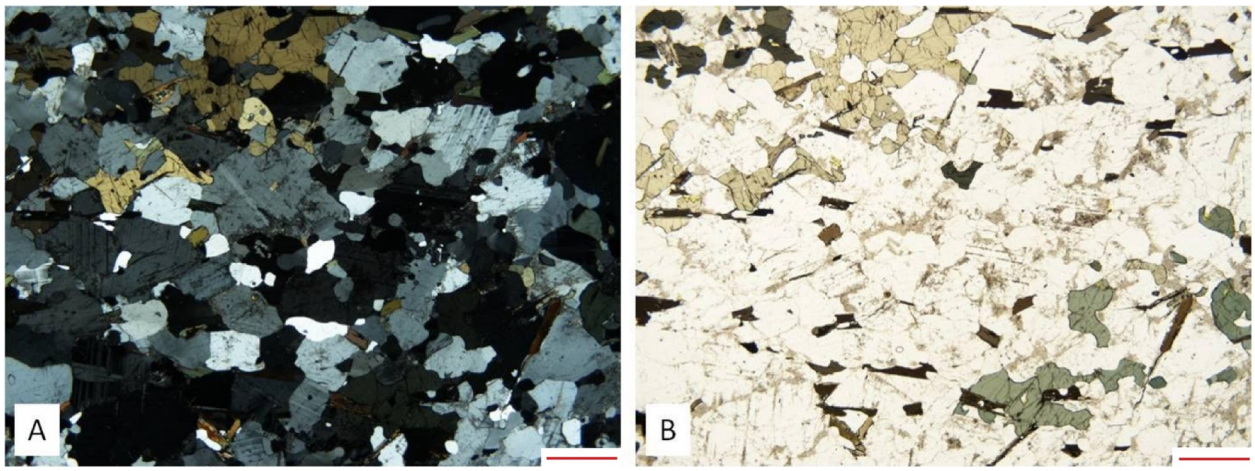

Fig. 25. Photomicrographs of thin section LL1110 F2 of pinkish grey gneiss at Toppeberg located in the Skene migmatite gneiss domain. The red scale bar = 1 mm. A) Crossed polarized light; Diffuse bands and lenses of dark minerals alternating with felsic domains define a weak foliation. Elongated individual grains of feldspar, quartz, biotite and hornblende are parallel to the foliation. B) Plane polarized picture of thin section LL1110 F2; Biotite and hornblende grains are parallel to the foliation defined by felsic domains alternating with diffuse bands and lenses of dark minerals.

size varies between 0.15 mm to 3.25 mm. The foliation (Figs. 26A-D) is defined by bands and lenses of dark minerals (biotite, hornblende and opaque minerals) alternating with felsic domains. Felsic domains contain few quartz ribbons (0.3-1.38 mm wide and 3.1-4.63 mm long) and elongated quartz and feldspar grains (0.25-1.35 mm wide and 1.18-3.25 mm long; Figs. 26A and C). Quartz ribbons, composed of large and relatively unstrained grains, define a lineation. Feldspars are irregular, moderately to severely sericitized and show smooth and occasionally irregular grain boundaries. Plagioclase is common and show well developed albite twins; antiperthite is absent. Microcline occurs as smaller grains but do not show well developed tartan twinning. Biotite occurs as aggregates and sub- to euhedral individual grains where few grains are partly to entirely chloritized. Biotite is dark-brown and hornblende is blue-green; individual grains are parallel to the foliation and lineation (pronounced in the thin section cut parallel to the lineation; Figs. 26C and D). A few opaque mineral grains have a corona of titanite. Garnet is absent.

Felsic gneisses in the Skene migmatite gneiss domain are commonly rich in microcline with well developed tartan twinning. Vräk is a felsic gneiss but the tartan twinning is not well developed.

4.4 Svarten gneiss domain

The gneiss in this domain is composed of feldspar, quartz, hornblende, biotite, garnet and clinopyroxene. Antiperthitic plagioclase is common but albite twins are seldom well developed. Biotite is red-brown and hornblende is brown-green. Clinopyroxene and almandine rich garnet are present while tartan twinning and titanite are absent.

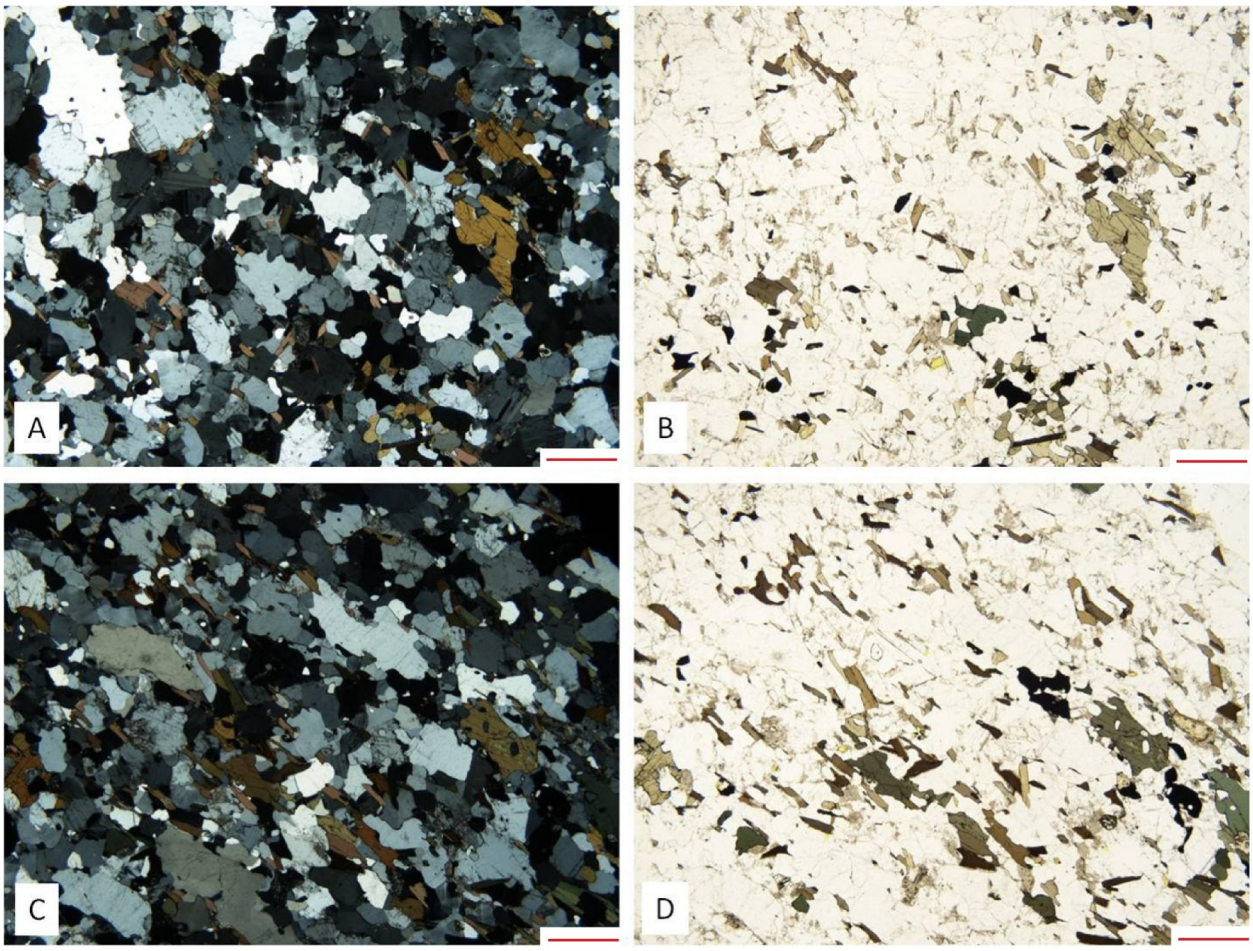

Fig. 26. Photomicrographs of thin section LL1111 TL and PL of a grey gneiss at Vräk located in the Skene migmatite gneiss domain. The red scale bar = 1 mm. A) Crossed polarized picture of thin section perpendicular to the lineation; Elongated felsic grains are parallel to the foliation defined by felsic domains alternating with bands and lenses of dark minerals. B) Plane polarized picture of thin section LL1111 TL; The foliation is defined by felsic domains alternating with bands and lenses of dark minerals. C) Crossed polarized picture of thin section parallel to the lineation; Biotite, hornblende, elongated felsic minerals are parallel to the foliation. D) Plane polarized picture of thin section LL1111 PL; Grains of biotite and hornblende are parallel to the foliation defined by bands and lenses of dark minerals alternating with felsic domains.

4.4.1 Köinge (LL1112 TL and PL)

The gneiss at Köinge is mainly made up of feldspars, quartz, hornblende, biotite, garnet and clinopyroxene. Accessory minerals are opaque minerals, apatite, zircon and allanite.

The rock is uneven grained and the thin sections show variation in microtextures. The grain size varies between 0.05 mm and 5.93 mm. The foliation (Figs. 27A-D) is defined by bands and lenses of dark minerals (hornblende, biotite, almandine rich garnet, clinopyroxene and opaque minerals) alternating with feldspar rich domains. The felsic domains contain few distinct quartz ribbons (0.5-0.9 mm wide and 2.53-12.7 mm long; Fig. 27C) in addition to elongated felsic grains (0.25-1.23 mm wide and 1.28-5.7 mm long; Fig. 27A). A pronounced lineation is defined by large and straight quartz ribbons made up of relatively unstrained grains (Fig. 27C). Feldspars are antiperthitic, irregular and show smooth grain boundaries. Albite twins are poorly developed. Alkali feldspar occurs as few, often granoblastic, polycrystalline domains (Fig. 27C). In one corner of the thin section cut perpendicular to the lineation (LL1112 TL) feldspars are severely sericitized: elsewhere the alteration is modest. Myrmekite is sparse. Biotite, hornblende and opaque mineral grains and aggregates are parallel to the foliation (Figs. 27B and D). Biotite occurs as subhedral individual grains and aggregates where some grains are partly to entirely chloritized. Biotite is red-brown and hornblende is brown-green. Some clinopyroxene grains show moderate rusty colored alteration. Opaque minerals are iron oxides (titanomagnetite, lamella of hematite and magnetite in the same grains) and iron sulfide (pyrite). Microcline (tartan twinning) and titanite is absent.

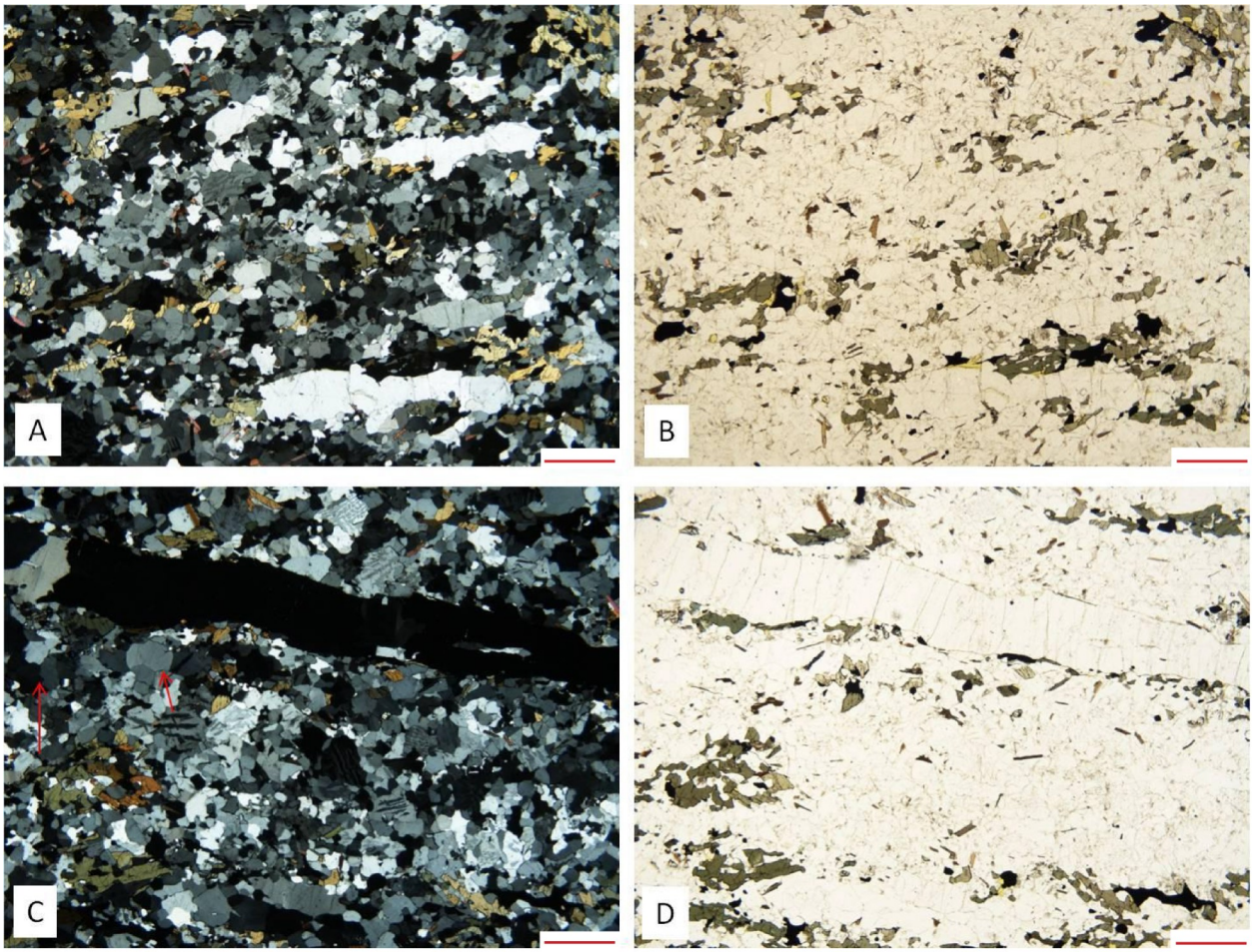

Fig. 27. Photomicrographs of thin sections LL1112 PL and TL of a grey gneiss at Köinge located in the Svarten gneiss domain. The red scale bar = 1 mm. A) Crossed polarized picture of thin section parallel to the lineation; Elongated felsic grains are parallel to the foliation defined by felsic domains alternating with lenses and bands of dark minerals. B) Plane polarized picture of thin section LL1112 PL where the darker color is due to carbon coating; Aggregates and individual grains of biotite, hornblende and opaque minerals are parallel to the foliation. C) Crossed polarized picture of thin section perpendicular to the lineation; Large and straight quartz ribbons is made up of relatively unstrained grains (define a lineation) and granoblastic alkali feldspar domains (marked with red arrows) occur in the felsic domains. D) Plane polarized picture of thin section LL1112 TL; Biotite, hornblende and opaque minerals are parallel to the foliation which is defined by bands and lenses of dark minerals alternating with felsic domains, including quartz ribbons.

5. Methods

5.1 Technical analyses

In order to assess the quality and the suitability of a rock for use as aggregates it is necessary to determine the technical properties of the rock. A number of standardized methods are routinely used to measure the technical properties. This thesis focuses on technical analyses which are used for quantitative evaluation of aggregate quality for road and railway construction. The methods used are described below.

5.1.1 Collecting material for technical analyses

Gneisses were collected from 12 sampling sites in four different tectonic domains in the Eastern Segment. Approximately 80 kg of fresh rock material was collected from each sample site using hammers and sledgehammers. Fresh, non-weathered rock was selected at each sampling site. One site, however, (Abild) included also material that showed indications of weathering when examined by the naked eye in the laboratory.

5.1.2 Studded tyre test

The studded tyre test value is a measure of the resistance to abrasion of a rock (Persson & Göransson, 2010b). A high value represents poor technical properties (low resistance to abrasion) i.e. significant loss of material during the test.

The studded tyre tests (A_N) were carried out according to SS-EN 1097-9 (Swedish Standards Institute, 2004a). The sample preparation started with crushing in two steps, first with a rotational jaw crusher (Svedala-Arbrå R 50-26-64) and then with a smaller jaw breaker (Morgårdshammar A23). Sieving was carried out with using a Gilson machine siever. All fractions (0-10; 10-11.2; 11.2-14; 14-16 and 16+ mm) were weighted and the density was determined by Archimedes principle (sample weight when dry compared to weight in water). Density determines the relative portion of the two fractions (11.2-14 mm and 14-16 mm) used in this test method. Flakey sorting sieving was carried out by hand eliminating most of the elongated and flaky grains, i.e. smaller than 6.3 mm. The sample, steel balls (7000 g) and two liters of water were put in a ball mill, where the ball mill will spin 5400 revolutions (c. 1 hour). The material was then sieved through an 8 mm and 2 mm sieves and steel balls are removed with a magnet. The sample was dried in an oven and then weighted.

The studded tyre test values was calculated according to following formula:

$$A_N = 100 \times (m_1 - m_2)/m_1$$

where m_1 and m_2 are the sample weight in grams before and after the abrasion process respectively.

5.1.3 Los Angeles test

Los Angeles test value corresponds to the fragility of a rock, resistance to fragmentation (Swedish Standards Institute, 1997a). High values represent poor technical properties i.e. a low resistance to fragmentation.

The Los Angeles tests (LA) were carried out according to SS-EN 1097-2 (Swedish Standards Institute, 1997a). Crushing, sieving and weighing were carried out in the same way as for the studded tyre test. The proportions of the fractions (10-14 mm) used in this test are fixed. The sample (5000 g) and 11 steel balls each with a diameter between 45 mm and 49 mm were added to the Los Angeles mill. The test is run with dry material. After 30 min (500 revolutions) the material is sieved for 10 min and then weighed (except for fraction 0-1.6 mm which is thrown away).

The LA test values are calculated according to:

$$LA = (m_1 - m_2)/50$$

where m_1 and m_2 are the sample weight in grams before and after the fragmentation process respectively.

5.1.4 MicroDeval test

The microDeval test value measures the resistance to abrasion of a rock (Swedish Standards Institute, 1997b). High values correlate with poor technical properties i.e. a low resistance to abrasion.

The microDeval tests (M_{DE}) were carried out according to SS-EN 1097-1 (Swedish Standards Institute, 1997b). Crushing, sieving and weighting were carried out in the same way as for the studded tyre and the Los Angeles tests. The proportions of the fractions (10-14 mm) used in this test are fixed. The sample (500 g), water (c. 2.5 l) and steel balls (5000 g) were put in a mill. After two hours (12000 revolutions) the steel balls are removed with a magnet and the remaining material was sieved through an 8 mm and a 1.6 mm sieve plane. The material was dried in an oven then weighed. Two subsamples were analyzed for each sampling site.

The following formula was used to calculate the microDeval test values:

$$M_{DE} = (m_1 - m_2)/5$$

where m_1 and m_2 are the sample weight in grams before and after the abrasion process respectively.

5.2 Water absorption analysis

In this study the water absorption analysis is used to determine if the rock material is suitable as aggregates for railway.

Water absorption analysis was made according to standard EN 13755 (European Committee for Standardization, 2008). One exception is the restrictions concerning the size and volume of the test specimens; they have not been followed due to limited hand sample volume. Samples are dried in an oven at constant temperature (70 ± 5ºC) and weighted every 24th hour (± 2 hours). Constant mass is achieved when mass difference is not greater than 0.1 % between two successive weighings. When constant weight has been attained the specimens are placed in a jar with a minimum distance of 15 mm between the samples. Tap water is successively added; at t_0 water is added to cover half the height of the samples. At $t_{0+60\pm5}$ min three-quarters of the height of the samples are covered with water and at $t_{0+120\pm5}$ min they are completely immersed. After 48 hours (± 2 hours) the samples are dried with a damp cloth and weighted within one minute. This is repeated every 24th hour (± 2 hours) until constant mass is attained with an accuracy of 0.01g.

Water absorption at atmospheric pressure is calculated by the following formula:

$$A_b=((m_s-m_d)/m_d)\times100$$

were A_b is the water absorption in weight percent, and m_d and m_s represent the weight of the sample after drying and water saturation respectively.

If the water absorption is below 0.5 wt % the aggregate is considered to be frost resistant according to SS-EN 13242+A1 (Swedish Standards Institute, 2007). According to SS-EN 1097-6 the maximum allowed water absorption is 1 wt % for rock material used as aggregates for railway (Swedish Standards Institute, 2004b).

5.3 Preparation of thin sections

Sawing of rock slabs for thin section preparation was carried out at the Department of Geology at Lund University. Two polished thin sections were made per sample (24 solid rock thin sections in total). The thin sections were cut parallel and perpendicular to the lineation (PL and TL, respectively) or perpendicular to the foliation (F1 and F2). Thin sections width ranges between 19 mm and 28 mm and the length between 37 mm and 47 mm. Manufacturing of the thin sections was made by Minoprep in Hunnebostrand.

The first step at Minoprep was to impregnate the thin sections with a mixture of Araldite and the fluorescent dye for filling of cracks and cavities with fluorescent media (Minoprep AB, personal communication, 12th of March, 2012). The thin sections were placed in vacuum for some minutes before they were polished and then glued on to rectangle glass pieces (36 × 53 mm). As a consequence, the impregnation material only occurs in pores and fissures. A sheet sander with a diamond bowl was used to polish the material to a thickness of 50 µm then manual polishing proceeded until the thin sections were 25 µm thick. This process begin with coarse polishing (6 µm of diamond paste and 8-9 hg load for 2-5 hours) and ends with fine polishing (1 µm diamond on a silk cloth for 1 hour).

5.4 Micro analyses

Micro analyses were carried out at the Swedish Cement and Concrete Research Institute in Borås except the perimeter analysis which was carried out at the Department of Geology at Lund University.

5.4.1 Image analysis

Fluorescent and polarized images of all samples were taken with fluorescent and optical microscopy (Åkesson et al., 2003). The thin section was fixed on a motorized stage were one fluorescent and one polarized image was taken. The stage was programmed to take images edge to edge creating mosaic images containing four or 12 images. The image size is 2.8 × 2.1 mm and resolution is 680 × 512 pixels for every image in the mosaic images (mosaic images made up of four images are 4.2 × 5.6 mm large and 8.4 × 8.4 mm when the image is made up of 12 images).

A Carl Zeiss Vision KS400 image analyzing software was used to combine fluorescent and polarized pictures. The combined pictures show the position of existing microcracks and voids in relation to existing minerals on a microscopic scale.

5.4.2 Microcrack analysis

Combined images (fluorescent and polarized) received from image analysis were used for quantitative analysis of microcracks in the thin sections. Travers lines perpendicular to each other were used to count the microcracks (Appelquist & Eliasson, 2011). Lines analyzed are equal in length in both directions and the total analyzed length is at least 100 mm. Cracks that cross the traverse lines are counted. Fluorescent areas in thin sections from Dagsås (LL1101) are restricted to orthopyroxene minerals; they do not show fractures and are therefore treated as cavities i.e. excluded from the calculation. Microcracks are divided into intragranular (inside a mineral grain), transgranular (crossing a grain boundary between minerals) and grain boundary cracks.

5.4.3 Mineral grain size and mineral grain size distribution analyses

Polarized images of the thin sections received from the image analysis are used to quantitatively determine the grain size and grain size distribution for each sample (Appelquist & Eliasson, 2011). Traverse lines have the same length in both directions and are perpendicular to each other. A ruler was used to measure the longest axis of mineral grains crossing the traverse lines. At least 200 mineral grains were measured per sample.

Minimum, maximum and mean grain sizes was calculated for each sample.

Cumulative grain size distribution curves were made according to NT BUILD 486 for each sample (Nordtest, 1998).

5.4.4 Perimeter analysis

The perimeter is the circumference of an object (Åkesson et al., 2003). Grain size and boundary complexity affect the perimeter. Comparing two equally large areas (images) the more fine grained material will contain more objects to be measured and therefore have a larger perimeter. Interfingering, sutured or cuspate grain boundaries will increase the perimeter. This analysis is then indirectly correlated to the grain size and the appearance of the grain boundaries, which can affect the technical properties.

NIS Elements BR 3.10 software was used to carry out perimeter analysis. The software was connected to an optic microscope, which made it possible to take pictures of all thin sections. One crossed polarized and one plane polarized picture was taken in each corner and in the middle of each thin section. The perimeter analysis was carried out on plane polarized pictures and objects analyzed were classified as different groups of phases. Red colored objects represent biotite, green color is pyroxene and amphibole, while blue represents opaque and garnet. The auto detect and draw object tools were used to define objects. Auto detect tool marks the object and its boundaries based on its intensity value (color). Sometimes mineral grains cannot be identified by color since the color contrast to other adjacent mineral phases is too low. This occurs for example when biotite grains are oriented in extinction angle and have a color similar to adjacent feldspars and quartz grains. The draw object tool can be used in these cases because the grain boundaries are identified by the software user and the circumference of the objects is drawn by hand. The software calculates the perimeter according to Crofton´s formula:

$$\text{Perimeter} = n \times (Pr_0 + Pr_{45} + Pr_{90} + Pr_{135})/4$$

where n is the number of points and Pr_X are projections in directions 0, 45, 90 and 135 degrees. Both the outer and inner boundaries (if there are large holes inside an object) of an object are measured. Minerals composing monomineralic aggregates are not measured individually; the perimeter of the aggregate is measured. The perimeter of a certain phase in one thin section is obtained by summarizing the perimeter of this phase from all five analyzed spots. Since there are two thin sections analyzed per sample, and all 24 thin sections have been analyzed, the perimeter of a phase for one sample is a mean value. To get the total perimeter of a sample the perimeter of all analyzed phases (mean values) in both thin sections are summarized.

5.4.5 Foliation index analysis (FIX)

The Foliation index (FIX) is a technique used to define the degree of foliation in various rocks. According to Åkesson et al. (2003) fabric dependent anisotropy is important in order to understand the mechanical behavior of foliated rocks since the foliation creates mechanically weak discontinuities. A rock with a lower FIX value than 1.10 is considered to be isotropic (Hellman et al., 2011).

Åkesson et al. (2003) showed that there is a good correlation between high FIX values and low length thickness index (LT-index; length and thickness relationship of crushed particles). This means that a rock with a high FIX value (> 1.10), ie. an anisotropic rock, will produce a higher proportion of highly elongated grains when crushed and probably contain more weak discontinuities than an isotropic rock. The energy required for crack propagation parallel to the foliation is much lower than for cracks propagating perpendicular to the foliation (Lindqvist et al., 2007; Tavares & das Neves, 2008). For this reason it is likely that an isotropic rock has a higher durability than an anisotropic rock and thereby is more suitable as road and railway aggregates.

Polarized images of the thin sections obtained from the image analysis and traverse lines used in the mineral grain size analysis were used as the basis for the FIX analysis. The traverse lines were categorized as parallel or perpendicular in respect to the mineral fabric (Åkesson et al., 2003). Grain boundaries crossing the traverse lines are counted. The analyzed length was 33.6 mm. The foliation index (FIX) was calculated according to the following formula:

$$FIX = \sum(P_L)_{\perp} / \sum(P_L)_{//}$$

were $\sum(P_L)_{\perp}$ and $\sum(P_L)_{//}$ is the sum of number of grain boundaries perpendicular and parallel to the mineral fabric measured from the traverse lines (Åkesson et al., 2003). Isotropic rocks have a FIX value near 1 and anisotropic material has FIX values higher than 1.10. The material is more anisotropic the higher FIX value it shows.

The term isotropic rock generally refers to rocks with no mineral fabric. In this case, concerning the FIX values, it represents a rock with an equally or almost equally strong mineral fabric in the two analyzed directions.

5.5 Chemical analyses

Whole rock chemical analyses were carried out for ten of the twelve samples. Sample Fridhemsberg (LL1108) and Töresjö (LL1109) were excluded since these samples were too heterogeneous in relation to the sample volume.

5.5.1 Chemistry

The chemical analyses were carried out by Acme Analytical Laboratories in Canada. Method 4A uses ICP-emission spectrometry, lithium metaborate/tetraborate fusion and dilute nitric digestion to determine the abundance of major oxides and several minor elements (Acme Analytical Laboratories 2011 & 2012). Major elements analyzed are Si, Al, Fe^{3+}, Mg, Ca, Na, K, Ti, P, Mn and Cr. In order to determine the rare earth and refractory elements the total trace elements were analyzed with ICP mass spectrometry, lithium metaborate/tetraborate fusion and nitric acid digestion (method 4B; Acme Analytical Laboratories 2011 & 2012).

5.5.2 CIPW norm calculations

Norm calculations were made using an excel spreadsheet program (Kurt Hollocher, Union College). Chemical data for major, minor and trace elements for all samples were used in the calculation. In order to continue the norm calculation some assumptions were made. The total analyzed amount were fix to 100 % and Fe^{3+}/total Fe ratio was set to 0.3. The iron ratio reflects the ratio normally occurring in granitoids (Jan Erik Lindqvist, personal communication, 5th of April, 2012). The normative mineralogy for each sample was then obtained.

5.5.3 Sample classification (TriPlot & GCD)

The TriPlot 4.1.2. software was used to plot the mineralogy in relation to the relative amount of quartz, feldspar and plagioclase for each sample (Le Maitre, 1989). Normative chemical mineralogy data received from CIPW norm calculations were used for plotting the mineralogy. The result is a QAP diagram which shows the mineralogy (rock type) for each analyzed sample.

The Geochemical Data Toolkit 2.3. (GCDkit) software is used to plot the mineralogy of samples in regard to major, minor and trace elements (Janoušek et al., 2006). Chemical data used for plotting were retrieved from the chemical analyses carried out by Acme Analytical Laboratories. The result is three diagrams showing the mineralogy (rock type) for each sample.

The R_1-R_2 diagram introduced by De la Roche et al. (1980) characterizes igneous rocks (Frost et al., 2001). The diagram compresses the basalt tetrahedron into two dimensions, R_1 and R_2, which are defined by cationic functions ($R_1 = 4Si - 11(Na + K) - 2(Fe + Ti)$; $R_2 = 6Ca + 2Mg + Al$). The diagram shows variation of silica saturation, changes in Fe-Mg ratio and plagioclase composition. The disadvantage with this approach is that K-feldspar and albite plot at the same point; i.e rocks with variable K/Na ratios are indistinguishable in the diagram.

Total Alkali Silica (TAS) classification diagram from Middlemost (1985) show total alkali content ($Na_2O + K_2O$) plotted against total silica content (SiO_2). The diagram shows variations and relations between silica and total alkali content. Rocks are divided into ultrabasic, basic, intermediate and acid depending on their silica content (Rollinson, 1993).

The P-Q diagram introduced by Debon & Le Fort (1983) show proportions of K-feldspar and plagioclase ($P = K - (Na + Ca)$ to quartz ($Q = Si/3 - (K + Na + 2Ca/3)$. Plagioclase is more common than K-feldspar in rocks plotting to the left in the diagram, i.e tonalitic rocks are located further to the left in the diagram than granitic rocks.

In the investigated thin sections, feldspar varieties could not everywhere be identified, mainly due to absence of twinning. Therefore no point counting was carried out.

6. Results

6.1 Technical properties, Los Angeles, studded tyre and microDeval tests

A compilation of the results from the technical analyses and water absorption analysis is shown appendix 4.

The samples show good correlation between microDeval test values and studded tyre test values (Fig. 28). According to Göransson et al. (2008) the correlation between these technical methods can be used as a tool for estimating the other when only one of them is known, for the tested materials. Comparing the correlation attained, $M_{DE} = 0.62 \times A_N + 0.55$ ($R^2 = 0.96$), with the same type of correlations achieved by Stenlid (2000; $M_{DE} = 0{,}86 \times A_N - 2{,}71$ ($R^2 = 0{,}95$)), Göransson et al. (2008; $M_{DE} = 0{,}89 \times A_N - 2{,}50$ ($R^2 = 0{,}89$)) and Bergström et al. (2008; $M_{DE} = 0{,}77 \times A_N - 1{,}51$ ($R^2 = 0{,}97$) it is obvious that they all show a common positive correlation.

The Los Angeles and studded tyre test values for all samples are shown in figure 29. Lower test values correspond with better technical properties and the possibility to use the material for more demanding road or railway qualities increases. Aggregate quality classification, a division into classes 1-3 made by the Geological Survey of Sweden, reflects how appropriate the material is for use as road construction material (Persson & Göransson, 2010a). In simplified words, aggregate quality class 1 represents good quality while, class 2 moderate, and class 3 poor aggregate quality. Samples which fall in classes 1 and 2 can be used for bound road layers while material in class 3 can only be used for unbound layers. The classification is based on established requirements for aggregates laid down by the Swedish Transport Administrations (Vägverket 2005a, 2005b). Most samples from the investigated area fall into class 3 (Fig. 29). Sample Ljungby (LL1103) and Dagsås (LL1101) located in the Varberg granulite gneiss domain fall into class 1 and 2 respectively. Sample Knobesholm (LL1104) located in the Hallandia gneiss domain and Vräk

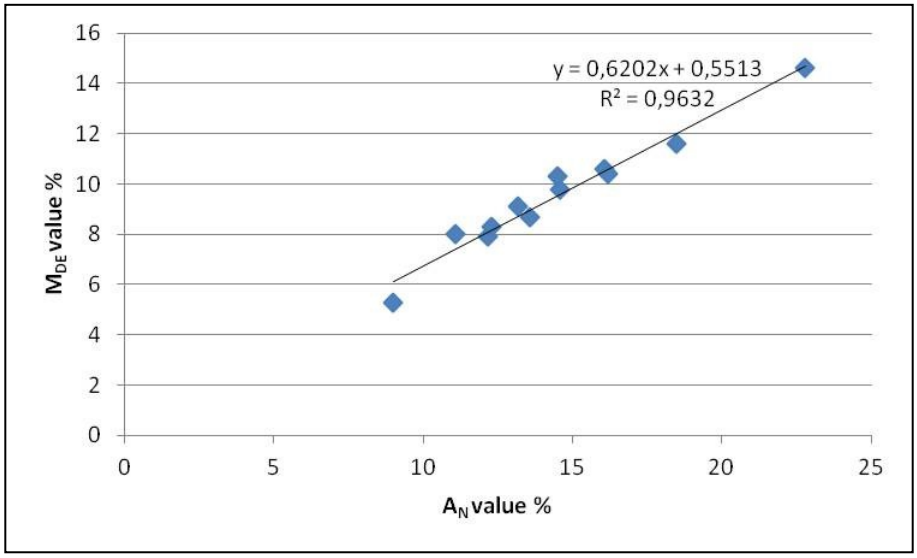

Fig. 28. The microDeval and studded tyre test values show a very good positive correlation, similar results achieved by Stenlid (2000), Göransson et al. (2008) and Bergström et al. (2008).

(LL1111) located in the Skene migmatite gneiss domain plot within the class 2.

All samples have too high LA values in order to be suitable as aggregates for bounded railway layers. Samples from Dagsås (LL1101) and Ljungby (LL1103) are exceptions.

Biotite and amphiboles are high-density minerals due to their high content of elements such as Fe, Mn and Ti. Feldspars and quartz on the other hand are light. A material containing dense minerals (Dagsås (LL1101) and Köinge (LL1112)) behaves in less brittle manner and has, a lower LA/A_N ratio (Fig. 30), as the LA test reflects the resistance to fragmentation. The content of free mica (amount of free mica grains in the crushed fine fraction, 0-10 mm) and occurrence of mica minerals in the rock (micas as orientated aggregates and bands or randomly oriented individual grains) affect the LA/A_N ratio (SGU, Mattias Göransson, personal communication, 12th of November 2012). High amounts of mica tend to lower the LA/A_N ratio (a rocks resistance to abrasion, A_N value increases with an increasing mica content). According to Lundqvist and Göransson (2001) rocks that are enriched in mica generally resist brittle fragmentation better than their mica poor equivalents. Mica rich rocks generally have, however, a low to very low resistance to abrasion. The occurrence of mica as bands, aggregates or individual grains oriented parallel to a present foliation or lineation correlate well with poor technical values (SGU, Mattias Göransson, personal communication, 12th of November 2012).

The energy it takes to produce a crack in a mineral, the fracture energy, varies between minerals and is directly correlated to the rocks resistance to fragmentation (LA values; Lindqvist et al., 2007; Tavares & das Neves, 2008). Amphiboles and pyroxenes have higher fracture energies than feldspars, which more easily slip along the crystal planes.

The investigated samples show a tendency towards decreasing LA/A_N ratio with increasing density (Fig. 30). There are two exceptions, samples from Mokrik (LL1106) and Töresjö (LL1109), which deviate from the trend. The unexpected low LA/A_N ratio shown by Töresjö can be explained by a high free mica content (22 %; unpublished CBI data).

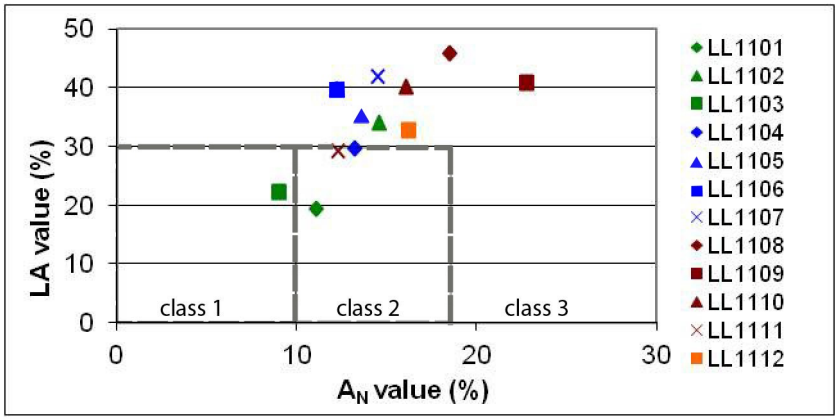

Fig. 29. Aggregate quality classification division (class 1-3) shows how appropriate the material is for use as road construction material. The lower the Los Angeles and studded tyre test values, the better is technical properties of the rock material. The samples have different color depending on their geographical location in the investigated area. Green color represent rocks located in the Varberg granulite gneiss domain, blue color represent rocks in the Hallandia gneiss domain, red color for rocks located in the Skene migmatite gneiss domain, and orange color for rocks restricted to the Svarten gneiss domain.

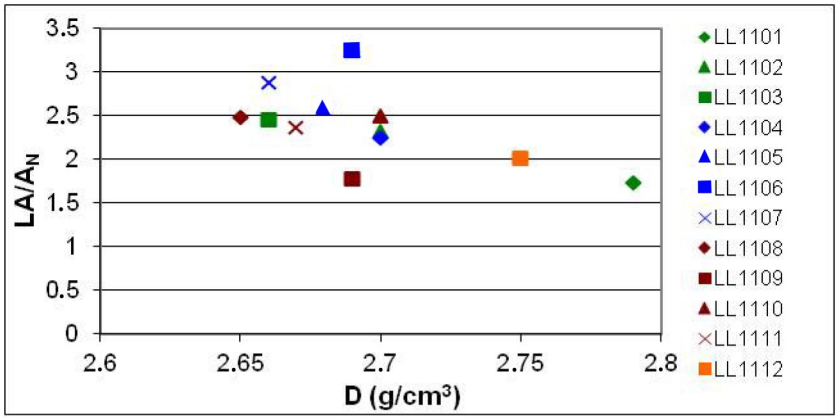

Fig. 30. The LA/A_N ratio for all investigated samples, plotted against their density. The occurrence and high contents of mica and heavy minerals (biotite and hornblende) tend to lower the LA/A_N ratio. Samples with higher density tend to have a lower LA/A_N ratio. The Mokrik (LL1106) sample shows a very high LA/A_N ratio and the opposite is shown by sample Töresjö (LL1109). Green color represent rocks located in the Varberg granulite gneiss domain, blue color represent rocks in the Hallandia gneiss domain, red color for rocks located in the Skene migmatite gneiss domain, and orange color for rocks restricted to the Svarten gneiss domain

6.2 Water absorption

Samples from Ljungby (LL1103), Hallandssten (LL1105) and Mokrik (LL1106) give the lowest water absorption values (0.1 wt %; Table 2). Highest values, 0.3 wt % and 0.4 wt %, are recorded for samples from Dagsås (LL1101) and Abild (LL1107) respectively. The presence of porous orthopyroxene in Dagsås and weathered material in Ablid can explain their water absorption values.

The water absorption values are restricted to a narrow interval and do not allow a correlation with the technical properties.

Table 2. Locality name, sample ID and water absorption values for each sample. The water absorption value (A_b) is presented in weight percent.

Locality name	Sample	A_b
Dagsås	LL1101	0.3
Stavsjö	LL1102	0.2
Ljungby	LL1103	0.1
Knobesholm	LL1104	0.2
Hallandssten	LL1105	0.1
Mokrik	LL1106	0.1
Abild	LL1107	0.4
Fridhemsberg	LL1108	0.2
Töresjö	LL1109	0.2
Toppeberg	LL1110	0.2
Vräk	LL1111	0.2
Köinge	LL1112	0.2

6.3 Micro analyses

The results of the micro analyses are listed in Appendix 5.

6.3.1 Microcracks

Rocks containing a high amount of light minerals such as quartz and feldspars behave in a brittle manner. These minerals have low fracture energies and therefore crack easily and obtain a high LA value (Lindqvist et al., 2007; Tavares & das Neves, 2008).

Various types of fractures and their relative frequencies in each sample are shown in figure 31. The frequency of the total fractures (purple line) correlates well with the frequency of grain boundary fractures (green line). In all analyzed samples the frequency of grain boundary fractures makes up the largest portion of the total frequency of fractures.

The total frequency of fractures in all samples is plotted against their LA values in figure 32.

The sample from Dagsås (LL1101) shows the lowest frequency of total fractures and the best LA value (0.65 fractures/mm, 19 %; Figs. 31 and 32). The fluorescent image (Fig. 33A) confirms the low frequency of fractures. The fluorescent dye seems to prefer the porous orthopyroxene (the fluorescent areas in Fig. 33A and B).

The sample from Ljungby (LL1103) shows the second best LA value (22 %), has a low frequency of total fractures, but shows the highest frequency of transgranular fractures (2.23 fractures/mm; 0.48 fractures/mm; Figs. 31, 32, 34A and B).

The highest frequency of total fractures and an intermediate LA value (33 %) is shown by the sample from Köinge (LL1112; 5.36 fractures/mm; Figs. 31, 32, 35A and B).

The sample from Knobesholm (LL1104) shows an intermediate LA value (30 %) and contains the second highest frequency of total fractures (4.62 fractures/mm; Figs. 31, 32, 36A and B).

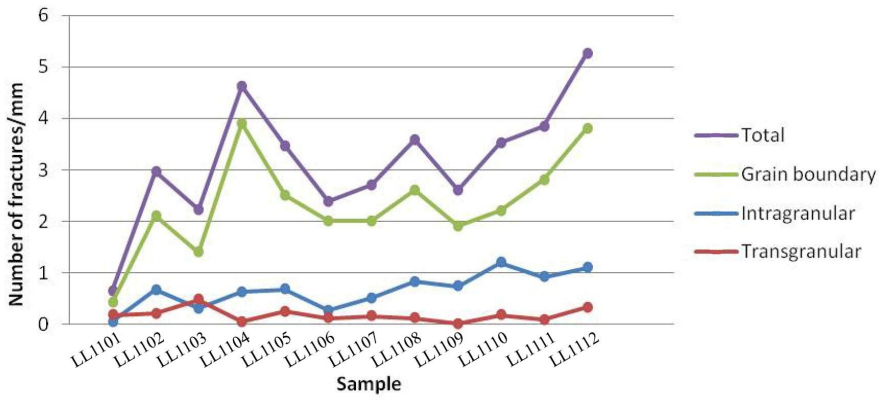

Fig. 31. Diagram showing the relative frequency of different types of fractures per mm in each sample. In all investigated samples the frequency of grain boundary fractures (green line) constitute the largest portion of the total frequency of fractures (purple line). LL1101 = Dagsås, LL1102 = Stavsjö, LL1103 = Ljungby, LL1104 = Knobesholm, LL1105 = Hallandssten, LL1106 = Mokrik, LL1107 = Abild, LL1108 = Fridhemsberg, LL1109 = Töresjö, LL1110 = Toppeberg, LL1111 = Vräk and LL1112 = Köinge.

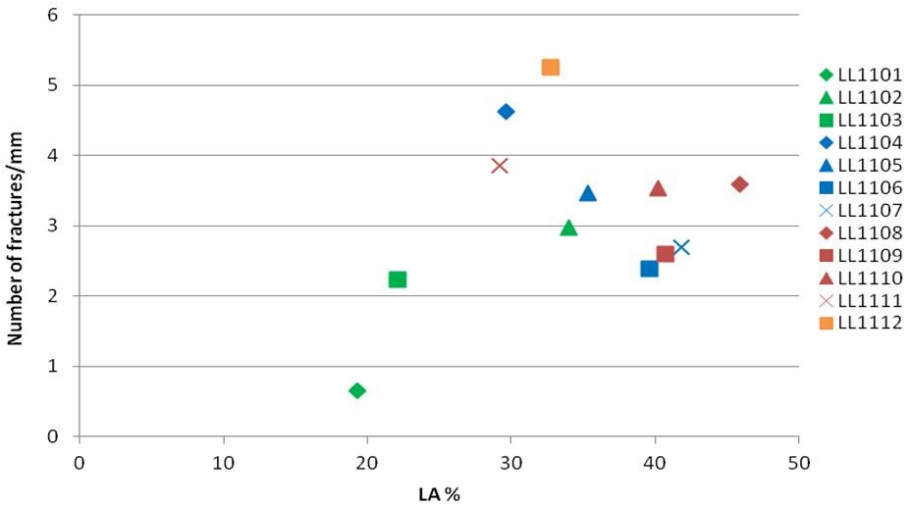

Fig. 32. Diagram showing the frequency of total fractures for all samples plotted against their LA values. LL1101 = Dagsås, LL1102 = Stavsjö, LL1103 = Ljungby, LL1104 = Knobesholm, LL1105 = Hallandssten, LL1106 = Mokrik, LL1107 = Abild, LL1108 = Fridhemsberg, LL1109 = Töresjö, LL1110 = Toppeberg, LL1111 = Vräk and LL1112 = Köinge.

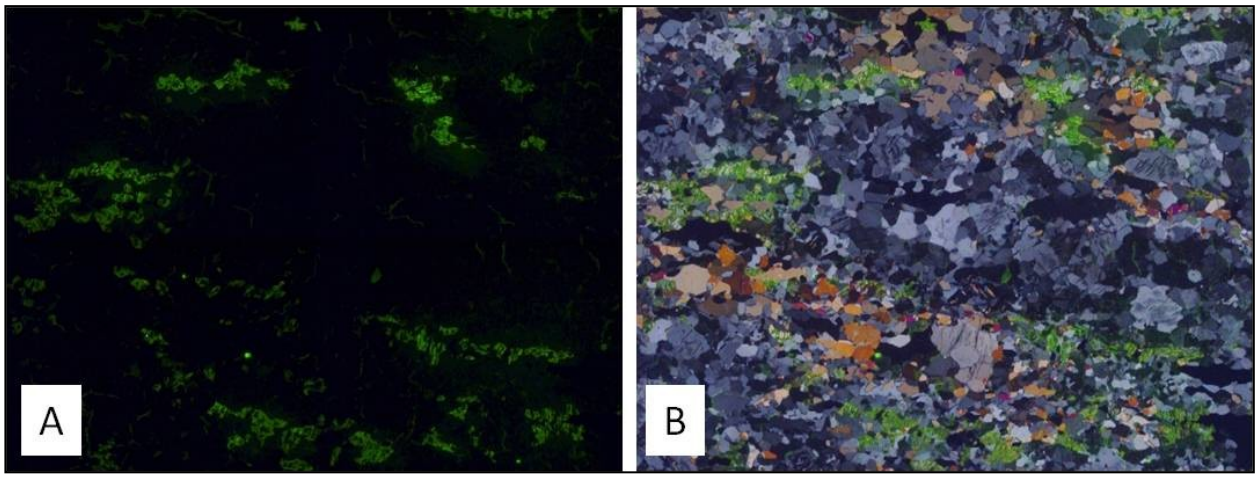

Fig. 33. Thin section images (4.2×5.6 mm) of LL1101 F1 (Dagsås). A) Fluorescent image and B) Combined image (polarized and fluorescent images); The thin section shows a low frequency of fractures. Fluorescent areas are orthopyroxene.

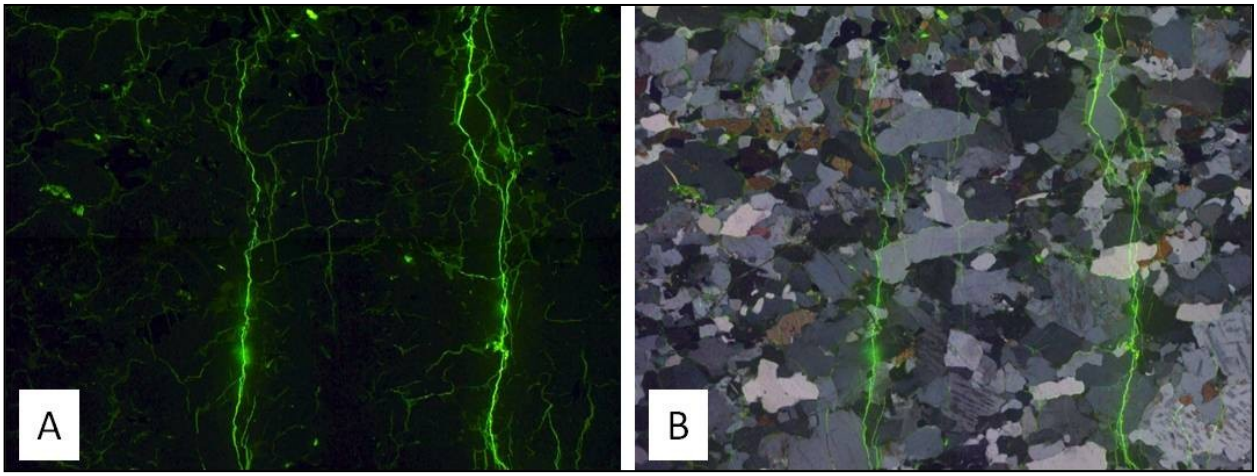

Fig. 34. Thin section images (4.2×5.6 mm) of LL1103 F1 (Ljungby). A) Fluorescent image and B) Combined image (polarized and fluorescent images); The rock has a low frequency of total fractures but shows the highest frequency of transgranular fractures.

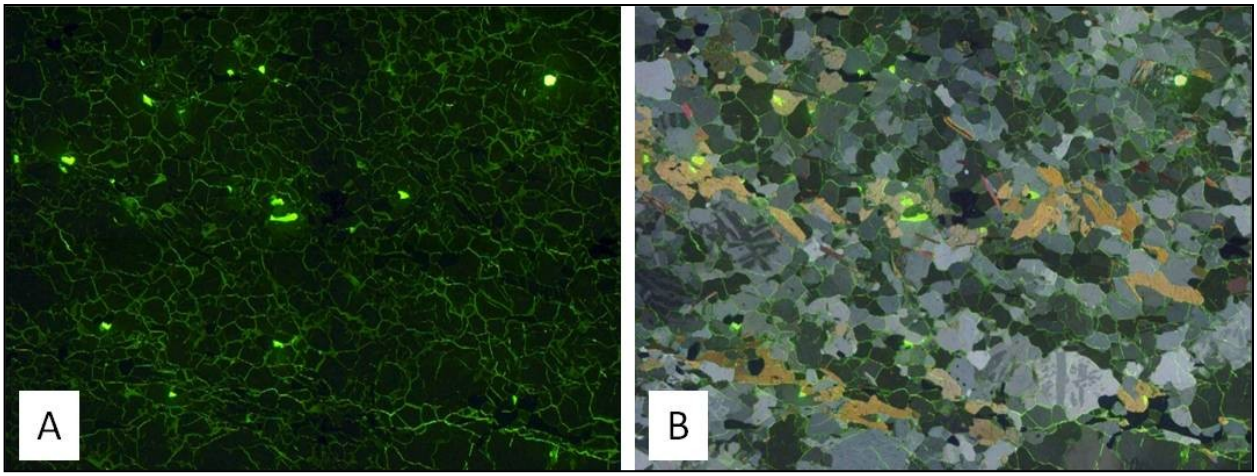

Fig. 35. Thin section images (4.2×5.6 mm) of thin LL1112 TL (Köinge). A) Fluorescent image and B) Combined image (polarized and fluorescent images); The highest frequency of total fractures occur in this rock.

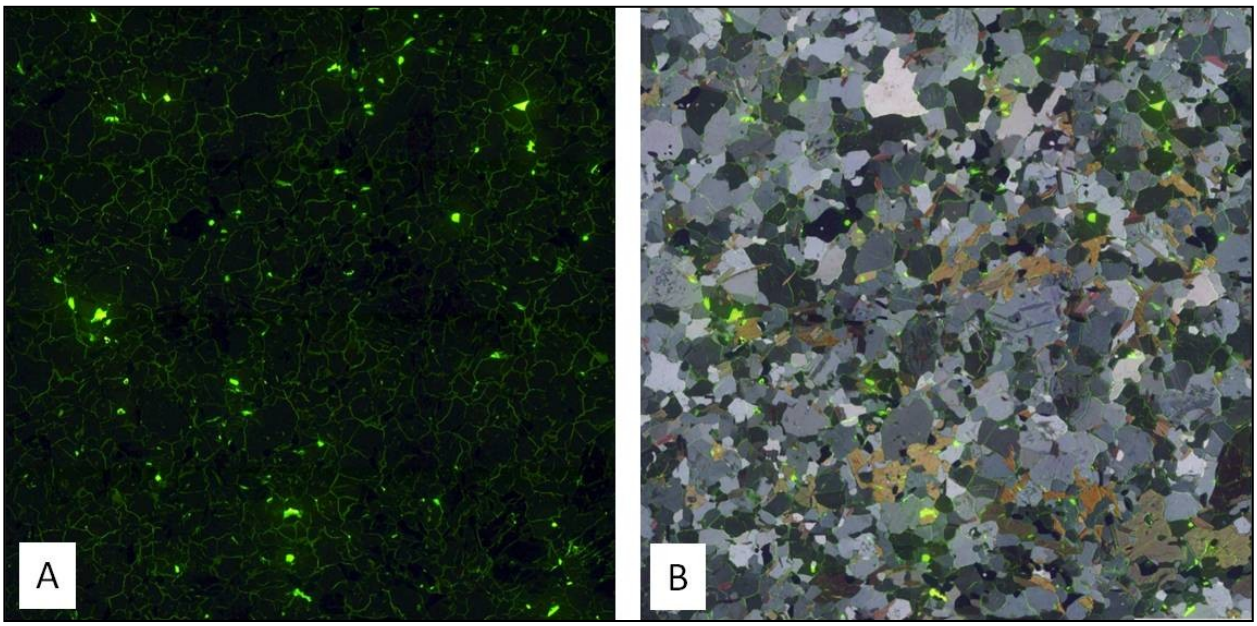

Fig. 36. Thin section images (8.4×8.4 mm) of LL1104 (Knobesholm). A) Fluorescent image and B) Combined image (polarized and fluorescent images); The rock has a high frequency of total fractures.

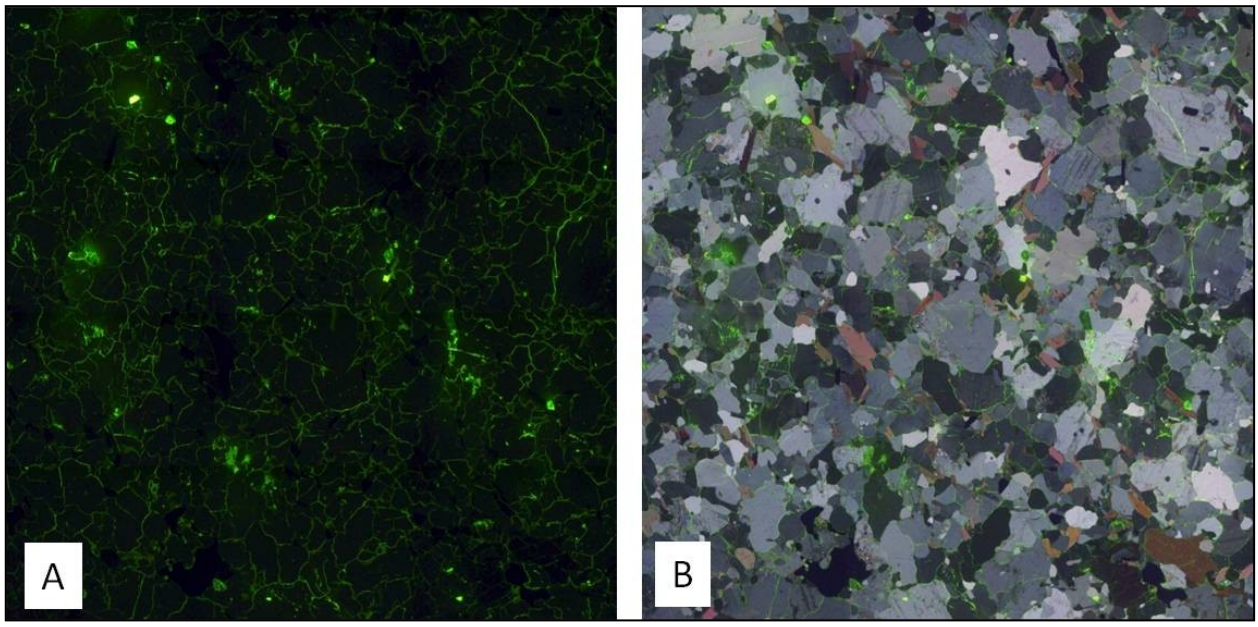

Fig. 37. Thin section images (8.4×8.4 mm) of LL1111 TL (Vräk). A) Fluorescent image and B) Combined image (polarized and fluorescent images); The rock has a high frequency of total fractures.

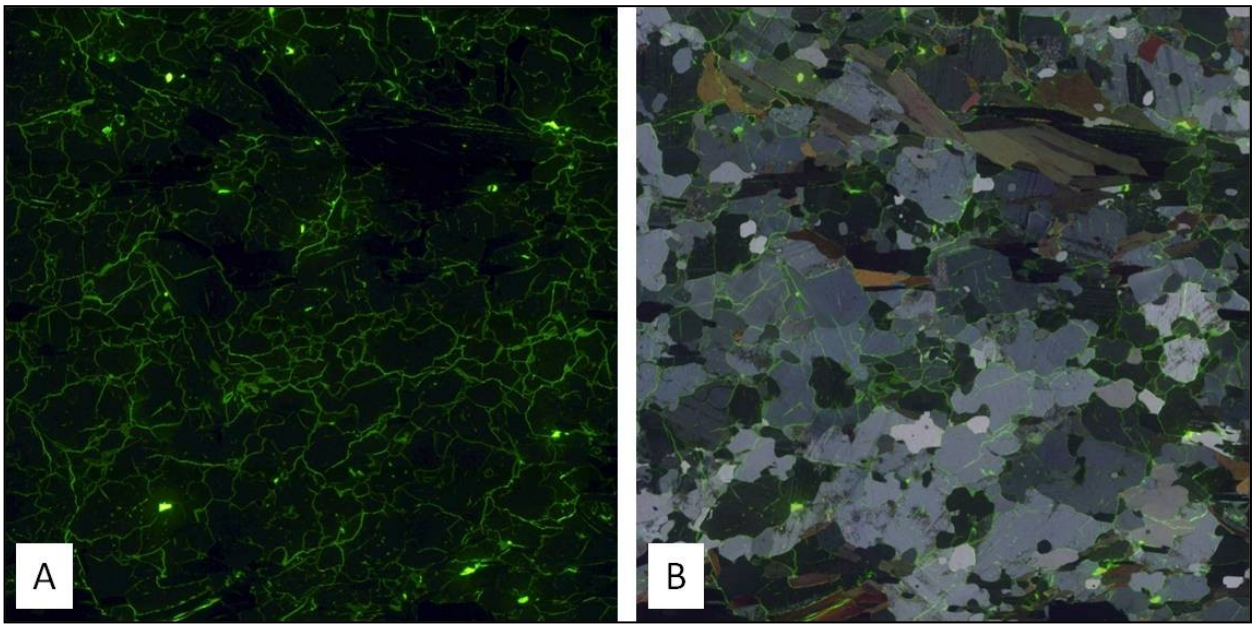

Fig. 38. Thin section images (8.4×8.4 mm) of LL1108 F1 (Fridhemsberg). A) Fluorescent image and B) Combined image (polarized and fluorescent images); The rock has a high frequency of fractures.

Intermediate LA value (29 %) and a high frequency of total fractures are shown in sample Vräk (LL1111; 3.85 fractures/mm; Figs. 31, 32, 37A and B).

The sample from Fridhemsberg (LL1108) shows a high frequency of total fractures (3.59 fractures/mm; Fig. 31). This is confirmed by the fluorescent and combined images (Figs. 38A and B). Fridhemsberg has a lower frequency of grain boundary fractures (and total fractures) than Knobesholm (LL1104) and Vräk (LL1111; 2.6 fractures/mm vs. 3.9 and 2.8 fractures/mm respectively) but higher frequency of transgranular fractures (0.12 fractures/mm vs. 0.05 and 0.09 fractures/mm respectively). Fridhemsberg shows the highest LA value (46 %; Fig. 32).

The results show that the fracture frequency has limited influence on the LA value for this population of rocks. The frequency of the fractures affects the LA values while the type of fractures does not seem to affect the LA values to the same extent.

6.3.2 Mineral grain size and mineral grain size distribution

Grain size is an important parameter that has to be considered when establishing the strength of various rock materials. A fine grained material is stronger than a coarse grained (Lundqvist & Göransson, 2001).

A good correlation between a low mean grain size and a low LA value is shown in figure 39. This trend is obvious for Dagsås (LL1101; 0.17 mm, 19 %) and Ljungby (LL1103; 0.33 mm and 22 %). Knobesholm (LL1104), Vräk (LL1111) and Köinge (LL1112) show low mean grain sizes but intermediate LA values (0.33 mm and 30 %; 0.36 mm and 29 %; 0.28 mm and 33 %). Fridhemsberg (LL1108) and Toppeberg (LL1110) have high mean grain sizes and high LA values (0.52 mm and 46 %; 0.72 mm and 40 %).

Knobesholm (LL1104) and Töresjö (LL1109) contain a large proportion of fine grained materials (87 % and 81 % is ≤ 1mm respectively; Fig.40). The former sample also contains a significant proportion of very fine grained materials (57 % is < 0.5 mm). Another sample containing a significant proportion of very fine grained grains is Dagsås (LL1101; 43 % is <0.5 mm; Fig. 40). Abild contains a large proportion of medium grained minerals (55 % >1 mm).

A high proportion of either very fine grained or fine grained materials seem to contribute to a better LA value.

6.3.3 Perimeter

A good correlation ($perimeter_{total}$ = -0.11 × LA + 6.4, R^2= 0.87; excluding samples Ljungby and Vräk) between high total perimeter and low LA value are shown in figure 41. This trend is shown by all samples except Ljungby (LL1103) and Vräk (LL1111). The low total perimeter of sample Ljungby can be explained by its very low content of biotite. Examining sample Vräk in thin section, it shows a low content of amphibole (pyroxene is absent) which can explain the low total perimeter. Sample Dagsås (LL1101) shows the highest total perimeter and lowest LA value (4.1 mm/mm^2 and 19 %) while sample Fridhemsberg (LL1108) shows the lowest total perimeter and the highest LA value (1.4 mm/mm^2 and 46 %; Fig. 41). This is likely due to that the more fine grained material (Dagsås) will contain more objects to be measures and therefore have a larger perimeter.

The samples plot on a line, with the exception of Vräk (LL1111), and show a trend where samples with high perimeter of amphibole + pyroxene tend to have a low LA value (Fig. 42). Since sample Vräk has a low content of amphibole (observation in the microscope), pyroxene is absent, explains the low perimeter of amphibole + pyroxene. Dagsås (LL1101) and Ljungby (LL1103) from the Varberg granulite gneiss domain show high perimeter of amphibole + pyroxene and low LA values (2.4 mm/mm^2 and 19 %; 1.4 mm/mm^2 and 22 %; Fig. 42). Stavsjö (LL1102), also located in the Varberg granulite gneiss domain, show high perimeter of amphibole + pyroxene but show an intermediate LA value (1.5 mm/mm^2 and 34 %; Fig. 42). Samples Fridhemsberg (LL1108) and Töresjö (LL1109) from the Skene migmatite gneiss domain

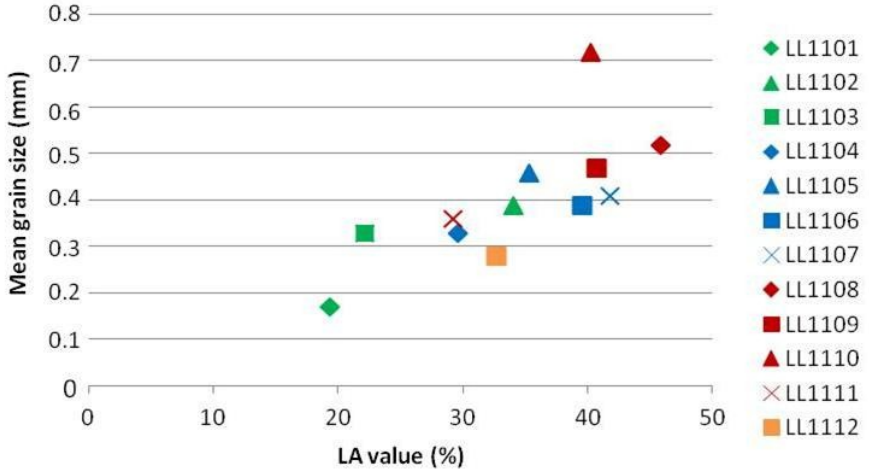

Fig. 39. Samples with low mean grain size tend to have a low LA value. LL1101 = Dagsås, LL1102 = Stavsjö, LL1103 = Ljungby, LL1104 = Knobesholm, LL1105 = Hallandssten, LL1106 = Mokrik, LL1107 = Abild, LL1108 = Fridhemsberg, LL1109 = Töresjö, LL1110 = Toppeberg, LL1111 = Vräk and LL1112 = Köinge.

have a low perimeter of amphibole + pyroxene and show high LA values (0.13 mm/mm^2 and 46 %; 0.00 mm/mm^2 and 41 %). Sample Vräk (LL1111), also located in the Skene migmatite gneiss domain, shows a low perimeter of amphibole + pyroxene but show an intermediate LA value (0.28 mm/mm^2 and 29 %; Fig. 42).

A plot of perimeter of opaque minerals + garnet against LA and A_N values reveals a slight decrease in LA and A_N values with increasing perimeter. The Dagsås sample (LL1101) is an exception and shows a distinctly higher perimeter in relation to the LA and A_N values (Figs. 43 and 44). This sample has the highest content of opaque minerals and gar-

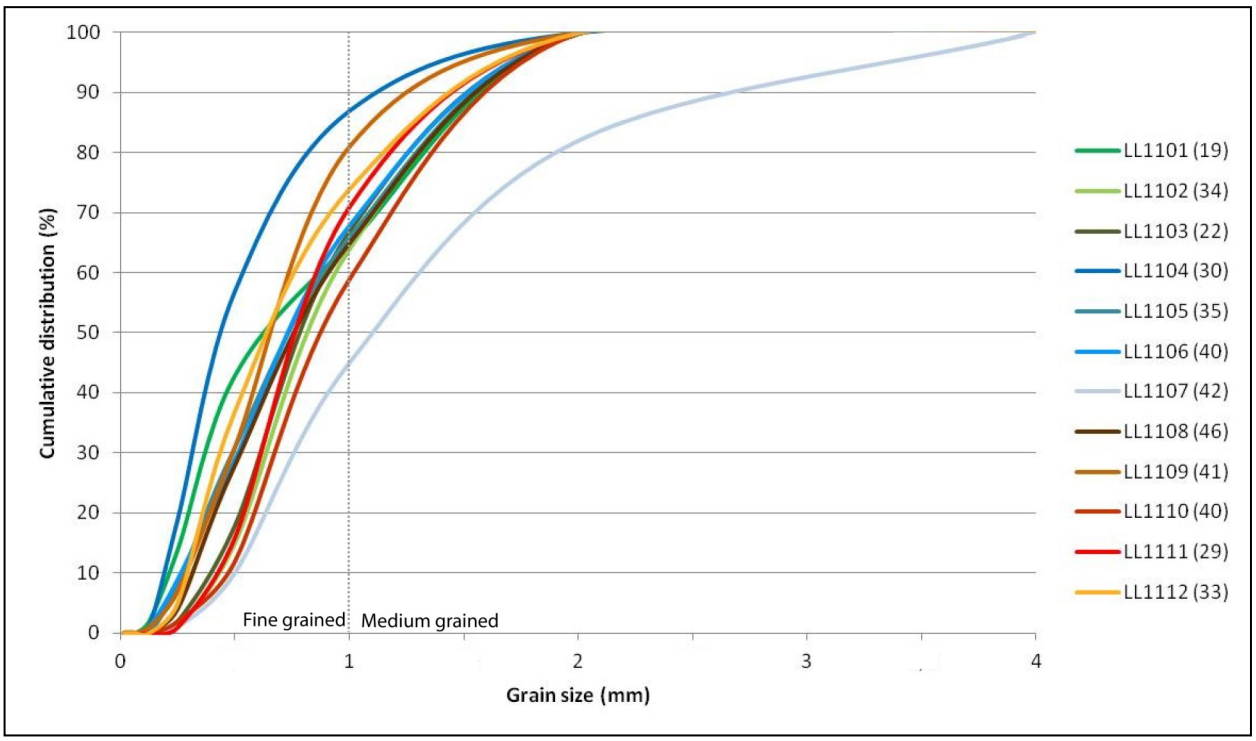

Fig. 40. Cumulative mineral grain size distribution for every sample. The LA value for each sample is in parentheses in the legend. LL1101 = Dagsås, LL1102 = Stavsjö, LL1103 = Ljungby, LL1104 = Knobesholm, LL1105 = Hallandssten, LL1106 = Mokrik, LL1107 = Abild, LL1108 = Fridhemsberg, LL1109 = Töresjö, LL1110 = Toppeberg, LL1111 = Vräk and LL1112 = Köinge.

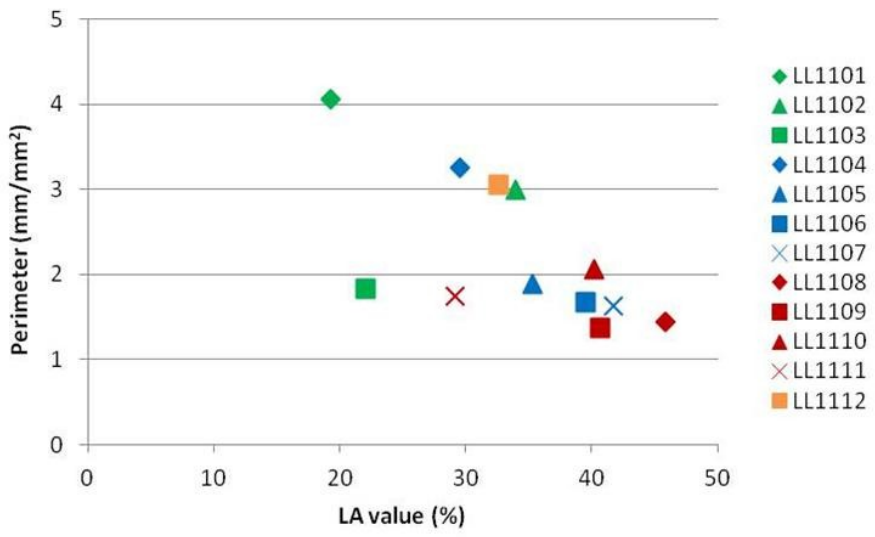

Fig. 41. A good correlation between high total perimeter and low LA values are observed. Ljungby (LL1103) and Vräk (LL1111) are two exceptions. LL1101 = Dagsås, LL1102 = Stavsjö, LL1103 = Ljungby, LL1104 = Knobesholm, LL1105 = Hallandssten, LL1106 = Mokrik, LL1107 = Abild, LL1108 = Fridhemsberg, LL1109 = Töresjö, LL1110 = Toppeberg, LL1111 = Vräk and LL1112 = Köinge.

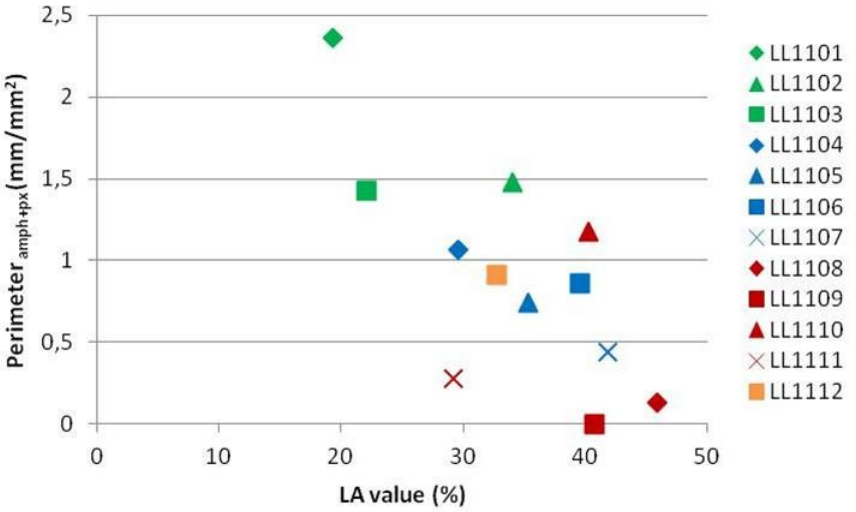

Fig. 42. The samples with high perimeter of amphibole + pyroxene tend to show a low LA value. Vräk (LL1111) plots of the line and shows an intermediate LA value and a low perimeter. LL1101 = Dagsås, LL1102 = Stavsjö, LL1103 = Ljungby, LL1104 = Knobesholm, LL1105 = Hallandssten, LL1106 = Mokrik, LL1107 = Abild, LL1108 = Fridhemsberg, LL1109 = Töresjö, LL1110 = Toppeberg, LL1111 = Vräk and LL1112 = Köinge.

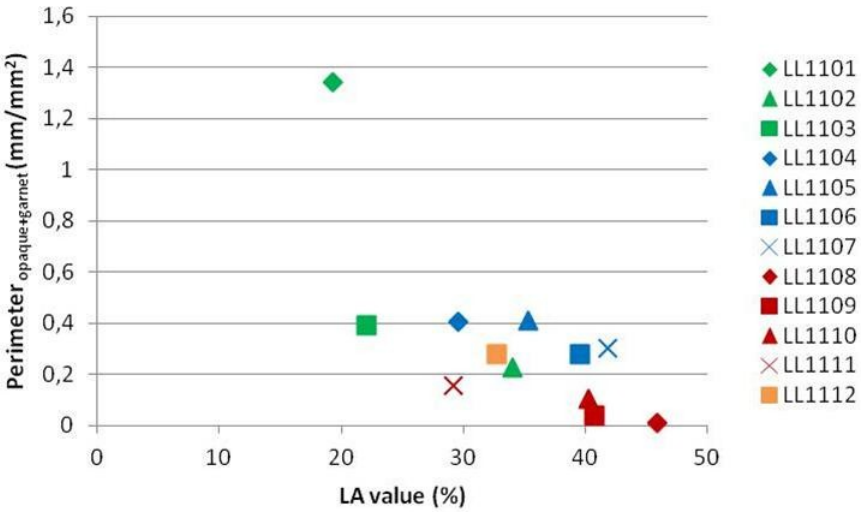

Fig. 43. A trend with high perimeter of opaque minerals + garnet and low LA values are observed. Dagsås (LL1101) plot of the line and shows a distinctly higher perimeter value. LL1101 = Dagsås, LL1102 = Stavsjö, LL1103 = Ljungby, LL1104 = Knobesholm, LL1105 = Hallandssten, LL1106 = Mokrik, LL1107 = Abild, LL1108 = Fridhemsberg, LL1109 = Töresjö, LL1110 = Toppeberg, LL1111 = Vräk and LL1112 = Köinge.

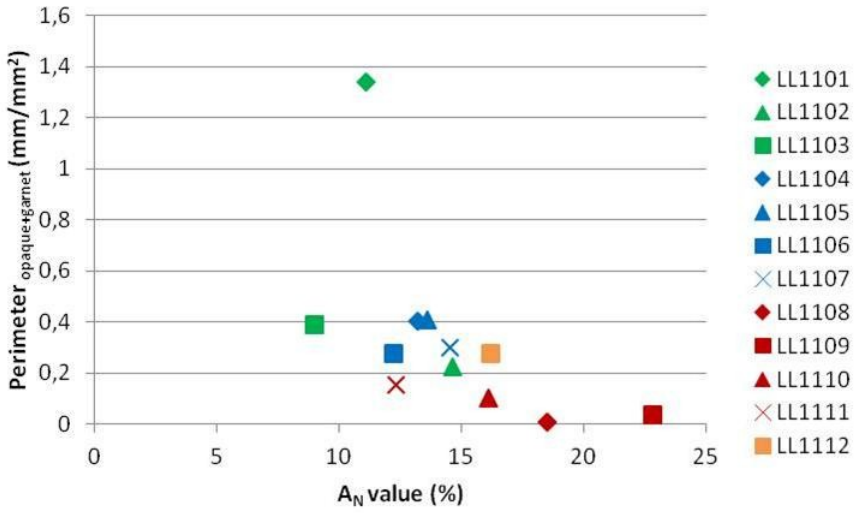

Fig. 44. The samples show a trend where high perimeter of opaque minerals + garnet tend to result in low A_N values. Dagsås (LL1101) plots off trend. LL1101 = Dagsås, LL1102 = Stavsjö, LL1103 = Ljungby, LL1104 = Knobesholm, LL1105 = Hallandssten, LL1106 = Mokrik, LL1107 = Abild, LL1108 = Fridhemsberg, LL1109 = Töresjö, LL1110 = Toppeberg, LL1111 = Vräk and LL1112 = Köinge.

net (microscope observation) but is also the most fine grained one, thus the high perimeter. The samples located in the Skene migmatite gneiss domain; Fridhemsberg (LL1108), Töresjö (LL1109), Toppeberg (LL1110) and Vräk (LL1111) show the lowest perimeters of opaque minerals + garnet (Figs. 43 and 44). They also show the highest LA and A_N values except Vräk which has intermediate LA and A_N values (29 % and 12 % respectively).

The mechanical properties of amphibole, pyroxene, garnet and opaque minerals differ from that of quartz and feldspars. The size of individual mineral grains as well as monomineralic aggregates of these minerals has a significant influence of the mechanical properties of the aggregate produced from these rocks.

6.3.4 Foliation index (FIX)

According to the FIX index, samples from Dagsås (LL1101), Stavsjö (LL1102), Knobesholm (LL1104) and Abild (LL1107) are classified as isotropic rocks (Table 3). The most anisotropic samples are Mokrik (LL1106) and Toppeberg (LL1110) with FIX values of 1.34 and 1.32 respectively. The rest of the samples show intermediate FIX values (values between 1.13-1.28).

Table 3. Locality name, sample ID and FIX value for each sample. According to Hellman et al. (2011) a material with a FIX value greater than 1.10 is anisotropic.

Locality name	Sample	FIX
Dagsås	LL1101	1.05
Stavsjö	LL1102	1.09
Ljungby	LL1103	1.23
Knobesholm	LL1104	1.08
Hallandssten	LL1105	1.16
Mokrik	LL1106	1.34
Abild	LL1107	1.09
Fridhemsberg	LL1108	1.28
Töresjö	LL1109	1.20
Toppeberg	LL1110	1.32
Vräk	LL1111	1.27
Köinge	LL1112	1.13

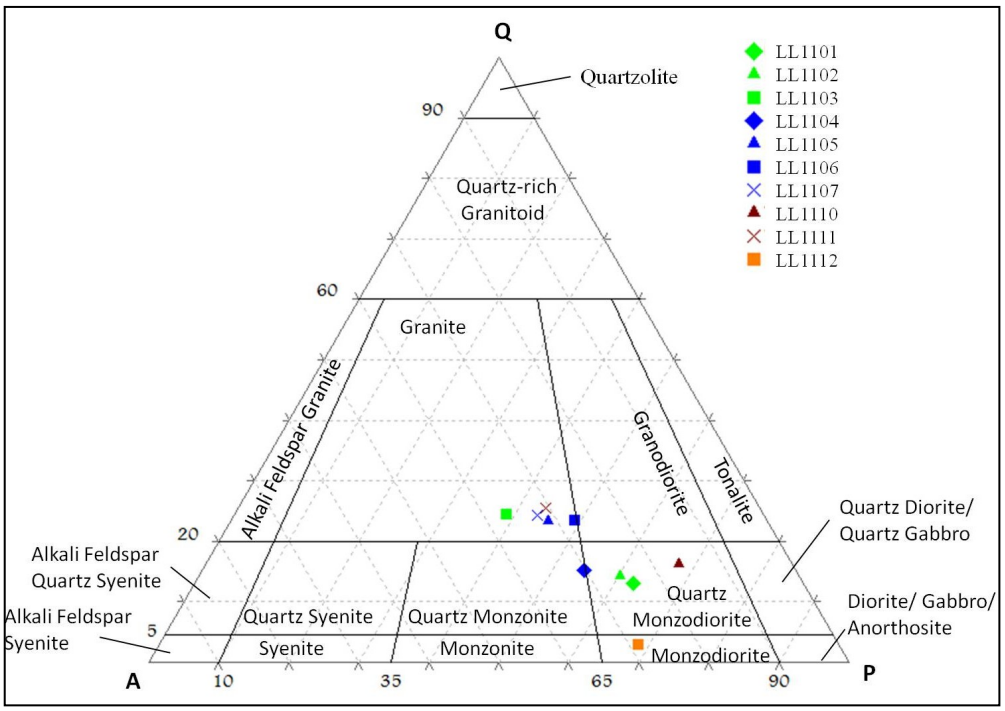

Fig. 45. QAP classification diagram showing the normative mineralogy for each sample. LL1101 = Dagsås, LL1102 = Stavsjö, LL1103 = Ljungby, LL1104 = Knobesholm, LL1105 = Hallandssten, LL1106 = Mokrik, LL1107 = Abild, LL1110 = Toppeberg, LL1111 = Vräk and LL1112 = Köinge. Modified from Le Maitre (1989).

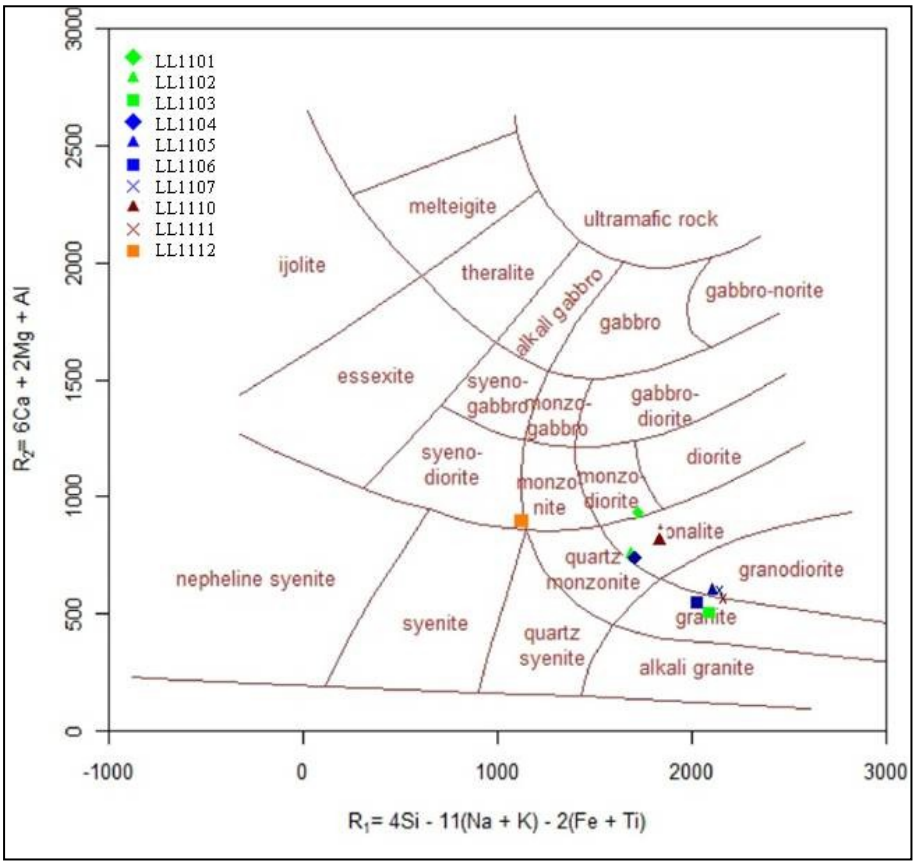

Fig. 46. R1-R2 classification diagram showing the bulk chemical composition of each sample with regard to silica saturation, Fe/Mg ratio and plagioclase composition. LL1101 = Dagsås, LL1102 = Stavsjö, LL1103 = Ljungby, LL1104 = Knobesholm, LL1105 = Hallandssten, LL1106 = Mokrik, LL1107 = Abild, LL1110 = Toppeberg, LL1111 = Vräk and LL1112 = Köinge. Modified from De La Roche et al. (1980).

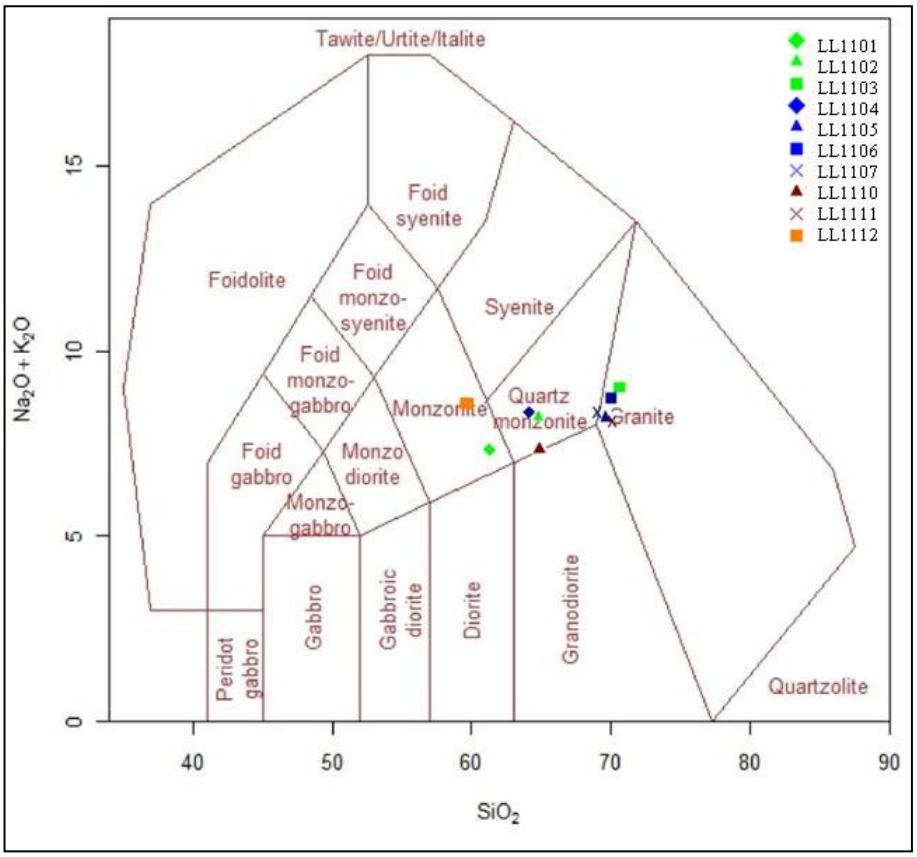

Fig. 47. TAS classification diagram showing the bulk chemical composition of each sample with respect to their total alkali (Na_2O + K_2O) and silica content (SiO_2). LL1101 = Dagsås, LL1102 = Stavsjö, LL1103 = Ljungby, LL1104 = Knobesholm, LL1105 = Hallandssten, LL1106 = Mokrik, LL1107 = Abild, LL1110 = Toppeberg, LL1111 = Vräk and LL1112 = Köinge. Modified from Middlemost (1985).

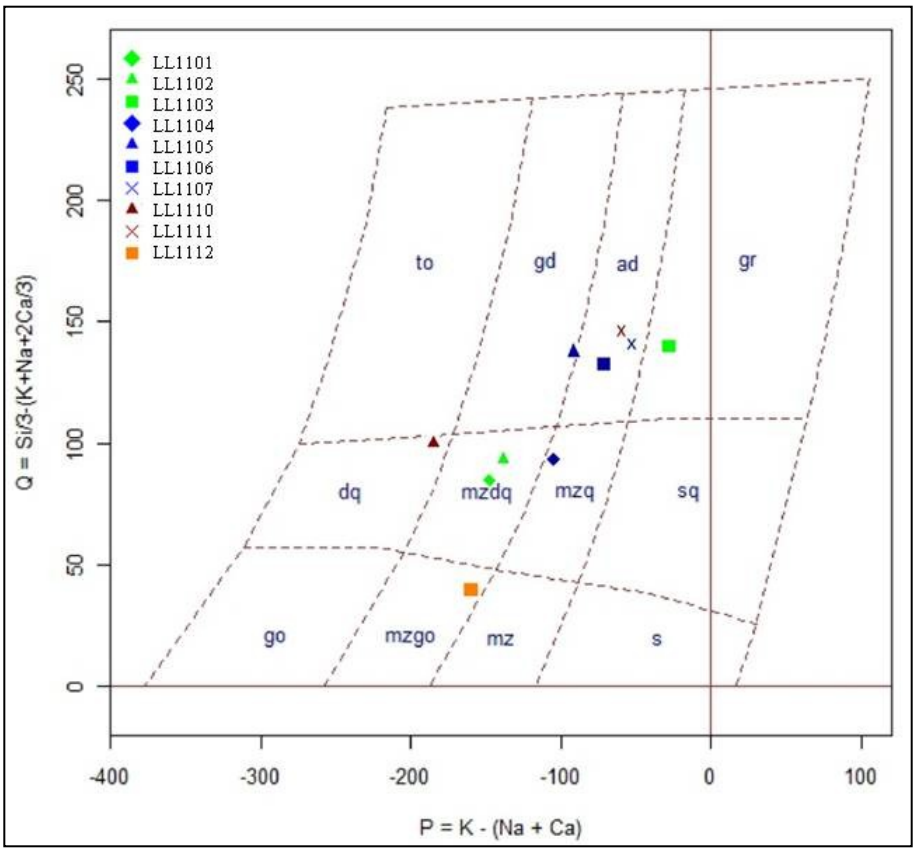

Fig. 48. P-Q diagram showing the bulk chemical composition of each sample with respect to the proportions of K-feldspar and plagioclase (P = K – (Na + Ca) to quartz (Q = Si/3 – (K + Na + 2Ca/3). to=tonalite, gd= granodiorite, ad= adamellite (quartz monzonite), gr= granite, dq= quartz diorite, mzdq=quartz monzodiorite, mzq= quartz monzonite, sq= quartz syenite, go= gabbro, mzgo=monzogabbro, mz=monzonite, s= syenite. LL1101 = Dagsås, LL1102 = Stavsjö, LL1103 = Ljungby, LL1104 = Knobesholm, LL1105 = Hallandssten, LL1106 = Mokrik, LL1107 = Abild, LL1110 = Toppeberg, LL1111 = Vräk and LL1112 = Köinge. Modified from Debon & Le Fort (1983).

6.4 Chemistry

The mineralogy (high or low content of light minerals such as quartz and feldspars) can give an indication of the mechanical behavior (degree of brittle manner) of a rock; which is reflected in the technical values of the samples.

The results from the chemical analyses are compiled in appendix 6.

6.4.1 Bulk rock geochemical classification

Geochemical classification diagrams of bulk geochemistry are shown in figures 45-48. The samples plot in several different compositional fields in the different diagrams.

Most of the samples from the Hallandia gneiss domain (blue color in the classification diagrams) seems to plot towards the silica rich compositional fields in the diagrams while the sample from the Svarten gneiss domain (orange color in the classification diagrams) and the majority of the samples located in the Varberg granulite gneiss domain (Dagsås and Stavsjö; green color in the classification diagrams) plots towards compositional fields containing less wt % SiO_2 (Figs. 45-48).

No clear trend can be observed between the geochemistry of the samples and their technical properties.

7. Discussion

Here the technical properties of the samples are compared to the quantitative results, field observations and thin sections descriptions in order to explain their mechanical properties. The results from the technical, qualitiative and quantitative analyses are compiled in Appendix 2-6. The discussion begins with the samples (Dagsås and Ljungby) showing the best technical properties, followed by the samples (Fridhemsberg and Töresjö) with poorest quality and ending with the samples showing intermediate values between these extremes.

Samples Ljungby (LL1103) and Dagsås (LL1101) are located in the Varberg granulite gneiss domain and are classified as aggregate quality class 1 and 2 materials respectively (Fig. 29). These two samples show the best LA and A_N values (19 % and 11 %; 22 % and 9 %; Fig. 29). In the field both samples lack a lineation, a metamorphic layering and veins are sparse to absent. In thin section both samples have antiperthitic feldspars, pyroxene, reddish brown biotite and brownish green hornblende. The biotite content is very low, titanite is absent and no tartan twinning is observed in the feldspar. The low content of biotite of both samples is probably contributing to their good (low) A_N values. Sample Dagsås (LL1101) has a higher A_N value probably due to a higher content of dark (Fe and Ti bearing) minerals, also shown by the geochemical analyses (Figs. 29, 45-48) and its high mea-

sured density (2.79 g/cm^3; Fig. 30). Both samples show a low frequency of fractures (Dagsås 0.65 fractures/mm; Ljungby (2.23 fractures/mm; Figs. 31 and 32), a low mean grain size (Dagsås 0.17 mm; Ljungby 0.33 mm; Fig. 39) and high perimeter values (except Ljungby when considering the total perimeter because the perimeter for the analyzed minerals cannot compensate for the very low biotite content (low perimeter of biotite); Figs. 41-44). This corresponds well to the good technical properties of the samples. Thin sections of the Dagsås sample show that this sample is much more fine grained in general and contains more fine grained material than the sample from Ljungby (Figs. 33B, 34B and 40). The higher LA value of the Ljungby sample can be explained by its higher frequency of fractures, lower perimeter values, are more coarse grained and has a coarser mean grain size than the Dagsås sample. A rock containing high frequency of microfractures tend to fragment more easily in the Los Angeles mill. The higher LA value of the Ljungby sample can explain the lower LA/A_N ratio shown by the Dagsås sample.

Fridhemsberg (LL1108) and Töresjö (LL1109) are both located in the Skene migmatite gneiss domain; these samples have the highest LA and A_N values of all and are classified as aggregate quality class 3 materials (46 % and 19 %; 41 % and 23 %; Fig. 29). In the field the rocks has a pronounced metamorphic layering consisting of leucosome and mesosome, and no remnants of primary igneous textures i.e. feldspar augens or a relict coarse grained fabric. Leucosome veins are abundant and has sugary texture (unstrained). In thin section tartan twinning is common and well developed, while antiperthite is sparse. Orthoclase occurs occasionally as remnant cores in larger microcline crystals. Biotite is dark brown and occurs as aggregates, bands and individual grains parallel to the foliation. Hornblende is bluish green when present. High contents of biotite in the samples can explain their high A_N values but also the very low LA/A_N ratio (1.8) and higher density of Töresjö (2.69 g/cm^3; Figs. 29 and 30). None of the samples have a very low or very high frequency of fractures. However, Fridhemsberg (LL1108) shows a slightly higher frequency (3.59 fractures/mm vs. 2.6 fractures/mm; Figs. 31 and 32). This result is expected for a rock with a lower density (higher content of light minerals such as quartz and feldspars) and therefore behaving in a more brittle manner (Fridhemsberg 2.65 g/cm^3; Fig. 30). Both samples show high mean grain sizes (Fridhemsberg 0.52 mm; Töresjö 0.47 mm; Fig. 39) and very low perimeter values which correlate well with their high technical values (Figs. 41-44). Töresjö (LL1109) contains a large proportion of fine grained materials (81 % < 1mm; Fig. 40). Both samples are anisotropic (high FIX values; Table 3); biotite occurs as individual grains, aggregates and bands parallel to the foliation, which might form weak discontinuities and contribute to their high LA values. Fridhemsberg (LL1108) shows a lower A_N value due to lower content of dark minerals (geochemistry and density) and a higher LA value probably due to a higher frequency of fractures, higher mean grain size, is less fine grained and a higher FIX value (more anisotropic).

Samples Knobesholm (LL1104) from the Hallandia gneiss domain and Vräk (LL1111) from the Skene migmatite gneiss domain show moderate LA and A_N values and are classified as aggregate quality class 2 materials (30 % and 13 %; 29 % and 12 %; Fig. 29). In the field the samples show a pronounced lineation (often defined by deformed pinkish feldspar aggregates). The samples have antiperthitic feldspars; tartan twinning is usually rare or not very well developed. The moderate A_N values of the samples can be explained by the intermediate content of dark minerals. The higher density of Knobesholm (LL1104; 2.7 g/cm^3) correlates with the geochemical composition (Knobesholm plots in more silica poor stability fields than Vräk; Figs. 30, 45-48). This explains the lower LA/A_N ratio of Knobesholm (Fig. 30). Knobesholm show high perimeter values while Vräk has low perimeter values (Figs. 41-44). Both samples have low mean grain sizes (Knobesholm 0.33 mm; Vräk 0.36 mm; Fig. 39) but the thin sections from Knobesholm looks more fine grained (Figs. 36B vs. 37B). The sample from Knobesholm contains a significant amount of fine grained material (87 % $\leq$ 1mm; Fig. 40). The low mean grain sizes of both samples may compensate for their high frequency of fractures (Knobesholm 4.62 fractures/mm; Vräk 3.85 fractures/mm; Figs. 31 and 32), and result in moderate LA values (Figs. 31, 32 and 39). The lower mean grain size, higher perimeter and more fine grained Knobesholm compensate for its higher frequency of fractures, resulting in technical properties similar to those for the sample from Vräk (LL1111).

The rest of the samples (Stavsjö, Hallandssten, Mokrik, Abild, Toppeberg and Köinge) are classified as aggregate quality class 3 material (Fig. 29) and have LA and A_N values plotting in between the samples with best and worst technical properties. The variation in LA values is more pronounced than the variation in A_N values. If the LA value for all samples was lowered they would all fall into aggregate quality class 2.

Sample Stavsjö (LL1102) is located in the Varberg granulite gneiss domain. The LA/A_N ratio (2.33), density (2.7 g/cm^3), mean grain size (0.39 mm), frequency of fractures (2.97 fractures/mm) and intermediate-high perimeter values correlate well with the moderate technical values (Figs. 30-32, 39, 41-44). The isotropy (1.09 FIX value) of the sample and the occurrence of biotite as randomly oriented individual grains and aggregates can contribute to keep the moderate technical values.

Hallandssten (LL1105) is located in the Hallandia gneiss domain. The technical values (LA is 35 % and A_N is 14 %) are average and correlate well with the intermediate values of the LA/A_N ratio (2.6), geochemistry (Hallandssten plots in the silica rich stability fields; Figs. 45-48), density (2.68 g/cm^3), frequency of

fractures (3.46 fractures/mm) and intermediate-high perimeter values (Figs. 29, 30-32, 41-44). These values might compensate for the high mean grain size (0.46 mm; Fig 39) and anisotropy (1.16 FIX value; Table 3) resulting in moderate technical values.

Sample Mokrik (LL1106), is also located in the Hallandia gneiss domain. It shows, however, an unexpected high LA/A_N ratio (3.2; Fig. 30). In this case either high LA value and/or low A_N value can obtain this ratio. The intermediate values of the mean grain size (0.39 mm; Fig. 39), perimeter values, the geochemistry analyses and density (2.69 g/cm^3; Fig. 30) correlate well with the technical values. This sample is the most anisotropic one (1.34 FIX value; Table 3) and the low frequency of fractures (2.39 fractures/mm; Figs. 31 and 32) do not seem to lower the LA value enough, thus resulting in a high LA value (40 %, Fig. 29).

Sample Abild (LL1107), located in the Hallandia gneiss domain, contains a significant amount of medium grained material (55 % >1 mm; Fig. 40) which is reflected in its high LA value (42 %; Figs. 29 and 40). The high LA/A_N ratio (2.9) is a reflection of the technical values. The LA value correlates well with geochemical analyses (Abild plot in the silica rich stability fields; Figs. 45-48), moderate density (2.66 g/cm^3), the intermediate-high mean grain size (0.41mm; Fig. 39) and the intermediate-low perimeter values (Figs. 41-44). The fact that the sample is isotropic (1.09 FIX value) and shows a low frequency of fractures (2.7 fractures/mm; Figs. 31 and 32) might contribute to and keep the technical values on a moderate level. The sample shows the highest water absorption value, 0.4 wt %, which does not correlate with the frequency of fractures but can be explained by weathered rock material.

Sample Toppeberg (LL1110), located in the Skene migmatite gneiss domain, has the highest mean grain size (0.72 mm) and should therefore show a higher LA value (40 %; Figs. 29 and 39). Some moderate values, such as the frequency of fractures (3.53 fractures/mm), density (2.7 g/cm^3), geochemistry, water absorption value (0.2 wt %) and intermediate-low perimeter values, correlating well with the technical values. The anisotropy (1.32 FIX value) and the occurrence of biotite as aggregates and grains parallel to the foliation, may form weak discontinuities, can contribute to the high LA value.

Sample Köinge (LL1112), located in the Svarten gneiss domain, has the highest frequency of fractures (5.3 fractures/mm) and should therefore show a higher LA value (33 %; Fig. 29). The sample is anisotropic (1.13 FIX value; Table 3); the occurrence of biotite as individual grains parallel to the foliation may act as weak discontinuities favoring a higher LA value. Köinge is fine grained (Fig. 35B), has a low mean grain size (0.28 mm; Fig. 39) and intermediate-high perimeter values (Figs. 41-44), which partially compensate for the high frequency of fractures (5.26 fractures/mm; Figs. 31 and 32), anisotropy and occurrence of biotite grains and aggregates parallel to the foliation and lineation, thus resulting in an moderate technical values. The moderate-high density (2.75 g/cm^3; Fig. 30) correlates with the geochemical composition (Köinge plots at silica poor stability fields; Figs. 45-48), indicating a high content of dark minerals and low LA/A_N ratio (2.0; Fig. 30).

In the samples from Stavsjö, Hallandssten, Mokrik, Abild, Toppeberg and Köinge, the grain size and perimeter are the dominating factors controlling the technical properties.

Results from the FIX analysis, for two samples, do not correlate well with the isotropic/anisotropic fabric observed in the field and under the microscope. Both samples Knobesholm (LL1104) and Abild (LL1107) are isotropic according to their FIX values (1.08 and 1.09 respectively) but in the field and under the microscope they are very anisotropic with a pronounced mineral stretching lineation. The opposite is the result for samples from Ljungby (LL1103) and Töresjö (LL1109) which only show a gneissic foliation in the field and under the microscope, but are anisotropic according to their FIX values (1.23 and 1.20 respectively). Samples such as Dagsås (LL1101) and Stavsjö (LL1102) only show a foliation (on both scales) which is reflected in their FIX values (1.05 and 1.09 respectively). The rest of the samples (Hallandssten, Mokrik, Fridhemsberg, Toppeberg, Vräk and Köinge) have LS fabric (both lineation and foliation) and depending on the relative strength of these two fabrics the rocks show various FIX values representing anisotropy. In the investigated high grade rocks, the grain boundary area reduction (GBAR) process may have proceeded far enough to form isotropic individual grains (exception is biotite and the distinct quartz ribbons consisting of individual elongated grains), however, the shape of the aggregates are anisotropic. A rock with isotropic minerals have a low FIX value, since the mineral fabric is equally or almost equally strong in both analyzed directions. The anisotropic aggregates will give the rock an anisotropic appearance in the field and under the microscope. This can explain why some samples show low FIX values (isotropic) while they are anisotropic both in the field and under the microscope.

8. Conclusions

- Considering the technical properties of all samples; samples from Dagsås (LL1101) and Ljungby (LL1103), located in the Varberg granulite gneiss domain, are the most suitable materials as aggregates for road and railway (bounded layers), while samples from Fridhemsberg (LL1108) and Töresjö (LL1109), located in the Skene migmatite gneiss domain, are the least suitable. Knobesholm (LL1104) and Vräk (LL1111) are suitable as aggregates

for bounded road layers.

- Features in the field that can be used as prospecting tools for rocks with good technical properties are: the absence of 1) a pronounced stretching lineation 2) high grade metamorphic banding (segregation of light and dark minerals) and 3) abundant veining.
- Rocks with the best technical properties have been deformed and metamorphosed at very high temperature conditions (granulite facies). Microtexutres which correlate well with high-T metamorphism are: 1) low biotite content, 2) reddish brown biotite, 3) brownish green hornblende, 4) antiperthitic feldspars, 5) pyroxene, and 6) the absence of titanite and tartan twinning in feldspars.
- A high content of biotite and the occurrence of biotite as individual grains, aggregates and/or bands parallel to present foliation correlate with poor technical values.
- Low mean grain size and high perimeter (total, amphibole + pyroxene and opaque minerals + garnet) show a good correlation to low LA values. A high proportion of very fine (c. 40 % < 0.5 mm) or fine grained materials (80 % < 1mm) seem to contribute to good LA values. The frequency of fractures has limited influence on the LA value where less fractures often result in better technical values. Samples with high density tend to have a lower LA/A_N ratio.

9. Acknowledgement

I would like to thank my supervisor Lotta Möller for thoroughly reviewing my thesis and all help she has given me throughout this time. Thanks to my co-supervisors Jenny Andersson and Mattias Göransson for your extensive work, advises and guidance. I could not have done this thesis without you. My co-supervisor Jan-Erik Lindqvist and Karin Appelquist at CBI in Borås, thanks for helping me with the micro analyses, reviewing my thesis and passing on your knowledge. Björn Schouenborg, thank you for thoroughly reviewing my thesis. Last but not least I want to thank my family and friends for all love, support and help you given me though this time.

10. References

Andersson, J., Eliasson, T., Möller, C., Lundqvist, I., Bergström, U. & Lundqvist, L. 2006: Abstract. *Bulletin of the Geological Society of Finland 1,* p. 9.

Appelquist, K. & Eliasson, E., 2011: Karaktärisering av Bohusgraniten i samband med utbyggnad av E6, norra Bohuslän. *Cement och Betong Institutet, CBI uppdragsrapport PX00536,* 32 pp.

Bergström, U., Göransson, M. & Shomali, H., 2008: Beskrivning till bergkvalitetskartan Partille och Lerums kommuner. *Sveriges geologiska undersökning K 94,* 33 pp.

Berthelsen, A, 1980: Towards a palinspastic analysis of the Shield. *International Geological Congress*, Colloquium C6, Paris, 5-21.

Bingen, B., Nordgulen, Ø. & Viola, G., 2008a. A four-phase model for the Sveconorwegian orogeny, SW Scandinavia. *Norwegian Journal of Geology 88*, 43-72.

Bingen, B., Andersson, J., Söderlund, U. & Möller, C., 2008b: The Mezoproterozoic in the Nordic countries. *Episodes 31,* 29-33.

Brander, L., Appelquist, K., Cornell, D. & Andersson, U.B., 2012: Igneous and metamorphic geochronologic evolution of granitoids in the central Eastern Segment, southern Sweden. *International Geology Review, 54*, 509–546.

Debon, F. & Le Fort, P., 1983. A chemical–mineralogical classification of common plutonic rocks and associations. *Transactions of the Royal Society of Edinburgh, Earth Sciences 73*, 135–149.

De La Roche, H., Leterrier, J., Grandclaude, P. & Marchal, M., 1980. A classification of volcanic and plutonic rocks using R1R2-diagram and major element analyses – its relationships with current nomenclature. *Chemical Geology 29*, 183–210.

European Committee for Standardization (2008) EN 13755. Natural stone test methods- Determination of water absorption at atmospheric pressure. European Committee for Standardization, Brussels.

Frost, B.R., Barnes, C.G., Collins, W. J., Arculus, R.J., Ellis, D.J. & Frost, C. D., 2001: A geochemical classification for granitic rocks. *Journal of petrology 42,* 2033-2048.

Group 4A, 2011: Lithogeochemical: Whole Rock by ICP. Acme Analytical Laboratories, Canada, Vancouver.

Group 4A, 2012: Lithogeochemical: Whole Rock by ICP. Acme Analytical Laboratories, Canada, Vancouver.

Group 4B, 2011: Lithogeochemical: Total Trace Elements by ICP-MS. Acme Analytical Laborato-

ries, Canada, Vancouver.

Group 4B, 2012: Lithogeochemical: Total Trace Elements by ICP-MS. Acme Analytical Laboratories, Canada, Vancouver.

Göransson, M., Bergström, U., Shomali, H., Claeson D. & Hellström, F., 2008: Beskrivning till bergkvalitetskartan delar av Kungsbacka och Varbergs kommuner. *Sveriges geologiska undersökning K 96*, 37 pp.

Harlov, D.E., Johansson, L., van der Kerkhof, A. & Foerster, H.J., 2006: The role of advective fluid flow and diffusion during localized, solid-state dehydration; Söndrum Stenhuggeriet, Halmstad, SW Sweden. *Journal of Petrology 47*, 3–33.

Hellman, F., Åkesson, U. & Eliasson, T., 2011: Kvantitativ petrografisk analys av bergmaterial- en metodbeskrivning. *Statens väg- och transportinstitut, VTI rapport 714*, 24 pp.

Hubbard, F.H., 1978: Geochemistry of the Varberg granite gneisses. *Geologiska föreningen i Stockholm förhandlingar 100*, 31–38.

Hubbard, F.H. & Whitley, J.E., 1979. REE in charnockite and associated rocks, southwest Sweden. *Lithos 12*, 1–11.

Janoušek, V., Farrow, C. M. & Erban, V., 2006. Interpretation of whole-rock geochemical data in igneous geochemistry: introducing Geochemical Data Toolkit (GCDkit). *Journal of Petrology 47*, 1255-1259.

Johansson, L., Lindh, A. & Möller, C. 1991: Late Sveconorwegian (Grenville) high-pressure granulite facies metamorphism in southwest Sweden. *Journal of Metamorphic Geology 9*, 283-292.

Le Maitre, R. W., 1989: *A classification of igneous rocks and glossary of terms*. Blackwell Scientific Publications, Oxford. 193 pp.

Lindqvist, J.E., Akessson, U. & Malaga, K., 2007: Microstructure and functional properties of rock materials. *Materials Characterization 58*, 1183–1188.

Lundqvist, S. & Göransson M., 2001: Evaluation and Interpretation of Microscopic Parameters vs. Mechanical Properties of Precambrian Rocks from the Stockholm Region, Sweden. *"Annales Géologiques des Pays Helléniques" Édition speciale Vol. XXXIX (Département de Géologie, Athènes).*

Middlemost, E. A. K., 1985. Naming materials in the magma/igneous rock system. *Earth-Sciences Reviews 37*, 215–224.

Möller, C., 1998: Decompressed eclogites in the Sveconorwegian (-Grenvillian) orogen of SW Sweden: petrology and tectonic implications. *Journal of Metamorphic Geology 16*, 641-656.

Möller, C., 1999: Sapphirine in SW Sweden: a record of Sveconorwegian (-Grenvillian) late-orogenic tectonic exhumation. *Journal of Metamorphic Geology 17*, 127-141.

Möller, C., Andersson, J., Lundquist, I. & Hellström, F., 2007: Linking deformation, migmatite formation and zircon U-Pb geochronology in polymetamorphic orthogneisses, Sveconorwegian Province, Sweden. *Journal of Metamorphic Geology 25,* 727-750.

NT BUILD 486 (1998). Aggregates: Size distribution. Nordtest.

Persson, L. & Göransson, M., 2010a: Beskrivning till bergkvalitetskartan del av Halmstads kommun. *Sveriges geologiska undersökning, K 298*, 27 pp.

Persson, L. & Göransson, M., 2010b: Beskrivning till bergkvalitetskartan Söderåsens kommun. *Sveriges geologiska undersökning, K 301*, 26 pp.

Rimsa, A., Johansson, L. & Whitehouse, M.J., 2007: Constraints on incipient charnockite formation from zircon geochronology and rare earth element characteristics. *Contributions to Mineralogy and Petrology 154*, 357–369.

Rollinson, H., 1993: *Using geochemical data: evaluation, presentation, interpretation*. Longman Group UK. Harlow, England. 352 pp.

Stenlid, L., 2000: Utvärdering av micro-Devalmetoden. *Slutrapport SBUF projekt nr 5002. Skanska Sverige AB, Vägtekniskt Centrum Nord, Bålsta*, 16 pp.

Svensk Standard (1997a): SS-EN 1097-2. Ballast – Mekaniska och fysikaliska egenskaper – Del 2: Bestämning av motstånd mot sönderdelning. Swedish Standards Institute, Sweden.

Svensk Standard (1997b): SS-EN 1097-1. Ballast – Mekaniska och fysikaliska egenskaper – Del 1: Bestämning av nötningsmotstånd (Micro-Deval). Swedish Standards Institute, Sweden.

Svensk Standard (2004a): SS-EN 1097-9. Ballast –

Mekaniska och fysikaliska egenskaper – Del 9: Bestämning av motstånd mot nötning av dubbdäck (Nordiska kulkvarnsmetoden). Swedish Standards Institute, Sweden.

Svensk Standard (2004b): SS-EN 1097-6. Ballast- Mekaniska och fysikaliska egenskaper- Del 6: Bestämning av korndensitet och vattenabsorption. Swedish Standards Institute, Sweden.

Svensk Standard (2007): SS-EN 13242+A1. Ballast för obundna material till vägbyggnad och anläggningsbygge. Swedish Standards Institute, Sweden.

Söderlund, U., Möller, C., Andersson, J., Johansson, L. & Whitehouse, M., 2002: Zircon geochronology in polymetamorphic gneisses in the Sveconorwegian orogen, SW Sweden: ion microprobe evidence for 1.46-1.42 and 0.98-0.96 Ga reworking. *Precambrian Research 113*, 193-225.

Tavares, L.M. & das Neves, P.B., 2008: Microstructure of quarry rocks and relationships to particle breakage and crushing. International Journal of Mineral Processing 87, 28-41.

Wahlgren, C.H., Cruden, A.R & Stephens, M.B., 1994: Kinematics of a major fan-like structure in the eastern part of the Sveconorwegian orogen, Baltic Shield, south-central Sweden. *Precambrian Research 70*, 67-91.

Wang, X.-D. & Lindh, A. 1996: Temperature-pressure investigation of the southern part of the Southwest Swedish Granulite Region. *European Journal of Mineralogy 8*, 51-67.

Wik, N.-G., Andersson, J., Bergström, U., Claeson, C., Juhujuntti, N., Kero, L., Lundqvist, L., Möller, C., Sukotjo, S. & Wikman, H., 2006: Beskrivning till regional bergsrundskarta över Jönköpings län. *Sveriges geologiska undersökning K 61*, 60 pp.

Wik, N.-G., Claeson, C., Bergström, U., Hellström, H., Jelinek, C., Juhujuntti, N., Jönberger, J., Kero, L., Lundqvist, L., Sukotjo, S. & Wikman, H. 2009: Beskrivning till regional bergrundskarta över Kronobergs län. *Sveriges geologiska undersökning K 142,* 60 pp.

Winter, J.D., 2001: *An introduction to igneous and metamorphic petrology.* Prentice-Hall Inc. New Jersey, United States of America. 697 pp.

Vägverket 2005a: Allmän teknisk beskrivning för vägkonstruktion. Kapitel E. Obundna material. ATB VÄG 2005 Publ. 2005:112, 105 pp.

Vägverket 2005b: Allmän teknisk beskrivning för vägkonstruktion. Kapitel F. Bitumenbundna material. ATB VÄG 2005 Publ. 2005:112, 90 pp.

Åkesson, U., Stigh, J., Lindqvist, J. E. & Göransson, M., 2003: The influence of foliation on the fragility of granitic rocks, image analysis and quantitative microscopy. *Engineering Geology 68,* 275-288.

11. Appendix

Appendix 1: Production data of the investigated quarries

Appendix 2: Field observations of the investigated samples

Appendix 3: Thin section descriptions of the investigated samples

Appendix 4: Technical values, density and water absorption values

Appendix 5: Micro analyses: Frequency of fractures, mineral grain size, mineral grain size distribution, FIX- and perimeter values

Appendix 6: Geochemistry classifications and SiO_2 content.

Appendix 1. Production data of the investigated quarries.

Locality name	Sample ID	Year	Total tons	Road	Concrete	Other	Ornamental stone	Dimension stone	Thrown away
Stavsjö	LL1102	2005	22580	22580	-	-	-	-	-
		2006	1114	1114	-	-	-	-	-
		2007	144300	138900	5400	-	-	-	-
		2008	187718	165718	22000	-	-	-	-
		2009	195455	171955	23500	-	-	-	-
Ljungby	LL1103	2011	40000	40000	-	-	-	-	-
		2012	70000	70000	-	-	-	-	-
Knobesholm	LL1104	2005	24720	24720	-	-	-	-	-
		2006	25000	25000	-	-	-	-	-
		2007	21379	15000	-	6379	-	-	-
		2008	17697	11770	-	5927	-	-	-
		2009	15544	7500	-	8044	-	-	-
Hallandssten	LL1105	2005	7750	-	-	-	1250	-	6500
		2006	4970	-	-	-	1523	-	3447
		2007	3990	-	-	-	1681	-	2309
		2008	4684	-	-	-	1296	-	3388
		2009	4274	-	-	-	1609	-	2665
Mokrik	LL1106	1996	31200	-	-	25500	-	5700	-
		1997	26300	21600	-	21600	4700	-	-
		1998	13225	10727	-	10727	2498	-	-
		1999	11971	9457	-	9457	2514	-	-
		2000	11200	1900	-	1900	2800	-	6500
		2001	9400	400	-	400	3300	-	5700
		2002	6800	-	-	4900	1900	-	-
		2003	15960	-	-	13400	2560	-	-
		2004	17700	-	-	950	3350	-	-
		2005	9100	-	-	6500	2600	-	-
		2006	12150	-	-	9450	2700	-	-
		2007	24600	-	-	22100	2500	-	-
		2008	3400	-	-	700	2700	-	-
		2009	4600	-	-	2000	2600	-	-

Appendix 2. Field observations of the investigated samples.

		Color						Layering		
Locality	Sample ID	Fresh cut	Weathered	Foliation	Lineation	Augen	Veins	Lithological	Stromatic	Metamorphic segregation
Dagsås	LL1101	Grey to dark grey	Rusty brown	Penetrative	-	-	-	-	-	-
Stavsjö	LL1102	Reddish grey	Yellowish brown to rusty colored	Yes	-	Dominated by pink K-feldspar	Extensive, granitic composition	-	-	-
Ljungby	LL1103	Reddish grey	Yellowish to rusty brown	Strong	-	Dominated by pink K-feldspar, deformed to various degree, occasionally show orthoclase core	Sparse	Yes	-	-
Knobesholm	LL1104	Reddish grey	Rusty brown	Weak	Pronounced	Deformed, dominated by pink K-feldspar, may contain orthoclase core	Abundant, pink, folded	-	-	-
Hallandsten	LL1105	Reddish grey	Yellowish brown to rusty brown	Yes	Pronounced	Deformed, dominated by pink K-feldspar	Abundant, two sets, pink, folded, surrounded by a biotite selvage	-	-	-
Mokrik	LL1106	Reddish grey	Yellowish brown to rusty colored	Yes	Pronounced	Dominated by pink K-feldspar	Abundant, two sets, pink, folded, occasionally surrounded by a dark mineral selvage	-	-	-

Appendix 2. Field observations of the investigated samples.

		Color						Layering		
Locality	Sample ID	Fresh cut	Weathered	Foliation	Lineation	Augen	Veins	Lithological	Stromatic	Metamorphic segregation
Abild	LL1107	Reddish grey	-	-	Yes	Dominated by pink K-feldspar, deformed to varous degree	Abundant, dominated by pink K-feldspar, ocasionally surrounded by a dark mineral selvage	-	-	-
Fridhemsberg	LL1108	Pink-whitish grey	Yellowish brown	Pronounced	Occasional	Pegmatitic	Abundant, pink, tree types, two types are surrounded by a biotite-hornblende selvage, unstrained, horizontally extensive	-	Yes	Yes
Töresjö	LL1109	Whitish grey	Yellowish brown to rusty colored	Yes	-	-	Abundant, coarse grained, white-pink, surrounded by a dark mineral selvage, unstrained, horizontally extensive	-	Yes	Yes
Toppeberg	LL1110	Pinkish grey	Yellowish brown to rusty colored	Yes	Weak	Occasional, deformed, dominated by pink K-feldspar	Sparse, unstrained	-	-	-
Vråk	LL1111	Grey	Rusty brown to grey	Weak	Yes	Stretched, dominated by bright pink K-feldspar	-	-	-	-
Köinge	LL1112	Pinkish grey	Pink-whitish grey to rusty brown	Yes	Yes	Stretched, dominated by pink K-feldspar	-	-	-	-

Appendix 3. Thin section descriptions of all the investigated samples.

Locality	Sample ID	Antiperthite	Tartan twinning	Quartz ribbons	Sericitization	Myrmekitization	Orthoclase	Alkali feldspar (occurence and alteration)
Dagsås F1	LL1101	Common	-	Yes	-	Modest	-	-
Dagsås F2								
Stavsjö F1	LL1102	Sparse	Common	-	Some are moderate to severely	-	-	-
Stavsjö F2				Yes				
Ljungby F1	LL1103	Common	-	Yes	Moderate	-	Few augen	Occasionally as granoblastic polycrystalline domains, show rust colored alteration
Ljungby F2								
Knobesholm TL	LL1104	Occasional	Sparse (few small grains)	-	Moderate to severely	-	-	Granoblastic monomineralic domains
Knobesholm PL				Yes				
Hallandssten F1	LL1105	Occasional	-	Yes	Occasionally moderate to severely	-	-	Granoblastic domains, show rust colored alteration
Hallandssten F2				-				
Mokrik F1	LL1106	Occasional	-	Yes	Occasionally moderate to severely	-	-	Granoblastic domains, show rust colored alteration
Mokrik F2								
Abild TL	LL1107	Occasional	Common	-	Moderate to severely	-	Occasionally as core in microcline grains	Occasionally as granoblastic domains
Abild PL				Yes				
Fridhemsberg F1	LL1108	Sparse	Common	-	Moderate to severely	Sparse	Core in few microcline augen	-
Fridhemsberg F2								
Töresjö F1	LL1109	-	Common	-	Occasionally moderate to severely	Occasionally	Core in few microcline augen	-
Töresjö F2								
Toppeberg F1	LL1110	Sparse	Common	-	Moderate to severely	Sparse	-	-
Toppeberg F2								
Vräk TL	LL1111	-	Not well developed	-	Moderate to severely	-	-	-
Vräk PL				Yes				
Köinge TL	LL1112	Yes	-	Yes	Severe in one corner, otherwise modest	Sparse	-	Few granoblastic polycrystalline domains
Köinge PL				-	Modest			

Appendix 3. Thin section descriptions of all the investigated samples.

		Color		Biotite					Pyroxene
Locality	Sample ID	Hornblende	Biotite	Content	Occurence	Cloritized	Titanite	Garnet	
Dagsås F1	LL1101	Brown-green	Red-brown	Low	Individual grains // S	-	-	Yes	Clino- and orthopyroxene are abundant
Dagsås F2									
Stavsjö F1	LL1102	Blue-green	Dark-brown	-	Individual grains and occasionally as aggregates, randomly oriented	-	Coronas surrounding few opauqe minerals	-	-
Stavsjö F2									
Ljungby F1	LL1103	Brown-green	Red-brown	Low	Individual grains // S	Some	-	Yes	Clinopyroxene shows severe rust colored alteration
Ljungby F2									
Knobesholm TL	LL1104	Brown-green	Red-brown	-	Individual grains and aggregates are randomly oriented	-	-	-	-
Knobesholm PL					Individual grains and aggregates // LS				
Hallandssten F1	LL1105	Brown-green	Red-brown	-	Individual grains and aggregates generally // S	Some are partly	-	-	-
Hallandssten F2									
Mokrik F1	LL1106	Brown-green	Red-brown	-	Individual grains and aggregates generally // S	Some are partly	-	Few	Occasional clinopyroxene shows severe rust colored alteration
Mokrik F2									
Abild TL	LL1107	Blue-green is dominating	Red-brown	-	Individual grains and aggregates // L	-	-	-	-
Abild PL									
Fridhemsberg F1	LL1108	Blue-green	Dark-brown	Biotite is abundant	Individual grains, aggregates and bands // S	Few are partly	-	-	-
Fridhemsberg F2									
Töresjö F1	LL1109	-	Dark-brown	Biotite is abundant	Individual grains, aggregates and bands // S	Few are partly	Individual grains and as coronas surrounding opaque minerals	Rare	-
Töresjö F2									
Toppeberg F1	LL1110	Blue-green	Dark-brown	-	Individual grains and aggregates // S	Often partly	Individual grains and as coronas surrounding opaque minerals	-	-
Toppeberg F2									
Vräk TL	LL1111	Blue-green	Dark-brown	-	Individual grains and aggregates // LS	Few are partly to entirely	Coronas surrounding few opauqe minerals	-	-
Vräk PL									
Köinge TL	LL1112	Brown-green	Red-brown	-	Individual grains and aggregates // LS	Some are partly to entirely	-	Yes	Some clinopyroxene grains show moderate rust colored alteration
Köinge PL									

Appendix 4. Locality name, Sample ID, technical values, density and water absorption values for all investigated samples.

Locality	Sample ID	A_N (%)	LA (%)	M_{DE} (%)	D (g/cm^3)	A_b (wt%)
Dagsås	LL1101	11	19	8	2.79	0.3
Stavsjö	LL1102	15	34	10	2.70	0.2
Ljungby	LL1103	9	22	5	2.66	0.1
Knobesholm	LL1104	13	30	9	2.70	0.2
Hallandssten	LL1105	14	35	9	2.68	0.1
Mokrik	LL1106	12	40	9	2.69	0.1
Abild	LL1107	15	42	10	2.66	0.4
Fridhemsberg	LL1108	19	46	12	2.65	0.2
Töresjö	LL1109	23	41	15	2.69	0.2
Toppeberg	LL1110	16	40	11	2.70	0.2
Vräk	LL1111	12	29	8	2.67	0.2
Köinge	LL1112	16	33	10	2.75	0.2

Appendix 5. Locality name, sample ID and results from micro analyses; Frequency of fractures, mineral grain size, mineral grain size distribution, FIX and perimeter.

		Frequency of fractures (number of fractures/mm)				Mineral grain size (mm)			Mineral grain size distribution: Accumulated material (%)								Perimeter (mm/mm^2)			
Locality	Sample ID	Intra granular	Trans granular	Grain boundary	Total	Min	Max	Mean	4 (mm)	2 (mm)	1 (mm)	0.5 (mm)	0.25 (mm)	0.125 (mm)	0.063 (mm)	FIX	Bt	Amph+ px	Opaque+ gt	Total
Dagsås	LL1101	0.05	0.18	0.42	0.65	0.02	1.56	0.17	100	100	65	43	14	2	0	1.05	0.36	2.36	1.34	4.06
Stavsjö	LL1102	0.67	0.21	2.10	2.97	0.06	1.21	0.39	100	100	64	15	1	0	0	1.09	1.29	1.48	0.22	2.99
Ljungby	LL1103	0.31	0.48	1.40	2.23	0.02	1.40	0.33	100	100	67	18	2	0	0	1.23	0.01	1.43	0.39	1.82
Knobesholm	LL1104	0.63	0.05	3.90	4.62	0.04	2.04	0.33	100	100	87	57	19	1	0	1.08	1.78	1.07	0.41	3.25
Hällandsåsten	LL1105	0.68	0.25	2.50	3.46	0.02	2.67	0.46	100	100	66	31	8	0	0	1.16	0.73	0.74	0.41	1.88
Mokrik	LL1106	0.27	0.12	2.00	2.39	0.02	2.00	0.39	100	100	68	29	9	1	0	1.34	0.53	0.86	0.28	1.67
Abild	LL1107	0.51	0.16	2.00	2.70	0.02	1.88	0.41	100	82	45	1	1	0	0	1.09	0.89	0.44	0.30	1.63
Fridhemsberg	LL1108	0.83	0.12	2.60	3.59	0.02	2.92	0.52	100	100	65	28	4	0	0	1.28	1.30	0.13	0.01	1.43
Töresjö	LL1109	0.74	0.01	1.90	2.60	0.04	2.25	0.47	100	100	81	31	7	1	0	1.20	1.33	0.00	0.04	1.37
Toppeberg	LL1110	1.20	0.18	2.20	3.53	0.04	2.79	0.72	100	100	59	12	2	0	0	1.32	0.78	1.17	0.11	2.06
Vråk	LL1111	0.92	0.09	2.80	3.85	0.04	1.63	0.36	100	100	71	16	1	0	0	1.27	1.30	0.28	0.16	1.74
Köinge	LL1112	1.10	0.33	3.80	5.26	0.04	1.44	0.28	100	100	74	37	5	0	0	1.13	0.85	1.64	0.55	3.05

Appendix 6. Locality name, sample ID, results from bulk rock classification diagrams and SiO_2 content.

		Rock classification (bulk rock geochemistry)				
Locality	Sample ID	Norm mineralogy (QAP)	TAS	P-Q	R_1-R_2	SiO_2 (wt %)
Dagsås	LL1101	Quartz Monzodiorite	Monzonite	Quartz Monzodiorite	Monzodiorite	61
Stavsjö	LL1102	Quartz Monzodiorite	Quartz Monzonite	Quartz Monzodiorite	Quartz Monzonite-Tonalite	64
Ljungby	LL1103	Granite	Granite	Granite	Granite	70
Knobesholm	LL1104	Quartz Monzonite-Quartz Monzodiorite	Quartz Monzonite	Quartz Monzonite	Quartz Monzonite-Tonalite	64
Hallandssten	LL1105	Granite	Granite	Granodiorite-Granite	Granite-Granodiorite	69
Mokrik	LL1106	Granite-Granodiorite	Granite	Granite	Granite	70
Abild	LL1107	Granite	Quartz Monzonite-Granite	Granite	Granite-Granodiorite	69
Fridhemsberg	LL1108	-	-	-	-	-
Töresjö	LL1109	-	-	-	-	-
Toppeberg	LL1110	Quartz Monzodiorite	Quartz Monzonite-Granodiorite	Quartz Diorite	Tonalite	64
Vräk	LL1111	Granite	Granite	Granite	Granite-Granodiorite	69
Köinge	LL1112	Monzodiorite	Monzonite	Monzogabbro	Syenodiorite-Monzonite	59

Tidigare skrifter i serien "Examensarbeten i Geologi vid Lunds universitet":

275. Vang, Ina, 2011: Amphibolites, structures and metamorphism on Flekkerøy, south Norway. (45 hp)
276. Lindvall, Hanna, 2011: A multi-proxy study of a peat sequence on Nightingale Island, South Atlantic. (45 hp)
277. Bjerg, Benjamin, 2011: Metodik för att förhindra metanemissioner från avfallsdeponier, tillämpad vid Albäcksdeponin, Trelleborg. (30 hp)
278. Pettersson, Hanna, 2011: El Hicha – en studie av saltstäppssediment. (15 hskp)
279. Dyck, Brendan, 2011: A key fold structure within a Sveconorwegian eclogite-bearing deformation zone in Halland, southwestern Sweden: geometry and tectonic implications. (45 hp)
280. Hansson, Anton, 2011: Torvstratigrafisk studie av en trädstamshorisont i Viss mosse, centrala Skåne kring 4 000 - 3 000 cal BP med avseende på klimat- och vattenståndsförändringar. (15 hp)
281. Åkesson, Christine, 2011: Vegetationsutvecklingen i nordvästra Europa under Eem och Weichsel, samt en fallstudie av en submorän, organisk avlagring i Bellinga stenbrott, Skåne. (15 hp)
282. Silveira, Eduardo M., 2011: First precise U-Pb ages of mafic dykes from the São Francisco Craton. (45 hp)
283. Holm, Johanna, 2011**:** Geofysisk utvärdering av grundvattenskydd mellan väg 11 och Vombs vattenverk. (15 hp)
284. Löfgren, Anneli, 2011: Undersökning av geofysiska metoders användbarhet vid kontroll av den omättade zonen i en infiltrationsdamm vid Vombverket. (15 hp)
285. Grenholm, Mikael, 2011: Petrology of Birimian granitoids in southern Ghana - petrography and petrogenesis. (15 hp)
286. Thorbergsson, Gunnlaugur, 2011: A sedimentological study on the formation of a hummocky moraine at Törnåkra in Småland, southern Sweden. (45 hp)
287. Lindskog, Anders, 2011: A Russian record of a Middle Ordovician meteorite shower: Extraterrestrial chromite in Volkhovian-Kundan (lower Darriwilian) strata at Lynna River, St. Petersburg region. (45 hp)
288. Gren, Johan, 2011: Dental histology of Cretaceous mosasaurs (Reptilia, Squamata): incremental growth lines in dentine and implications for tooth replacement. (45 hp)
289. Cederberg, Julia, 2011: U-Pb baddelyit dateringar av basiska gångar längs Romeleåsen i Skåne och deras påverkan av plastisk deformation i Protoginzonen (15 hp)
290. Ning, Wenxing, 2011: Testing the hypothesis of a link between Earth's magnetic field and climate change: a case study from southern Sweden focusing on the 1st millennium BC. (45 hp)
291. Holm Östergaard, Sören, 2011: Hydrogeology and groundwater regime of the Stanford Aquifer, South Africa. (45 hp)
292. Tebi, Magnus Asiboh, 2011: Metamorphosed and partially molten hydrothermal alteration zones of the Akulleq glacier area, Paamiut gold province, South-West Greenland. (45 hp)
293. Lewerentz, Alexander, 2011: Experimental zircon alteration and baddeleyite formation in silica saturated systems: implications for dating hydrothermal events. (45 hp)
294. Flodhammar, Ingrid, 2011: Lövestads åsar: En isälvsavlagring bildad vid inlandsisens kant i Weichsels slutskede. (15 hp)
295. Liu, Tianzhuo, 2012: Exploring long-term trends in hypoxia (oxygen depletion) in Western Gotland Basin, the Baltic Sea. (45 hp)
296. Samer, Bou Daher, 2012: Lithofacies analysis and heterogeneity study of the subsurface Rhaetian–Pliensbachian sequence in SW Skåne and Denmark. (45 hp)
297. Riebe, My, 2012: Cosmic ray tracks in chondritic material with focus on silicate mineral inclusions in chromite. (45 hp)
298. Hjulström, Joakim, 2012: Återfyllning av borrhål i geoenergisystem: konventioner, metod och material. (15 hp)
299. Letellier, Mattias, 2012: A practical assessment of frequency electromagnetic inversion in a near surface geological environment. (15 hp)
300. Lindenbaum, Johan, 2012: Identification of sources of ammonium in groundwater

using stable nitrogen and boron isotopes in Nam Du, Hanoi. (45 hp)

301. Andersson, Josefin, 2012: Karaktärisering av arsenikförorening i matjordsprofiler kring Klippans Läderfabrik. (45 hp)
302. Lumetzberger, Mikael, 2012: Hydrogeologisk kartläggning av infiltrationsvattentransport genom resistivitetsmätningar. (15 hp)
303. Martin, Ellinor, 2012: Fossil pigments and pigment organelles – colouration in deep time. (15 hp)
304. Rådman, Johan, 2012: Sällsynta jordarts-metaller i tungsand vid Haväng på Österlen. (15 hp)
305. Karlstedt, Filippa, 2012: Jämförande geokemisk studie med portabel XRF av obehandlade och sågade ytor, samt pulver av Karlshamnsdiabas. (15 hp)
306. Lundberg, Frans, 2012: Den senkambriska alunskiffern i Västergötland – utbredning, mäktigheter och faciestyper. (15 hp)
307. Thulin Olander, Henric, 2012: Hydrogeologisk kartering av grund-vattenmagasinet Ekenäs-Kvarndammen, Jönköpings län. (15 hp)
308. Demirer, Kursad, 2012: U-Pb baddeleyite ages from mafic dyke swarms in Dharwar craton, India – links to an ancient supercontinent. (45 hp)
309. Leskelä, Jari, 2012: Loggning och återfyllning av borrhål – Praktiska försök och utveckling av täthetskontroll i fält. (15 hp)
310. Eriksson, Magnus, 2012: Stratigraphy, facies and depositional history of the Colonus Shale Trough, Skåne, southern Sweden. (45 hp)
311. Larsson, Amie, 2012: Kartläggning, beskrivning och analys av Kalmar läns regionalt viktiga vattenresurser. (15 hp)
312. Olsson, Håkan, 2012: Prediction of the degree of thermal breakdown of limestone: A case study of the Upper Ordovician Boda Limestone, Siljan district, central Sweden. (45 hp)
313. Kampmann, Tobias Christoph, 2012: U-Pb geochronology and paleomagnetism of the Westerberg sill, Kaapvaal Craton – support for a coherent Kaapvaal-Pilbara block (Vaalbara). (45 hp)
314. Eliasson, Isabelle Timms, 2012: Arsenik: förekomst, miljö och hälsoeffekter. (15 hp)
315. Badawy, Ahmed Salah, 2012: Sequence stratigraphy, palynology and biostratigraphy across the Ordovician-Silurian boundary in the Röstånga-1 core, southern Sweden. (45 hp)
316. Knut, Anna, 2012: Resistivitets- och IP-mätningar på Flishultsdeponin för lokalisering av grundvattenytor. (15 hp)
317. Nylén, Fredrik, 2012: Förädling av ballast-material med hydrocyklon, ett fungerande alternativ? (15 hp)
318. Younes, Hani, 2012: Carbon isotope chemostratigraphy of the Late Silurian Lau Event, Gotland, Sweden. (45 hp)
319. Weibull, David, 2012: Subsurface geological setting in the Skagerrak area – suitability for storage of carbon dioxide. (15 hp)
320. Petersson, Albin, 2012: Förutsättningar för geoenergi till idrottsanläggningar i Kallerstad, Linköpings kommun: En förstudie. (15 hp)
321. Axbom, Jonna, 2012: Klimatets och människans inverkan på tallens etablering på sydsvenska mossar under de senaste århundradena – en dendrokronologisk och torvstratigrafisk analys av tre småländska mossar. (15 hp)
322. Kumar, Pardeep, 2012: Palynological investigation of coal-bearing deposits of the Thar Coal Field Sindh, Pakistan. (45 hp)
323. Gabrielsson, Johan, 2012: Havsisen i arktiska bassängen – nutid och framtid i ett globalt uppvärmningsperspektiv. (15 hp)
324. Lundgren, Linda, 2012: Variation in rock quality between metamorphic domains in the lower levels of the Eastern Segment, Sveconorwegian Province. (45 hp)

LUNDS UNIVERSITET

Geologiska institutionen
Lunds universitet
Sölvegatan 12, 223 62 Lund